Université
de Liège

Analysis of performance and robustness of biological switches:
local tools for non-local dynamical phenomena.

PhD thesis of Laura Trotta

Supervised by Pr. Rodolphe Sepulchre

Co-supervised by Pr. Eric Bullinger

Faculty of Applied Sciences

Department of Electrical Engineering and Computer Science

The present dissertation has been evaluated by the jury members

Pr. V. Seutin, Chair, University of Liège

Pr. R. Sepulchre, Advisor, University of Liège

Pr. E. Bullinger, Co-advisor, University of Liège

Pr. P. Geurts, University of Liège

Pr. G-B. Stan, Imperial College London (UK)

Pr. B. Gutkin, Ecole normale supérieure de Paris (France)

Pr. J-A. Sepulchre, Université de Nice Sophia Antipolis (France)

Abstract

Biological switches are frequently encountered in mathematical modeling of biological systems because binary decisions are at the core of many cellular processes. A bistable switch presents two stable steady-states, each of them corresponding to a distinct decision. These two decisions are assumed to result from the interactions between biochemical effectors at the molecular level. Because these molecular interactions are particularly complex, involving many effectors, mathematical models of biological switches are often high dimensional and nonlinear. Therefore, an analysis of these systems is challenging. In this dissertation, we try to identify principles and tools to study the performance and robustness of biological switches. Our first contribution is to highlight the dynamical nature of these switches. A biological switch encodes a decision-making process rather than a static binary code. It captures dynamical phenomena that are important for the decision-making process, such as decision latencies and reversibility. Our second contribution is methodological. While most of the classical analysis tools are based on a linearization of the system around a stable steady-state, a switch is a non local phenomenon involving a transition between two stable steady-sates. Rather than studying the system around stable equilibria, we identify the local rulers of the decision-making process in both the state and parameter spaces and propose a local analysis in the vicinity of these particular points. Our third contribution is to emphasize the added value of an abstract (that is, mathematical) framework for the analysis of biological switches. By studying different models, we point out that the same principles can be used to encode dynamical phenomena in very different cellular processes. Physiological processes as different as apoptosis, the cellular choice of death, and action potential, the cellular choice to emit an electrical spike, share common features when regarded as decision-making processes.

Résumé

L'objet de cette thèse est l' étude de la performance et de la robustesse des modèles d'interrupteurs en biologie. Mathématiquement, ces interrupteurs sont modélisés par des systèmes bistables, c'est-à-dire des systèmes dans lesquels deux états stationnaires stables coexistent. Ces modèles sont utilisés en biologie systémique pour représenter des décisions cellulaires binaires, résultant de réactions biochimiques. Etant donné la complexité de ces interactions et le nombre potentiellement élevé d'effecteurs, ces systèmes sont souvent de grande dimension et nonlinéaires, rendant leur étude complexe. La thèse tente d'identifier des principes et outils d'analyse permettant de mieux comprendre et contrôler ces interrupteurs biologiques. Notre première contribution réside dans la mise en lumière du caractère dynamique des interrupteurs biologiques. Nous considérons les interrupteurs bistables comme des processus de prise de décision temporels qui permettent d'implémenter des phénomènes dynamiques tels qu'une latence dans la décision ou la réversibilité de la décision. Notre seconde contribution est méthodologique. Nous partons du constat qu'il existe une inéquation entre les outils d'analyse classiques basés sur une étude locale du système autour d'un état d' équilibre stable et le caractère non local de la prise de décision impliquant une transition entre deux états d'équilibre différents. En réponse à ce problème, nous proposons une analyse locale non pas effectuée aux points d'équilibre stables du système mais en des points que nous identifions comme des régulateurs clés du processus de décision dans l'espace d'état et des paramètres. Notre dernière contribution vise à mettre en évidence l'intérêt d'une analyse mathématique des modèles d'interrupteurs bistables indépendamment de leur contexte biologique. En effet, notre analyse fournit un cadre d'étude commun à des phénomènes distincts en biologie. Elle montre que des processus cellulaires de nature très différentes, tels que que l'apoptose cellulaire ou la génération de potentiels d'actions dans les neurones, partagent des caractéristiques essentielles.

Acknowledgements

I wish to express my personal gratitude to all of those who contributed to make the preparation of this thesis a pleasant and enriching experience.

First and foremost, I am heartily thankful to my advisor, Professor Rodolphe Sepulchre. Most of this work is due to his outstanding advice, support and perpetual enthusiasm about research.

I also mention with gratitude the help received from my co-advisor, Professor Eric Bullinger. I have greatly benefited from his technical advice in systems biology.

Many thanks are also due to my colleagues of the University of Liège who all contributed to create a stimulating working environment. In particular, I would like to thank Anne Collard, a great colleague and friend whose organizational skills in work and cheerfulness in life were very precious when completing this thesis. It was a real pleasure to share the office with Gilles Meyer and Fulvio Forni, two very kind and attentive persons. Pierre Sacré is specially thanked for his reliable and precious help in work and his nice company. Special thanks go to Alexandre Mauroy and Raphael Liégeois, for rewarding scientific and philosophical discussions during the fortuitous breaks of the afternoon. Thanks to Bamdev Mishra for sharing with us so many curiosities about sciences and technology, to Alain Sarlette for his valuable opinion and comments about various scientific matters, to Guillaume Drion, Julie Dethier, Mattia Zorzi and Enrico Amico for animated coffee breaks. The optimism of Alessio Franci and his useful advices in the work carried out together have been particularly appreciated.

I gratefully thank Professor Quentin Louveaux, Dominique Lamy and Laurent Poirrier for the very nice teaching lessons in Numerical Analysis.

Like for any piece of work distributed over a long period of time, achieving the present thesis would not have been possible without a caring and distracting life environment. Special thanks to Emilie Gretry-Sibilla and her husband Laurent Sibilla for their friendly support, to the biomed girls, Laura Symul, Marie Schrynemackers, Jessica Schrouff, Sabine Paeme-Regnier and Melinda Choua for the enjoyable and unforgettable moments spent together and to the team of the Friday 'Boulet' for these pleasant lunch times.

The members of the Jury are acknowledged for their interest and time devoted to this work.

Last but not least, I offer my regards and blessing to my family. I owe my parents, Bernadette and Toni, many thanks for unconditional support and devotion over all these years. I greatly appreciated the humor and patience of my little brother Antoine. I am indebted to my sister, Marie and his partner Valentin, for valuable comments and support that were essential for the completion of this thesis but also for an extra-work source of motivation, the little girl, Léa. Finally, my deepest gratitude goes to César.

Introduction

The cell is the functional unit of life able to grow, replicate and respond to its environment. In the 20th century, major advances have been made in the understanding of the cell machinery with the discovery of genetic and proteinic mechanisms of regulation. Proteins carry the information encoded in the genome. They are the key effectors of the cell, composing its structure, ruling its metabolism and participating to various signaling pathways.

The question underlying molecular and cellular physiology is, how to bridge the gap between biochemical interactions such as interactions among proteins and a given cell behavior? Whereas, the main biochemical signaling pathways governing the cellular functions have been identified, understanding how such complex interactions can give rise to robust behaviors is still challenging. These questions have recently motivated the emergence of new disciplines such as systems and synthetic biology. In these fields, biological phenomena are studied in the light of theories inherited from engineering such as systems and control theories while mathematical modeling is proposed as a tool to understand, design and control the interactions between biochemical effectors.

In this thesis, we study the performance and robustness of biological switches. Bistable switches model cellular binary decisions. Mathematically, those models are called bistable, which means that two attractors (for instance, equilibria) coexist, each corresponding to a possible alternative for the cell. These two decisions are assumed to result from the interactions between biochemical effectors at the molecular level.

Because these molecular interactions are particularly complex, involving many effectors, nonlinear phenomena and taking place on different time-

scales, mathematical models built to represent these systems are particularly difficult to analyze. Classical analysis methods fail to capture the properties of bistable switches. This is because they are mostly based on local analysis (linearization) around a stable steady-sate, whereas bistability modeling is about capturing the transition between the two stable equilibria. Biological switches are non-local phenomena, not determined by the local behavior about each stable steady-state. This explains why most current studies about biological switches modeling is through numerical simulation. The system is simulated for various initial conditions and parameters values and performance and robustness measures are drawn from the results of these simulations. This approach quickly becomes formidable as the number of equations and parameters grows. It rarely captures qualitative mechanisms, which are what modeling is about.

Systems biology is still a young field, and its methodology is under development. In this thesis, we propose a mathematical methodology to study biological switches. Our hope is that this methodology when coupled to other approaches, will help at understanding and designing performant and robust switches.

Contributions

Our first contribution lies in our particular viewpoint on bistable switches. Rather than reducing a bistable model to its two stable steady-state responses, we consider bistable switches as open dynamical decision-making processes, that is we focus on the temporal transition that determines the switch between the two states. Time is associated to transient phenomena that are at the core of the decision making process, allowing for instance the decision-making to be slowed down or even reversed. The decision-making process also depends on time trough the input history, i.e the decision-making process has a memory.

Our second contribution is methodological. We propose a new methodology to study bistable switches. The methodology is standard, in the sense that is is based on local analysis, but the local analysis is not performed around the stable steady-states. Rather, we identify in the state-space and in the parameter space particular points that act as local

rulers of the (non-local) decision-making process. In the first part of the thesis, we focus on the role of the saddle-point, an unstable equilibrium that typically separates the basins of attraction of the two stable attractors, and show that a local analysis around that unstable equilibrium is an excellent predictor of the non-local analysis of bistablity. In the second part of the thesis, we further explore this idea with the concept of singularity, that locally organizes bistability both in state-space and in parameter space. The idea that isolated points of high sensitivity organize the global behavior of complex dynamical models does not seem to have been previously exploited in systems biology.

Finally, a third contribution is to show the added value of analyzing in a unified framework decision models that have a very different physiological background. Our thesis aims at showing that two biological phenomena that seem very different from a physiological viewpoint, such as apoptosis, the controlled cell death and the mechanism of spike generation in neurons share common features that shed light on each other.

Outline

In Chapter 1, we present three distinct examples of important decision-making processes taking place at the cellular level. The first process is apoptosis, the controlled cell death. Facing pro-apoptic signals, the cell has to choose between the survival and death. The second example is inherited from electrophysiology and is the problem of first spike latency in neurons. The last one is a switch in particular enzymes known to participate to long term potentiation, a phenomenon underlying synaptic plasticity and memory.

In Chapter 2, we identify the main characteristics of a switch model by surveying the history of models in the literature. This survey shows how the switch concept is coupled to the mathematical concept of bistabitlity but also how it evolved from a static input-output relationship to a dynamical process. Through the multiplicity of examples, we try to convince the reader, that the concept of switch is a dominant concept of systems biology.

Based on this analysis, we propose, in Chapter 3, a definition of performance and robustness for biological bistable switches and review the advantages and limitations of existing methods to quantify these measures. Our analysis reveals a paradox. The switch is a non local phenomenon describing a transition between two stable steady-states. Yet, the theoretical methods from control theory are generally local relying on the linearization of the system around a particular stable steady-sate. To cope with this problem, most of studies of performance and robustness of biological models are based on extensive numerical simulations. However, results from these simulations are often difficult to interpret in terms of biology.

The study of planar bistable models in Chapter 4 identifies the key rulers of the switch in the state space and sheds light on the interplay between the system dynamics and properties of these local rulers. The saddle point is central to the decision-making in the phase portrait like a mountain pass connecting two valleys. A local analysis at this point is proposed to quantify the switch performance and robustness. In this chapter, we furthermore emphasize the role played by bifurcations such as saddle-node bifurcations in the decision-making process. In chapter 5, we extend our analysis to high-dimensional models.

Chapter 6 illustrates the power of the proposed analysis by studying the performance and robustness of two cellular decision-making processes, the apoptotic process and long term potentiation, in high-dimensional models of the literature. We identify the saddle point in all these models and perform a local analysis at this point. We compare our results with results from non local methods such as numerical simulations and diagrams of bifurcation. Results suggest that theoretical concepts illustrated on toy conceptual models in the previous chapters do generalize with high predictive value to high-dimensional models.

Chapter 7 introduces singularities, in particular hysteresis singularities and cusp. These singularity organize bistability in both the state and the parameter spaces.

In chapter 8, we study the problem of the first spike latency in neuronal models. Based on the concepts developed in the previous chapters, we

show how this property is naturally connected to the concept of bistability and we stress the interplay between the first spike latency and a particular type of excitability called regenerative excitability.

Trough all the dissertation, we illustrate our argumentation with various models and biological experiments of the literature and try to convince the reader that same principles are shared across various biological processes.

Publications

The material of Chapter 4 to 6 has been partly published in:

Laura Trotta, Eric Bullinger and Rodolphe Sepulchre, Global analysis of dynamical decision-making models through local computation around the hidden saddle, *Plos ONE*, 7(3), 2012.

Laura Trotta, Rodolphe Sepulchre and Eric Bullinger. Delayed decision making in bistable models. *In Proceedings of the 49th IEEE Conference on Decision and Control*, pp 816-821, Atlanta (USA), December 2010.

The material of Chapter 8 has been presented in:

Laura Trotta, Alessio Franci and Rodolphe Sepulchre. First spike latency sensitivity of spiking neuron models. *Twenty second annual computational neuroscience meeting : CNS 2013*, 14, P354, Paris (France), July 2013. (Poster)

It is the topic of an article in preparation:

Laura Trotta, Alessio Franci and Rodolphe Sepulchre. Slow regenerative ion channels regulate first-spike latency in neuronal spiking, *unpublished manuscript*.

Contents

<div style="text-align: right">

Chapter 1

</div>

Three examples of decision-making processes in cellular biology

Three cellular phenomena lie at the heart of this disseration, apoptosis, the controlled cell death, the first spike latency, a signaling phenomenon underlying neuronal excitability and long-term potentiation, a mechanism involved in synaptic plasticity. All these three phenomena involve a decision-making process: to die or not to die in apoptosis, to spike or not to spike in first spike latency, to remember or to forget in long term potentiation. This chapter briefly introduces these phenomena and the main issues related to the modeling of these complex processes.

1.1 Apoptosis, the controlled cell death

Apoptosis, the predominant form of programmed cell death, is used by multicellular organisms to remove superfluous, damaged or potentially harmful cells (Elmore, 2007; Green and Evan, 2002). In response to pro-apoptotic signals such as radiation, nutrient deprivation or oxidative stress, the cell triggers a biochemical signaling cascade which leads to its own destruction. This cellular suicide, highly regulated and controlled, is involved in several physiological functions including morphogenesis, regulation of the immune system and early-stage embryonic development (Jacobson et al., 1997; Nijhawan et al., 2000; Opferman and Korsmeyer, 2003). Failure in the apoptotic process is associated with severe diseases including cancers and neurodegenerative diseases such as Parkinson's and Alzheimer's diseases (Lowe and Lin, 2000; Thompson, 1995). Anti-cancer drugs have been shown to induce apoptosis in tu-

<div style="text-align: center">

1

</div>

mor cells revealing the therapeutic potential of controlling the apoptotic pathway (Fulda and Debatin, 2006; Lowe and Lin, 2000). However, the design of these new drugs requires a fine and quantitative understanding of the apoptotic process which is still lacking. Whereas, most of the regulators of the apoptotic pathways have been identified, understanding how their complex interactions leads to a robust binary life-death process is still challenging (Elmore, 2007). The current description is still largely qualitative and descriptive and there is an increasing need for quantitative measures and models.

In the last decade, the need for a quantitative description of the physiological pathways of apoptosis has motivated the development of new mathematical models, see Huber et al. (2009) for a review of apoptotic signaling models. These models are built on several mathematical formalisms including ordinary differential equations (ODEs), boolean networks, partial derivative equations (PDEs) and stochastic differential equations (SDEs). Among these formalisms, ODE's models have been the most popular (Albeck et al., 2008; Bagci et al., 2006; Chen et al., 2007; Cui et al., 2008; Eissing et al., 2004; Fussenegger et al., 2000; Legewie et al., 2006). In an ODE model, a state variable is associated to the concentration of each key biochemical enzyme or protein. Therefore, the dimension of the model is fixed by the number of regulators included in the physiological description. The dynamics of each variable are then determined by the kinetic laws which govern the interactions of this enzyme with the other regulators of the system.

The first model of apoptosis was developed in 2000 (Fussenegger et al., 2000). At that time, the development of new experimental procedures such as fluorescent reporters imaging techniques shed light on the dynamics of the apoptotic process at the level of a single cell. In particular, these experiments permitted to follow the dynamics of key regulators of apoptosis called effector caspases (Rehm et al., 2002; Tyas et al., 2000). Effectors caspases are particular proteases whose activation is recognised as a hallmark of the cellular death (Wolf and Green, 1999). Once fully activated, these effectors trigger the ensemble of cellular mechanisms leading to the cellular death. Experiments at the single cell level showed that the activation of the effector caspases is a fast all-or-none phenomenon (Rehm et al., 2002; Tyas et al., 2000), see Figure 1.1. In

each cell, the concentration of effector caspases rises sharply and suddenly in a switch-like manner after the application of a sufficiently strong pro-apoptotic signal. This all-or-none activation at the single cell level contrasts with the response of a population of cells presenting a graded increase in the concentration of effector caspases (Hentze et al., 2002; Scaffidi et al., 1998). Since that time, the idea that a switch governs the apoptotic process at the single cell level has been at the core of the development of new mathematical models. The goal of these models is to identify how the switch from life to death might arise from the complex interactions between the key biochemical effectors of apoptosis and how this switch could be possibly controlled.
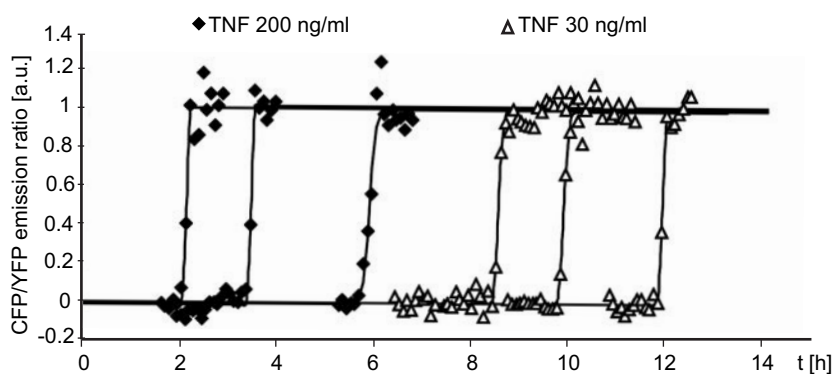
Figure 1.1: Experimental recording of effector caspases activation. Figure from Rehm et al. (2002).

Mathematical modeling has attributed the switch in apoptosis to various physiological mechanisms (Albeck et al., 2008; Bagci et al., 2006; Chen et al., 2007; Eissing et al., 2004; Legewie et al., 2006). Current models of apoptosis try to get a finer description of the process by incorporating more and more physiological details. Mathematically, further details translate into further states and parameters in the model (Bentele et al., 2004; Schliemann et al., 2011). As the number and complexity of biological models increases, there is a need for methods to quantify the performance and robustness of these models.

1.2   First spike latency in single neurons

Neurons are excitable cells that transmit and process information. In neural coding theory (Borst and Theunissen, 1999; Koch, 1999), it is assumed that this information is encoded in the pattern of action potentials generated by a single or a collection of neurons in response to specific stimuli. Several neuronal codes have been proposed including rate codes where the information is encoded by the rate at which the neuron fires action potentials and spikes timing codes which depend on the precise timing of spikes (Maass and Bishop, 1999; Rieke, 1997; Thorpe et al., 2001). First spike latency coding is one of these spike timing codes where information is presumably encoded by the latency preceding the first action potential of a neuron subjected to a sufficiently strong stimulus (Fgure 1.2). Recent studies have shown that first latency could code for stimulus recognition in several sensory systems (Chase and Young, 2007; Gollisch and Meister, 2008; Johansson and Birznieks, 2004; Storchi et al., 2012; Zohar et al., 2011). However, physiologically, mechanisms that allow neurons to implement this code reliably are still unclear.
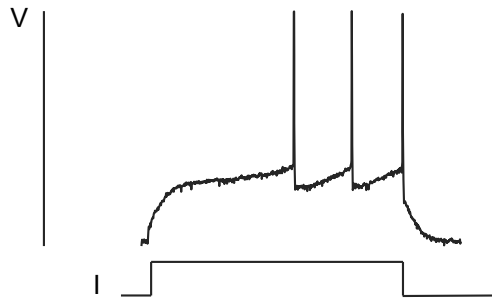
Figure 1.2: Schematic representation of a first spike latency recording.

Each neuron possesses a cellular membrane separating its cytoplasm from the extracellular medium (Figure 1.3). Because of the selective permeability of this membrane to ions and the active transport of ions by cellular pumps, there is a gradient of ion concentrations across the membrane (Hille, 1984; Keener and Sneyd, 2009). When the neuronal membrane is depolarized, following an incoming electrical signal, voltage-dependent ion channels of the membrane can open or close, thereby

modifying the permeability of the membrane to these ions. Ions flow through the membrane driven by their electrochemical gradient. This flow of ions modifies the intracellular potential resulting in a sudden rise and fall of the voltage called action potential. Conductance-based models of neurons describe the variations observed in the difference of potential (neuron voltage) resulting from this (in)activation of ion channels following the application of some external current. They typically model a neuron as an electrical circuit including a capacitor, the neuron membrane, in parallel with resistors, the ion channels (Figure 1.4). In electrophysiology, it is common to use conductances instead of resistors. These conductances can be variable reflecting the fact that (in)activation of some ion channels are time and voltage dependent. The size of the model depends on the number of ion channels incorporated in the system. Due to the zoo of ion channels which have been shown to regulate neuronal excitability (Hille, 1984), the size of conductance-based models can be particularly large. How can we identify currents which give rise to a specific mechanism such as the first spike latency in these models? How can we estimate the robustness of the proposed models? Are these models capturing true physiological properties or just reflecting the fine-tuning of some parameters?
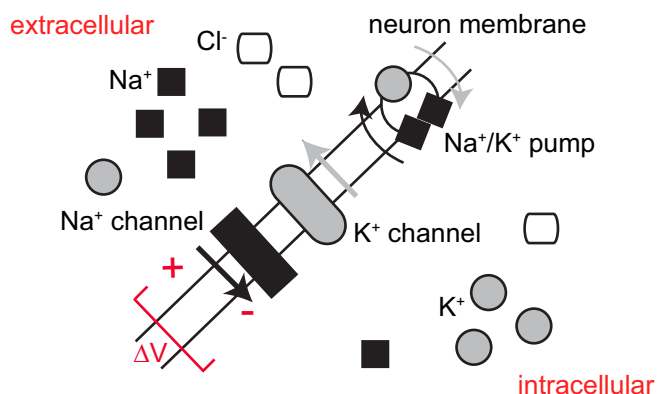
Figure 1.3: Neuron membrane potential resulting from the selectivity of the neuron membrane to ion channels.
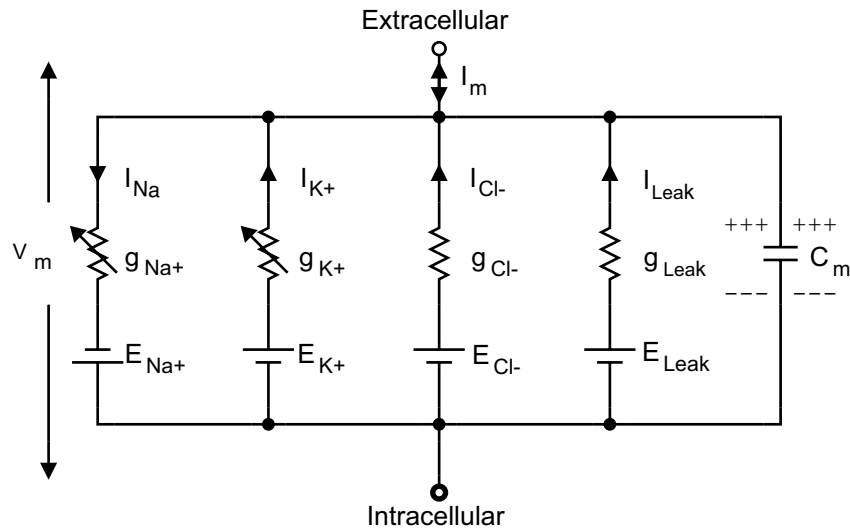
Figure 1.4: Neuron as a RC circuit. The neuron membrane is a capacitor. Each ion channel has a specific (voltage-dependent) conductance.

1.3   Long term potentiation and synaptic plasticity

Our last illustration is a decision-making process involved in memory formation, called long term potentiation. In the brain, it is assumed that long-term information storage is achieved through changes in synaptic efficiency. An electrical signal at the postsynaptic membrane translates into chemical signals which in turn trigger mechanisms to generate an increase in the synaptic strength (Bliss and Collingridge, 1993). Long term potentiation (LTP) describes the longlasting increase in synaptic strength described in learning and memory processes (Frey and Morris, 1997). When submitted to weak stimuli, an early-phase of long term potentiation is triggered which lasts for 2-4h, while when submitted to strong stimuli, a late phase of long term potentiation (L-LTP) is triggered which lasts much longer (Frey et al., 1988). Several studies have proposed that long-term memory could be accomplished trough a molecular bistable switch (Aslam et al., 2009; Lisman and Zhabotinsky, 2001; Miller et al., 2005). In particular, Aslam et al. proposed a model of late LTP in agreement with experimental data where long term potentiation is achieved thanks to the autophosphorylation of the kinase α-CaMKII,

an enzyme regulated by calcium (Aslam et al., 2009).The importance of the model lies in its ability to reproduce experimental results, in particular to account for the different effects of applying inhibitors during the induction or the maintenance phase of L-LTP: if applied during the induction of L-LTP, protein synthesis inhibitors can block L-LTP but they do not reverse the potentiation when applied during the maintenance phase of L-LTP (Fonseca et al., 2006; Frey and Morris, 1997). Moreover blocking the αCaMKII activity stops the L-LTP induction phase but not the maintenance phasz (Malinow et al., 1989; Otmakhov et al., 2004) (Figure 1.5). The reversibility of the switch in the αCaMKII activity, associated with memory formation, depends on the time of application of the reversing stimulus.

1.4   Conclusion

In this chapter, we introduced three cellular decisions which illustrate current research in systems biology and neuroscience. While in all these phenomena, the key regulators of the process have been identified, it is still unclear how to relate the molecular interactions to a robust signaling function. Mathematical modeling is viewed as a tool to answer these questions. Because these models try to include a precise physiological description of the phenomenon, they are often high-dimensional and nonlinear. Therefore, understanding which parameters and state governs the dynamical phenomena of interest in these complex models is challenging. In this thesis, we will try to show that, because these three nonlinear phenomena are of the same nature, a switch between two stable attractors, they can be studied using the same mathematical framework. We will propose some mathematical tools to study these phenomena and apply them on several models of the literature. Our analysis relies on several concepts including the notions of biological switch and bistability, introduced in Chapter 2 and the concepts of performance and robustness of biological systems, discussed in Chapter 3.
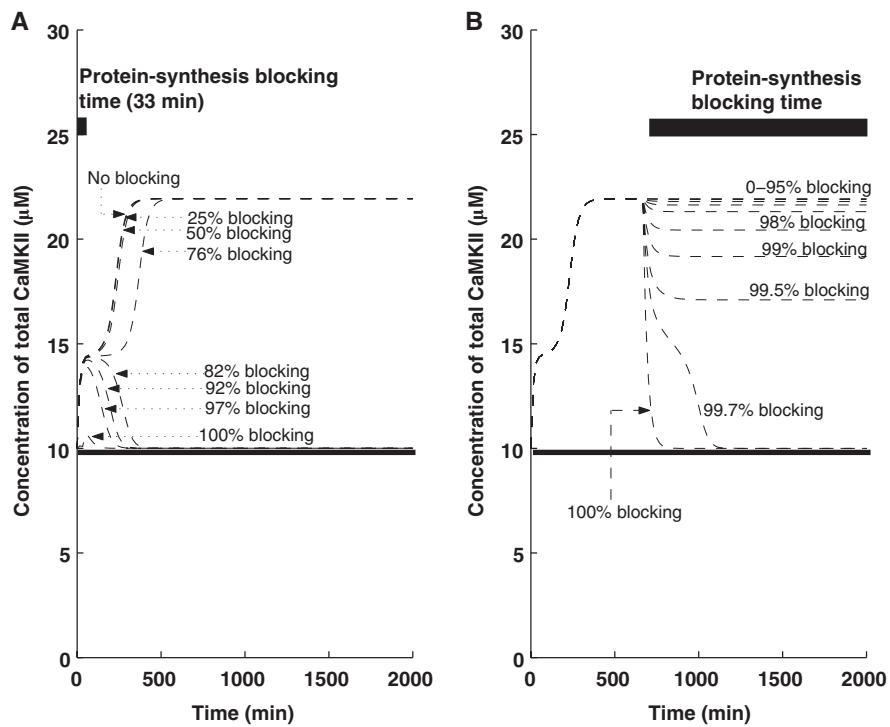
Figure 1.5: Reversibility of a bistable switch in a model of long-term potentiation proposed by Aslam et al. (2009). The reversibility is achieved by blocking the protein synthesis in the early phase while the switch is difficult to reverse when blocking the protein synthesis in the late phase. Figure from Aslam et al. (2009).

Mathematical models of biological switches: a historical perspective

By presenting experimental advances from early developments in chemistry to recent findings in new disciplines including systems biology and synthetic biology, we highlight the main characteristics of a biological switch. Through this chronological description, we attempt to formulate a switch definition. As the concept of switch is closely related to mathematical modeling, mathematical concepts relevant for the modeling of biological switches are introduced in parallel.

2.1 Preliminaries: kinetics laws and enzymatic regulation

Kinetics laws govern the interactions among species in chemical and enzymatic reaction networks. An introduction to chemical kinetics can be found in any text book on mathematical modeling in biology including Keener and Sneyd (2009).

The law of mass action

A chemical reaction between two reactants A and B interacting to produce the product C, is graphically modeled by:

$$A + B \rightarrow C$$

In this chapter, we denote the concentrations by lower case letters. The derivatives with respect to time are denoted by a dot. The rate of accumulation of the product, $\dot{c}$, is the rate of the reaction. The law

of mass action predicts that the rate of the reaction is proportional to the product of the concentrations of reactants. This law is a model based on the hypothesis that the rate of reaction is proportional to the number of collisions between the two reactants per unit of time. The number of collisions is assumed to be proportional to the product of the concentrations of the two reactants A and B,

$$\dot{c} = kab$$

with a and b, the concentrations of the reactants and c, the product concentration. The factor k depends on the temperature of the mixture and on the geometry of the reactants.

Michaelis-Menten kinetics

In biological processes, most of the chemical reactions are catalyzed by enzymes. Enzymes speed up the chemical reaction by decreasing the energy of activation of the reaction. An enzyme E links to a substrate S, forming the complex C. This complex is necessary for the production of the product P.

$$S + E \underset{k_2}{\overset{k_1}{\rightleftarrows}} C \overset{k_3}{\rightarrow} P + E$$
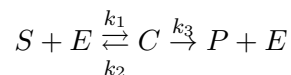
Applying the mass action law to these reactions leads to the system of equations,

$$
\begin{aligned}
\dot{s} &= -k_1 se + k_2 c \\
\dot{e} &= -k_1 se + k_2 c + k_3 c \\
\dot{c} &= k_1 se - k_2 c - k_3 c \\
\dot{p} &= k_3 c
\end{aligned}
$$

As the enzyme is not consumed during the reaction, we can write an equation of conservation:

$$(\dot{c + e}) = 0 \Leftrightarrow e = e_0 - c$$

and the system can be reduced to a three-dimensional model:

$$
\begin{aligned}
\dot{s} &= -k_1 s(e_0 - c) + k_2 c \\
\dot{c} &= k_1 s(e_0 - c) - (k_2 + k_3)c = k_1 \left[se_0 - (K_m + s)c \right] \\
\dot{p} &= k_3 c
\end{aligned}
$$

with $K_m = \dfrac{k_2 + k_3}{k_1}$.

The relation of Michaelis-Menten is based on *the quasi-steady state approximation.* The hypothesis is that the complex c is instantaneously at equilibrium. This means that after a fast transient, the complex stays constant:

$$\dot{c} = 0$$

It follows than c can be expressed as a function of s,

$$c = \frac{se_0}{K_m + s}$$

and

$$\dot{p} = k_3 c = \frac{V_{max}s}{K_m + s}, \quad \text{where } V_{max} = k_3 e_0$$

The relation between the substrate concentration and the rate of the reaction is nonlinear. While for small concentrations of substrate, the relation is linear, there is a saturation effect for high concentrations of the substrate.

Hill kinetics and the sigmoid input-output relation curve

At the beginning of the 20th century, a particular interest was paid to hemoglobin, a protein contained in the red blood cells of vertebrates which carries oxygen from the respiratory system to the tissues of the whole organism (Hill, 1910; Pauling, 1935). The affinity of the oxygen for hemoglobin strongly depends on the pressure of oxygen. When the pressure is high as in the lungs, the affinity is large and oxygen binds to hemoglobin. In contrast, when the pressure is low, as in tissues burning nutrients to produce energy, the affinity is low and oxygen can dissociate from hemoglobin.

The experimental dissociation curve of oxygen to hemoglobin was presenting a sigmoid shape which could not be described in terms of mass action kinetics. However, this curve was well fitted by a simple relation proposed by Hill in 1910, (Hill, 1910),

$$y = \frac{x^n}{x^n + K^n}$$

with y the percentage of saturation of hemoglobin in oxygen and x the partial pressure of oxygen.

At that time, nothing was known about enzymatic regulation and scientists were facing serious troubles to provide a valid explanation for this experimental observation.

In the 1960's, major discoveries in the field of enzymatic regulation provided an explanation for the binding of oxygen to hemoglobin (Monod, 1966; Monod et al., 1963, 1965). The fixation of oxygen to hemoglobin was explained in term of a particular mechanism of regulation proposed by Jacob and Monod, called allosteric transition. Allostery is a mechanism of regulation where the fixation of a ligand to one binding site modifies the affinity of the ligand for another, distant binding site. Hemoglobin presents four binding sites called hemes. When the oxygen binds to one heme, a conformational change of the protein is assumed to increases the affinity of the oxygen for the hemoglobin (Changeux and Edelstein, 2005; Hsia, 1998). This is an example of positive cooperativity where the affinity for a binding site is enhanced by the fixation of a ligand to another binding site. There exist many models of enzymatic cooperativty (Dixon and Webb, 1979).

A simple model to represent cooperaitivty is to consider that n molecules of substrate must bind to the receptor for the reaction to occur. This model is a simplification because it is not realistic to assume that $n+1$ molecules meet simultaneously. The reaction scheme,

$$nS + E \underset{k_2}{\overset{k_1}{\rightleftarrows}} C \overset{k_3}{\rightarrow} P + E$$
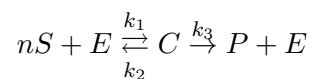
leads to the system,

$$
\begin{aligned}
\dot{s} &= nk_2c - nk_1s^n e \\
\dot{e} &= (k_2 + k_3)c - k_1s^n e \\
\dot{c} &= k_1s^n e - (k_2 + k_3)c \\
\dot{p} &= k_3c
\end{aligned}
$$
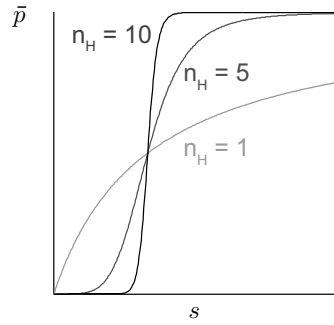
Figure 2.1: Ultrasensitive response resulting from a cooperative behavior described by a Hill kinetics. As the Hill factor n_H increases, the sigmoidal relation between the substrate concentration and the product concentration at steady-state becomes steeper.

By assuming a quasi steady-state approximation and assuming the enzyme concentration is small with respect to the concentration of substrate, we get,

$$\dot{p} = k_3 c = \frac{V_{max} s^n}{K_m + s^n}$$

The Hill equation is generally used when a cooperative behavior is suspected to describe the rate of reaction but intermediate steps are not necessarily well understood or known. If we assume that the product is degraded at a rate k_4, we get at equilibrium:

$$\dot{p} = k_3 \bar{c} - k_4 \bar{p} = 0 \Leftrightarrow \bar{p} = \frac{1}{k_4} \frac{V_{max} s^n}{K_m + s^n}$$

The relation between the substrate and the product concentration is sigmoidal (Figure 2.1). The steepness of the sigmoid depends on the Hill coefficient n. For small concentrations in the substrate, we observe very small quantities of the product. If we increase this concentration, the rate of production remains small until reaching some kind of threshold in the concentration of substrate. For concentrations above this threshold, the rate of production is almost instantaneously maximal, leading to a sudden and sharp increase in the product concentration. A behavior characterized by a sigmoidal input-output response curve is called *ultrasensitive*.

Besides cooperativity, several others mechanisms of enzymatic regulation can lead to an ultrasensitive behavior including zero-order ultrasensitivy and multi-step phosphorylation reactions (Goldbeter and Koshland, 1984).

Example 2.1.1. Zero-order ultrasensitivty is achieved by two converters enzymes, E_1 and E_2 operating close to stauration, i.e in the zero-order kinetic region of the Michalis-Menten kinetics. These two enzymes act in opposite direction on the same protein W whose total quantity is conserved.

$$W + E_1 \underset{d_1}{\overset{a_1}{\rightleftarrows}} WE_1 \overset{k_1}{\rightarrow} W^* + E_1$$

$$W^* + E_2 \underset{d_2}{\overset{a_2}{\rightleftarrows}} W^*E_2 \overset{k_2}{\rightarrow} W + E_2$$
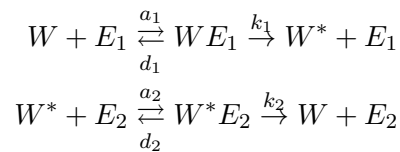
with the concentration of the protein, a conserved quantity $w_T = w + we_1 + w^*e_2 + w^*$. At steady-state, the fraction of activated protein $\dfrac{w^*}{w^T} = f(\dfrac{v_1}{v_2}, \dfrac{K_{m_1}}{w_T}, \dfrac{K_{m_2}}{w_T})$, with $v_1 = k_1 e_{1T}, v_2 = k_2 e_{2T}$. When the 2 enzymes, E_1 and E_2 work close to saturation, i.e $K_{m1}, K_{m2} << 1$, the function f is a sigmoid function of the ratio $\dfrac{v_1}{v_2} = \dfrac{k_1 e_{1T}}{k_2 e_{2T}}$. If we assume that the enzyme E_1 is activated by an input effector S, for instance by a simple Michaelian mechanism, we get that the fraction of activated protein $\dfrac{w^*}{w^T}$, is a Hill-function of the input signal s.

The Hill equation is a sigmoid input-output relation curve. For small input signals, the system exhibits very small responses. However, when the signal s reaches a particular threshold s^*, the system becomes fully activated and the response increases sharply. The response is therefore *switch-like*. We will call mechanisms presenting an ultrasensitive response as *switch-like responses* while the term of *switch* will be devoted to the concept introduce in the next section. We will see later that the concept of biological switch and the concept of ultrasensitive response are tightly coupled.

2.2 Emergence of the switch concept

In 1965, Jacques Monod, André Lwoff and Francois Jacob were awarded the Nobel prize of Physiology or Medicine for their work on genetic reg-
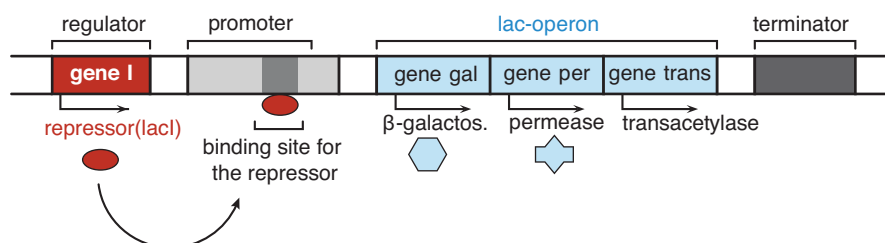
Figure 2.2: Lac operon in E. coli.

ulation (Jacob and Monod, 1961). One of their major discoveries is the concept of operon. An operon is a set of genes corresponding to a single transcriptional unit, see Figure 2.2. An operon corresponds to a DNA unit including a promoter, an operator, a set of structural genes and a terminator. The transcription of structural genes into mRNA is initiated when a specific enzyme called RNA-polymerase binds to the promoter region. An operon can be regulated by specific proteins called activators and repressors trough specific mechanisms of regulation called induction and repression which control the transcription of the gene.

The Lac operon is generally considered as one of the first example of a biological switch (Figure 2.2). The lac operon consists in a set of three genes coding for the metabolism and uptake of lactose and other sugars in intestinal bacteria such as Escherichia Coli (Jacob and Monod, 1961; Müller-Hill, 1996; Ozbudak et al., 2004). This set of genes encodes an enzyme called β-galactosidase which allows for the effective digestion of lactose. Novick and Wiener showed experimentally that the induction of β-galactosidase by a specific inducer called TGM is an all or none phenomenon (Novick and Weiner, 1957). Under high concentrations of TGM, the β-galactosidase is produced at maximum rate almost instantaneously. However, at low concentrations of inducers, the rate of enzyme synthesis per bacteria increases linearly. Novick and Wiener showed that the population of bacteria consist in bacteria which can be either fully induced or not induced at all. When submitted to low concentrations of inducers, all the bacteria are not fully activated simultaneously. As the fraction of fully induced cells in the population increases, the rate of synthesis increases linearly. The all-or-none enzyme induction at the scale

of a single bacteria can be considered as one of the first examples of a biological switch (Laurent and Kellershohn, 1999; Ozbudak et al., 2004).

In 1968, Griffith studied in a theoretical work mechanisms of gene induction. In particular, he studied a mechanism of induction of a gene by the protein for which it codes.

Example 2.2.1. Posititve feedback to one gene. In this model, the mRNA (RNA messenger), M codes for the protein E. This enzyme E acts as an inducer of the gene and therefore produces a positive feedback on M.

$$\dot{m} = -\alpha m + \frac{e^m}{K + e^m} \tag{2.1}$$

$$\dot{e} = -\beta e + m \tag{2.2}$$

The theoretical analysis of Griffith showed that the self-induction proposed by Monod and Jacob where an enzyme induces the production of the gene that codes for this particular enzyme, leads to ' sufficient stability in the two states required (Griffith, 1968)' only if the induction is a cooperative mechanism with $m \geq 2$, (Griffith, 1968).

In dynamical systems theory, the behavior described by Griffith is called bistability. The system presents two stable equilibria, an inactivated state corresponding to low concentrations of M and E (the gene is not induced) and an activated state where both concentrations are high (the gene is fully induced). The stability of both states requires that the inducing mechanism or positive feedback is described by a Hill equation, i.e an ultrasentitive mechanism.

In the 1990's, ultrasensitivity was discovered in cell signaling systems (Ferrell, 1996). In signalling cascade, ultrasensitive mechanisms allow to convert a graded signal, typically a concentration into a switch-like response. By adding a positive feedback loop to the cascade, the switch becomes bistable and or-all-none (Ferrell and Machleder, 1998). As for the model of Griffith, the combination of an ultrasensitive mechanism and of a positive feedback loop leads to bistability.

Experimentally it is not always possible to distinguish between an ultrasensitive response and a bistable switch (Sha et al., 2003), see Figure
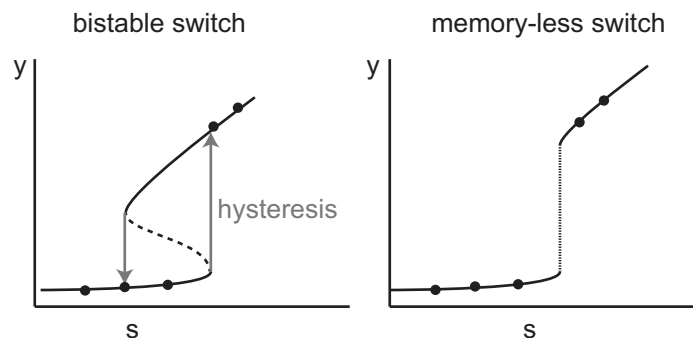
Figure 2.3: Comparison of a bistable and an ultrasensitive, memory-less, switch like, response. The black dots represent experimental observations. The bistable system presents two branches of stable equilibria (black lines) and a branch of unstable equilibria (black-dashed line). For the same value of the signal s, the system can be in two distinct operating conditions, i.e the system shows hysteresis. Conversely, the ultrasensitive, switch-like, system only presents one stable equilibrium for each signal input. This figure has been inspired by Sha et al. (2003)

2.3. Discontinuity in the sigmoidal stimulus-response curve may be due to either a bistable process or a very steep ultrasensitive mechanism. One way to distinguish between these two mechanisms is by testing a defining property of bistable systems, hysteresis. A system presents hysteresis when the stimulus threshold needed to trigger a transition from the rest to the excited state differs from the threshold needed to trigger the opposite transition from the excited state from the resting state. Evidence for hysteresis was demonstrated experimentally in the cell cycle (Pomerening et al., 2003; Sha et al., 2003; Thron, 1997). Systems with hysteresis have memory because once the transition from the rest state to the excited state as been initiated, the system remains in the high state even if the stimulus is decreased below the low-to-high state threshold.

2.3 Modern developments

Thanks to the development of new techniques in biology such as cloning or genome sequencing but also the development of computer-assisted

computation, new disciplines such as synthetic biology and systems biology have emerged at the beginning of the 21th century.

Synthetic biology is the engineering of new biological processes trough the practical implementation of theoretical design concepts (Serrano, 2007). In 2000, Gardner et al. engineered a synthetic bistable switch in the bacteria E. Coli (Gardner et al., 2000). The switch was designed as a mutually inhibitory network between two repressible promoters. This experiment demonstrated the practical implementation of modules with functions predicted by the theory such as memory. The experiment of Gardner et al. (2000) also shed light on one important issue for the design of robust switches, the stochastic nature of gene expression. In the E Coli toggle switch, natural fluctuations in the gene expression blur the switching threshold resulting in a transient bimodal distribution of cell responses for concentration of inducers close to this threshold (Figure 2.4). Relation between (transient) bimodality in a cell population and stochasticity was further discussed in Ozbudak et al. (2004) and more recently in Robert et al. (2010) where it was shown that other factors such as epignetic inheritance could also be involved in this mechanism. Bimodal cellular phenomena require single-cell method analysis and can not be captured by average models on a cell population. For these systems, a stochastic approach is needed (Ullah and Wolkenhauer, 2010).

Another concept discussed in Gardner et al. (2000) is reversibility. In response to transient inputs, the system can be reversed in a long-term scale. Encouraged by the success of the experiment of Gardner, other teams have proved the practical implementation of switches (Kramer et al., 2004; Palani and Sarkar, 2011). These new experiments try to reproduce switches with some design specifications such as reversibility. Originally applied to small modules, synthetic biology is currently trying to engineer complex multicellular systems (Basu et al., 2005; Kobayashi et al., 2004). Interfacing several modules to create a system performing nontrivial dynamical behavior is particularly challenging. Challenging issues include the problem of handling noise, formulating effective bioengineering design principles, developing computational tools to study large-scale models and developing programming abstractions which allow to capture the essential features of the system without including complex details (Purnick and Weiss, 2009).
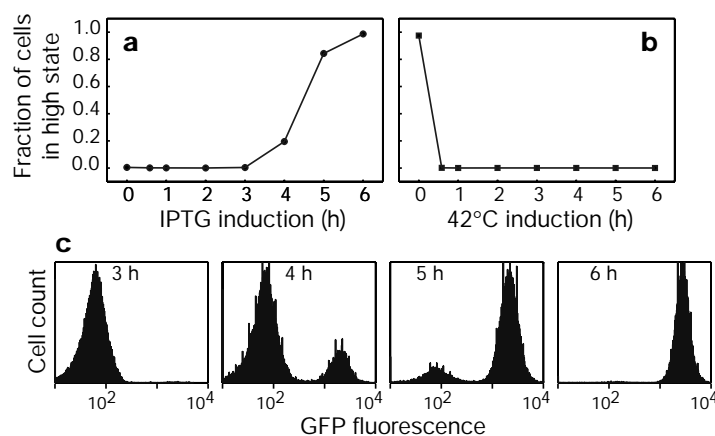
Figure 2.4: Bimodal distribution of cell responses in the experiment of Gardner et al. (2000). Figure from Gardner et al. (2000).

Systems biology aims at understanding the interactions between the components of complex biological processes (Alon, 2006; Chuang et al., 2010; Kitano, 2002). Methods used in systems biology are various including both top-down and bottom-up approaches (Bruggeman and Westerhoff, 2007). Among all the possible methods and formalisms, models based on ordinary differential equations (ODE) have been applied to the analysis of several biological switches (Kotaleski and Blackwell, 2010; Yao et al., 2011; Zi et al., 2011). As illustrated for apoptosis in Chapter 1, a general tendency in systems biology is to build high-dimensional models in order to get a fine description of the system's physiology. Models of apoptosis (Albeck et al., 2008; Chen et al., 2007; Legewie et al., 2006; Schliemann et al., 2011) can include up to 58 states which is a high-dimension with respect to the classical analyses tools of nonlinear dynamical systems. As a consequence, analysis of these models is often based on extensive numerical simulations. Which kind of biological information can be extracted from the analysis of these systems? What are the parameters which the most affect the system behavior? Rigorous means are required to link models to experimental data and understand which aspects of a model are supported by data (Spencer and Sorger, 2011).

2.4   From cellular to population models

One of the main challenges in current biology is to bridge the gap between the single cellular level and the large-scale multi-cellular network level (Purnick and Weiss, 2009). We briefly discuss challenges encountered when trying to switch from the single cell level to multicellular models.

Biological systems are subjected to various sources of heterogeneity (Balázsi et al., 2011; Hilfinger and Paulsson, 2011; Raj and van Oudenaarden, 2008; Sanchez et al., 2013). Several methods can be used to study heterogeneous systems. One possible approach is cell ensemble modeling. In this approach, some given kinetic parameters such as expression rates are drawn from a given statistical distribution for each cell in the population (Henson, 2003). The system is simulated for a large number of cells differing slightly in their parameters and results are derived from these numerical simulations. Cell ensemble modeling has been applied to the study of apoptosis (Schliemann et al., 2011) revealing that heterogeneity reduces sensitivity to tumor necrosis factor (TNF) stimuli.

Intrinsic noise seems to play a critical role in cellular decision-making processes (Balázsi et al., 2011). If we assume that heterogeneity at the macroscopic scale arises from intrinsic noise at the microscopic scale such as protein interactions, several mathematical formalisms can be used depending on the nature of the physical assumption characterizing interactions among species (Gillespie, 1976). A short review of stochastic methods and simulations will be presented in Chapter 3.

At the scale of population of individuals, such as a population of neurons or an insect colony, bistable models have been successfully used to represent a collective decision-making process (Hopfield, 1982; Seeley et al., 2012; Usher and McClelland, 2001; Wilson and Cowan, 1972). The theoretical works of Wilson and Cowan (1972) and Hopfield (1982) show how hysteresis and memory can arise from collective interactions among excitatory units. More recently, the leaky-competing accumulator model has been proposed to represent the decision-making process between subpopulations of neurons inhibiting each other. In its two dimensional

nonlinear form, this stochastich system exhibits biomdality (Usher and McClelland, 2001). In Seeley et al. (2012), a colony of honeybees has to choose between two alternative nest sites. Each honeybee or agent is represented as a single microscopic unit which can interact stochastically with other single units. Provided that the number of single units is not too small, the macroscopic behavior is drawn by using averaging techniques. At the population level, the decision-making process is well described by a two-dimensional bistable model where the variables represent the fraction of honeybees committing to each decision.

2.5 Conclusions

The switch is a concept which has been used from the early development in biochemistry to modern developments in systems and synthetic biology. Initially, the switch was associated to a nonlinear static input-output response curve between the stimulus and the response of the system. A distinction can be made between switch-like, memory-less switches and bistable switches. Memory-less switches present an ultrasensitive behavior, i.e they present a continuous sigmoidal input-output relation curve which is well described by a Hill function. This ultrasensitive behavior is achieved through different mechanisms of regulation including cooperativity and zero-order ultrasensitivity. By adding a positive feedback loop to an ultrasensitive mechanism, it is possible to build a bistable switch. Bistable switches present two stable steady-states for a particular set of experimental conditions. Their input-output relation curve is discontinuous, i.e the system shows hysteresis and memory. Their activation is all-or-none, i.e they present an activation threshold.

With the development of new experimental technologies allowing the study of the dynamics of concentrations at the single cell level, the concept of switch evolved towards a dynamical concept. Questions such as reversibility by transient signals or latencies prior to switch where shown to be important for the control of several physiological processes. Some of these properties were used as design principles to build new synthetic switches. Because, new models try to incorporate more physiological details, their dimension can be particularly large. As a result, system questions are generally addressed by means of numerical simulations.

Bistable models have been used to describe decision-making processes at the molecular, cellular and population scale. Bridging the gap between these scales would require to deal with heterogeneity and multi-scale systems. Modeling a biological system is a matter of scale and of finding the good level of representation to capture the essential characteristics of the phenomenon under investigation. Yet, fundamental phenomena such as bistability seem to be conserved across scales and systems.

Chapter 3

Performance and robustness of bistable switches

This chapter introduces the concepts of performance and robustness of biological switches. First, we review the general considerations which need to be taken into account when trying to define the robustness and performance of a biological system. Based on these general considerations and the analysis of Chapter 2, we identify performance criteria for biological switches. Finally, we present a short survey of the methods that have been used to quantify the performance and robustness of biological bistable switches. We try to identify the advantages and limitations of each method in the light of our previous analysis.

3.1   Performance and robustness of biological systems

Chapter 2 illustrated how the complexity of biological models rapidly increases when a certain level of physiological description is incorporated in the model. The goal of systems biology is not only to provide models for numerical simulations but also to identify the functional principles ruling the behavior of biological processes. A major issue in systems biology is to understand how complex biological systems can implement a function robustly. The formulation of a definition of robustness for biological systems is a challenging issue which has recently received a particular attention (Kitano, 2004, 2007; Stelling et al., 2004b). Classical approaches such as methods from control theory face serious challenges when dealing with biological systems. Failure of classical approaches is not only due to the complexity of models which results from the inherent nonlinear and possible stochastic nature of biological phenomena under investigation. The nature of questions related to the study of biological

systems can also be quite different from the questions raised when engineering a new device. This section reviews the considerations which need to be taken into account when formulating these definitions. This review is mainly based on the work of Kitano (Kitano, 2004, 2007, 2010), a pioneer in the study of the robustness of biological models.

The robustness of a biological system is generally defined as its capacity to maintain its function against perturbations:

> 'robustness is a property that allows a system to maintain its functions against internal and external perturbations' (Kitano, 2004).

> 'robustness, the ability to maintain performance in the face of perturbations and uncertainty, is a long-recognized key property of living systems' (Stelling et al., 2004b).

With regard to the previous definitions, the robustness of a biological system is defined with respect to a given system, function and set of perturbations. The system may be defined at a scale ranging from the molecular level to the scale of an entire organism or population. The function typically corresponds to a physiological function that the organism needs to perform under normal physiological conditions. The characteristics of the physiological process dictate the performance criteria that the model should satisfy. Obviously, this definition implies that the system has a given and well-characterized function. In practice, this function may be unknown. In addition, a biological system generally present several functions and could be robust to one of them while presenting high fragility with respect to another one.

The set of perturbations is very broad in biology. These perturbations are due to a fluctuating external environment but also to internal perturbations (Hilfinger and Paulsson, 2011; Swain et al., 2002). Among others, internal perturbations include molecular noise resulting from the possible low copy number of molecules interacting in a biochemical reaction and intrinsic gene expression noise (Blake et al., 2003; Ozbudak et al., 2002; Sanchez et al., 2013) which has been shown to participate to cell to cell phenotypic variability. Identifying the system, the function and the set of perturbations are all three current research issues

revealing the complexity hidden in the seemingly simple definition of robustness proposed at the beginning of this paragraph.

One other major point raised by Kitano is that robustness is a concept which is too often confused with homeostasis or stability (Kitano, 2007). Homeostasis is the maintaining of physiological parameters which need to stay relatively constant. This is the set of mechanisms which allow the system to maintain steady-states in the organism (Cannon, 1932).

> 'Whereas homeostasis and stability are somewhat related concepts, robustness is a more general concept according to which a system is robust as long as it maintains functionality, even if it transits through a new steady state or if instability actually helps the system to cope with perturbations (...). Such transition between states is often observed in biological systems when facing stress conditions' (Kitano, 2007).

The concept of homeostasis is related to the capacity of a system to maintain a given state and not a given function. As illustrated in Chapter 1, the apoptotic switch from life to death is an important function of the system associated with a crucial decision. Failure in this process can lead to severe diseases emphasizing the importance of a precise regulation of this switching mechanism. A definition of apoptotic robustness only based on homeostatic regulation of the survival sate would certainly miss the true function of the apoptotic switch.

> 'A theory that takes into account multistability and evolution of unstable systems needs to be developed and new theoretical avenues need to be explored to provide a broad and unified account of robustness of biological systems' (Kitano, 2007).

Whereas some simple concepts inherited from control theory such as the trade-off between robustness and performance seems to have applications in biology, they warrant careful investigation (Kitano, 2010). For instance, robust control, a field dedicated to design of systems able to perform in presence of disturbances, could provide a framework for the study of biological robustness. However robust control generally assumes that there is a criterion to optimize. We already mention the difficulty

to define such kind of criteria for biological systems. Furthermore, assuming that a biological system is optimized is a hypothesis subject to discussion (Kitano, 2010). Another drawback of this approach is that these techniques generally rely on control theory which mainly focuses on stability and performance of monostable systems.

Biological systems deserve a specific theory which takes into account their heterogeneity and structural nature. There is still a gap to fill between the level of description used in thermodynamics and physical sciences and a description at the scale of networks of biological interactions. These considerations should motivate new advances in theories of dissipative systems in thermodynamics or in the field of nonlinear dynamical analysis and chaos (Kitano, 2007).

A proper definition of performance and robustness criteria for biological switches should cover all the aspects presented in this section. In this thesis, we will try to formulate a definition of robustness and performance of biological switches which is consistent with the previous considerations. In the next section, we identify performance criteria relevant for the analysis of biological switches. These criteria are motivated by the analysis presented in Chatper 2.

3.2 Definition of criteria for biological switches

In Systems Biology, the **system** typically corresponds to a subnetwork of enzyme and protein interactions which are supposed to give rise to the switch behavior. Performance criteria are motivated by the need to control these complex processes and design effective drugs. In the light of Chapter 2, we define the following criteria to study the performance of biological switches:

All-or-none sharp activation In models of biological switches, the fast, all-or none increase (or decrease) in one or several concentrations of the system is assumed to be a good indicator of the physiological process under investigation. In apoptosis, the switch typically corresponds to the fast nonlinear increase in activated effector caspases. The switch is a nonlocal phenomenon that can not be characterized in the vicinity of stable equilibria and does not correspond to homeostatic conditions.

Rather, bistable switches correspond to a sharp transition between two different stable steady-states corresponding to distinct physiological behaviors.

Switching threshold   Bistable switches present an activation threshold. This threshold is defined as the minimal input necessary to trigger the switch. This threshold depends on the type of input considered. Common inputs in biological models include transient, pulse-like inputs and constant step-like inputs. In apoptosis models, inputs have been used to represent an instantaneous increase in the initial concentration of pro-apoptotic effectors (Eissing et al., 2004; Schliemann et al., 2007). The contamination process in prion diseases that is responsible for progressive neurodegenerative disorders, has been simulated by a pulse of a pathogenic isoform of the prion protein (Kellershohn and Laurent, 2001). In experiments on the cell cycle, the input typically corresponds to an increase in the total concentration of cyclin, a quantity conserved in the system (Sha et al., 2003; Solomon et al., 1990; Tyson and Novak, 2008). Therefore, the input is similar to a step input corresponding to a sustained rise in one concentration of the system. In experiments on the lac-operon in E. coli, the bacterias are grown in a medium with different concentrations of inducers (Gardner et al., 2000) also corresponding to a constant input signal.

Hysteresis and memory   We showed in Chapter 2 that memory and hysteresis are a characteristic of bistable systems. As it will be recalled in the next chapter, a hysteresis occurs when the signal modifies the steady-states of the system. This situation is typically encountered for step inputs.

Latency and decision time   The example of apoptosis has highlighted a particular mechanism of latency at the single cell level. These latencies correspond to a period following the application of the stimulus and preceding the fast all-or-noe transition in the output concentration. Understanding the relation between stimulus strength and latencies is not only important for apoptosis. It is also particularly important for understanding the dynamics of infectious diseases. Indeed, this mechanisms as been shown to regulate long-term period of incubation in prion

propagation and progression towards Alzheimer's disease (De Caluwé and Dupont, 2013; Kellershohn and Laurent, 2001). In these systems, it is necessary to understand how the input, a concentration step or impulse, is related to the time necessary to trigger the switch. The first spike latency in neurons, presented in chapter 1, is an additional example of a switch where the latency plays a critical role. In this thesis, the decision time will refer to the time between the stimulus application and the sharp transition. A system will be said to present latencies, if it presents long transient following the application of the stimulus and preceding the switch.

Reversibility Some switches can be reversed by applying a signal to them. What is the type and strength of the input signal needed to reverse the switch? Are all switches reversible? What is the best time to apply the reversing signal? As illustrated in Chapter 1, reversibility is important for long term potentiation and synaptic plasticity.

Bimodality Bimodality is the property of some populations to exhibit two distinct responses for the same input. Bimodality occurs due to natural fluctuations in gene expression (Blake et al., 2003; Gardner et al., 2000). In a population of cells presenting (transient) bimodality, an all-or none switch at the single cell level is traduced in a graded signal at the population level when considering a global variable such as the total concentration in a particular enzyme (Cui et al., 2008; Gardner et al., 2000).

As mentioned in Chapter 2, the primary function of a bistable switch is to encode a binary decision. We should note that our performance criteria are related to general questions about binary decision-making processes. What is the minimum amount of an enzyme or a drug to trigger the decision-making process? Which factors control the decision time? Can we revert the decision taken by the system? In this dissertation, we particularly focus on dynamical properties of biological switches. The switch is not only a static input-output relation but primarily a dynamical system encoding a decision-making process.

3.3 Existing methods and limitations

In the previous section, we introduced some measures of performance for biological switches. In this section, we review the methods to quantify performance and robustness in biological sytems. We try to identify the main advantages but also the limitations of these methods with regard to the study of bistable switch models. The list of methods is not exhaustive.

3.3.1 Network motifs

One attempt to understand the complex interactions of biochemical networks is the identification of network motifs (Alon, 2006; Tyson and Novák, 2010; Tyson et al., 2003). Complex biochemical networks are decomposed into small networks motifs which are assumed to perform a particular function. Among popular motifs for switches, one can cite the one-way switch and the toggle switch proposed in systems biology (Tyson et al., 2003) and the excitatory-excitatory (E-E) and inhibitory-inhibitory (I-I) motifs proposed in neural networks (Hopfield, 1982; Wilson and Cowan, 1972). These four motifs are two-dimensional and encode a positive feedback loop either by mutual excitation or by mutual inhibition (Figure 3.1).
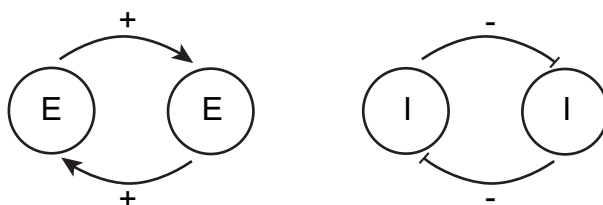
Figure 3.1: Positive feedback in two-dimensional networks motifs of bistability. The positive feedback loop results from mutual excitation (E-E) or mutual inhibition (I-I) between two units.

The method of motifs tries to identify key structural mechanisms leading to a biological function. This is an interesting approach for biological systems where interactions are generally represented by graphical models and qualitative relations. However, this method mainly works for

two or three dimensional models (Tyson and Novák, 2010). As the size of the system increases, it becomes difficult to identify networks which lead to a specific behavior. In addition, it is also difficult to estimate the robustness of the small motif when it is embedded in a larger network even if some features of biological networks can be used to simplify the picture including the separation of time-scales between different processes (Alon, 2007). Finally, these networks motifs only capture static properties of the switch.

3.3.2 Parametric robustness

Another important consideration is parametric robustness. Because heterogeneity is present in every biological system, it is assumed that a model should be robust to perturbations of its parameters. A variety of methods has been proposed to quantify the robustness of biochemical networks to parametric perturbations (Hafner et al., 2009; Ma and Iglesias, 2002; Shoemaker and Doyle, 2008; Stelling et al., 2004a). These methods include local and global methods.

Sensitivity analysis is a classical tool to quantify the parametric robustness (Turányi, 1990) that has been applied to various biological models including models of switches (Bentele et al., 2004; Kikuchi et al., 2003; Rehm et al., 2006) and models of oscillators (Bagheri et al., 2007; Stelling et al., 2004a). A classical way to define the parametric sensitivity, s_{ij} of the ith observable c_i to the jth parameter p_j is :

$$s_{ij} = \frac{\partial c_i(t)}{\partial p_j}$$

This method, generally applied to a stable equilibrium, is local in the state and parameter spaces. When trying to study the dynamics of the process like the switching between two stable steady-sates, these sensitivity measures can be computed over trajectories and normalized by $\frac{1}{T}$, with T the integration period, to get a time-average valued:

$$s_{ij} = \frac{1}{T} \int_0^T |s_{ij}(t)| \, dt$$

Obviously the sensitivity measure is then dependent of the chosen trajectory. Therefore, sensitivities must be computed for various initial
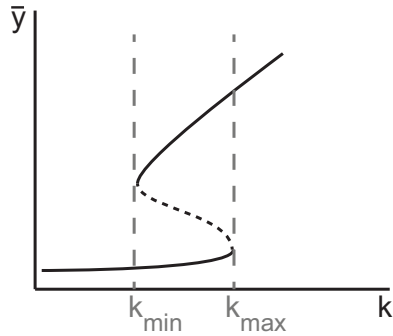
Figure 3.2: Diagram of bifurcation of a bistable model as a function of the parameter k. The solid black curves represent branches of stable equilibria while the dashed black curve represents a branch of unstable equilibria. The stable equilibria disappear in local bifurcations $k_{\min}$ and $k_{\max}$.

conditions to get a global picture of the switch robustness in the state space, which can be time consuming.

A classical method to get a non local robustness measure of the system in the state space is to draw diagrams of bifurcation. A one-parameter diagram of bifurcation represents the steady-states of a system as a function of the value of one parameter. In bistable switches, the system typically presents two stable steady-states for a fixed value of one parameter k (Figure 3.2). These diagrams allow to identify local bifurcations, i.e points when the system changes stability. Typically, these diagrams can be drawn using specific softwares, see Appendix A. Among others, this analysis has been applied to quantify the robustness of the apoptotic switch, (Eissing et al., 2005) and the mitotic control, (Borisuk and Tyson, 1998).

As an illustration, we will consider in later chapters a robustness measure proposed by Ma and Iglesias (Ma and Iglesias, 2002). This method has been used to quantify the robustness of apoptotic models, (Eissing et al., 2007). The DOR (degree of robustness) of a bistable model with respect to a particular parameter $k > 0$ (all remaining parameters being fixed) is defined by:

$$\text{DOR} = 1 - \max\left\{\frac{k_{\min}}{k}, \frac{k}{k_{\max}}\right\} \tag{3.1}$$

where $(k_{\min}, k_{\max}) \subseteq (0, \infty)$ denotes the parameter interval in which the system presents two stable attractors (Figure 3.2). A degree close to one means that the system is very robust to parameter k and a degree

close to zero means that it is very sensitive to this parameter. The advantage with respect to classical local sensitivity analysis is that the measure does not depend on a given state or trajectory, it is non-local in the state space. However, the computation of the range of bistability for each parameter variation is a computationally demanding task. Moreover, softwares dedicated to bifurcation analysis are difficult to run when the size of the system increases, in particular if the system is stiff which is generally the case in models of biological switches. In addition, the sensitivity can only be computed for one or at most two parameters at the same time. These measures are local in the parameter space, they are computed around a nominal set of parameters which is not necessarily easily defined. Finally, these methods only focus on the presence of stable attractors, i.e on the static properties of the system and are not suited to capture a dynamical transition between two steady-states.

To get a global robustness measure in both the state and parameter spaces, parametric robustness is mostly computed trough simulation-based methods. The system is simulated for various values of initial conditions and parameters and results of numerical simulations are compared with some performance criteria dictated by biology. These methods include Monte-Carlo based simulations where parameters are randomly selected according to a given statistical distribution in a predefined range (Robert and Casella, 1999). The robustness of the model corresponds to the volume of parameters which lead to the desired behavior. These methods have been applied to quantify the switch robustness in bacterial chemotaxis (Barkai and Leibler, 1997) and apoptosis (Eissing et al., 2007; Shoemaker and Doyle, 2008). However these are computationally demanding and results are often difficult to interpret from a biological point of view.

A possibly promising approach is the coupling between both local analysis and global methods. Such methods have recently been applied to the study of circadian oscillators, (Hafner et al., 2010, 2009) and the study of the ErbB signaling pathway (Chen et al., 2009). To study such complex systems, interdisciplinary teams try to integrate the various concepts including networks motifs, sensitivity analysis, noise robustness, population dynamics. This type of analysis has been used to design artificial tissue homeostasis (Miller et al., 2012).

3.3.3 Noise robustness

In biology, decision-making processes are subject to different sources
of noise (Balázsi et al., 2011). First, biological systems are exposed
to perturbations from their external environment (extrinsic perturba-
tions). But there are also subject to a different source of noise often
called intrinsic noise. This noise arises when the copy number of units
(ions, molecules or individuals) in a population is low. In this case, the
deterministic ordinary differential equations which describe the system
behavior at the macroscopic (population) level fail to provide a faith-
ful representation of the system. The interactions among species are
then probabilistic. Intrinsic noise has been particularly investigated in
the context of molecular reactions, see Gillespie (2007) for a review of
stochastic simulation of chemical kinetics. In particular the chemical
master equation (CME) gives a good description of the system based on
a probabilistic description of the interactions between species. It con-
sists in describing the system as a continuous-time Markov jump process.
However, solving the CME is a computationally demanding task even if
efficient algorithms including the SSA algorithm (Gillespie, 1976, 2007)
have been designed to simulate sample paths of the process.

The diffusion approximation can be used to approximate the CME by
a stochastic differential equation (SDE) when the number of species is
large enough (but not large enough to be described by deterministic
equations). A SDE is an ordinary differential equation with a noise
term. In chemical kinetics, SDE arise as a natural approximation of the
CME under the diffusion approximation. On the other hand, SDE or
Langevin-type equations have also been used in a broad variety of fields
to describe the dynamics of macroscopic (or collective) variables which
are subjected to microscopic (individual) perturbations. It is based on
the hypothesis that the macroscopic variables vary slowly with respect to
the microscopic perturbations. SDE can be simulated using the Euler-
Maruyama scheme (Higham, 2001).

3.4 Conclusion

Based on general observations on performance and robustness of biological systems, we introduced performance criteria for biological switches. Instead of focusing on static properties of the system such as the presence of two stable steady-sates, the performance is defined with respect to dynamical properties of the switch such as latencies and reversibility. The introduction of these dynamical criteria is motivated by the fact that most models of biological switches represent a binary decision-making process. The questions which seemed important for the control of the switch can be related to general questions about the dynamics of this decision-making process.

We presented a short and non-exhaustive survey of methods to quantify the robustness of biological models and identified their advantages and limitations in studying the robustness of dynamical switches:

- Methods that are local in both the state and parameter spaces such as local sensitivity analyses are easy to implement. However, these methods usually consider the linearization of the system around a stable equilibrium. This methodology is suited for the analysis of biological phenomena such as homeostasis, but it is not suited to phenomena characterized by a nonlocal transition between two stable steady-sates.

- To get a non-local picture of the switch robustness in the state space, sensitivity analysis can be applied along trajectories. Trajectories are simulated for different initial conditions and the sensitivity is computed over all these trajectories.

- Methods such as diagrams of bifurcations are also non local in the state space, capturing in one diagram all the states of the system. However, they only describe the static properties of the switch, they are difficult to run for high-dimensional models and local in the parameter space.

- Global methods generally address the problem of robustness by means of extensive simulations. The system is simulated for various initial conditions and sets of parameters. This type of analysis

quickly becomes intractable as the dimension of the system increases. In addition, results are often difficult to interpret from a biological point of view and it is not clear yet what biological insight could be gained from such methods.

Studying the robustness of biological switches is challenging. Because these systems describe a dynamical decision-making process, involving a transition between two stable steady-sates, classical theoretical tools based on a local linearization around one stable steady-state fail to capture the switch performance and robustness. This explains why most studies currently address this problem by means of extensive numerical simulations.

Chapter 4

The saddle point: a local organizer of bistability

Quantifying the performance and robustness of bistable switches is a challenging issue which can be addressed with various theoretical and numerical methods. The analysis presented in this chapter relies on dynamical systems theory. The goal is to identify general mathematical properties that rule the switch behavior and propose some simple tools to quantify its performance and robustness. These principles are introduced in planar models in the present chapter and then extended to high-dimensional models in the next chapter. In contrast to methods previously proposed in the literature, our goal is to provide local tools that can be used to estimate the global performance and robustness of the switch.

4.1 The saddle point, a key ruler of the switch
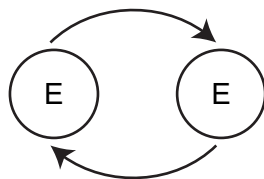
Figure 4.1: EE motif corresponding to mutual activation between two excitatory units. Each unit produces a nonlinear positive feedback on the activation of the other unit.

Bistability is a phenomenon that is well understood in planar models.

There are many examples of two-dimensional bistable models including the famous Lotka-Volterra equations for two competing species population dynamics (Lotka, 1925; Volterra and Brelot, 1931), the model of genetic control proposed by Griffith (Griffith, 1968) and the "excitatory-excitatory" (E-E) and "inhibitory-inhibitory" (I-I) models of Hopfield for neural networks (Hopfield, 1982).
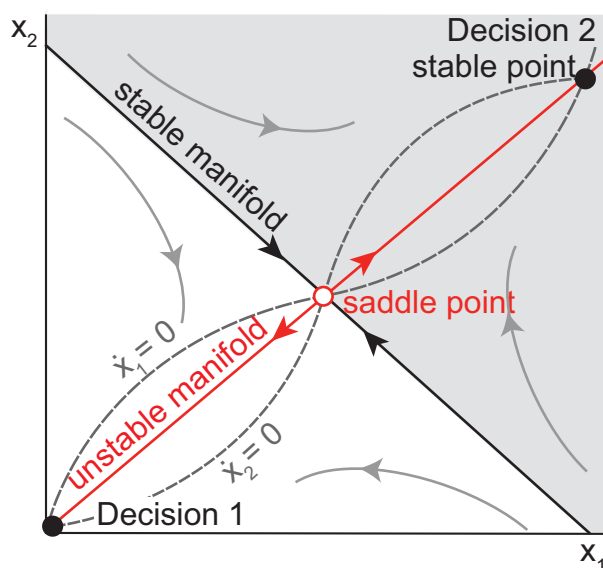
Figure 4.2: Phase plane of a typical bistable model resulting from mutual activation. The system has two stable steady-states (black dots) and a saddle point (white dot). The stable manifold of the saddle (black curve) separates the phase plane into the two basins of attraction of stable equilibra while its unstable manifold (red curve) connects the three equilibra. Depending on the initial condition, the system converges to the 'off' state associated with decision 1 or the 'on' state associated with decision 2.

In all these models, bistability is achieved thanks to the presence of a positive feedback loop, a mechanism particularly important for bistability (Cinquin and Demongeot, 2002; Thomas, 1994). This positive feedback results from different mechanisms of interactions such as self-induction

(Lotka-Volterra model), mutual activation (Griffith and E-E models) or mutual inhibition (I-I model). As a toy example for this section, we use a model of mutual activation between two simple components (Figure 4.1),

$$
\begin{aligned}
\dot{x}_1 &= -x_1 + \mathrm{sat}(x_2) \\
\dot{x}_2 &= -x_2 + \mathrm{sat}(x_1)
\end{aligned}
\tag{4.1}
$$

where $x_1, x_2 \in \mathbb{R} \geq 0$ are the level of activation of two interacting components (activation of neurons, expression level of genes, concentration level of proteins, . . .). The positive, nonlinear function sat, typically sigmoidal or step-like, describes the positive feedback of one component on the other. In this section, $\mathrm{sat}(x)$ is chosen as a Hill function, $\mathrm{sat}(x) = \frac{1}{\gamma}\frac{x^n}{1+x^n}$ with $\gamma > 0, n = 2$. For suitable values of the parameter $\gamma > 0$, the system is bistable.

In addition to the two stable equilibria, two-dimensional bistable models must include a saddle point as an extra equilibrium. Figure 4.2 depicts the typical phase plane of a bistable model resulting from mutual activation. Equilibrium points are located at the intersection of the nullclines (black-dashed curves), i.e the curves $\dot{x}_1 = 0$, $\dot{x}_2 = 0$. Nullclines present a typical sigmoidal shape which is related to ultrasensitivity and cooperative behaviors introduced in Chapter 2. Due to the s-shape nonlinearity of nullclines, the system has three equilibria. Two are stable and correspond to experimentally observable conditions (black dots): the 'off' state where both x_1 and x_2 are inactivated and the 'on' state where both x_1 and x_2 are fully activated. The third equilibrium is unstable and is therefore not seen in experiments (white dot). This point is a saddle point, i.e an equilibrium point with attractive and repulsive directions. The saddle point has a central role in the decision model: it is like a mountain pass between two valleys. Its stable manifold (black curve) divides the phase plane into the two basins of attraction of stable equilibrium points while its unstable manifold (red curve) connects the three equilibria.

4.2 Local analysis at the saddle point

The local stability of an equilibrium, x_0 is determined by computing the Jacobian matrix of the system at this point.

For the system 4.1:

$$J = \begin{pmatrix} -1 & \partial_{x_2}\mathrm{sat}(x_2) \\ \partial_{x_1}\mathrm{sat}(x_1) & -1 \end{pmatrix}\Bigg|_{x=x_0} = \begin{pmatrix} -1 & m \\ q & -1 \end{pmatrix}$$

with $m = \partial_{x_2}\mathrm{sat}(x_2)|_{x_0}$ and $q = \partial_{x_1}\mathrm{sat}(x_1)|_{x_0}$.
The local stability of x_0 is determined by the real part of the eigenvalues
of J, λ_1 and λ_2.

$$\begin{aligned} \mathrm{Tr}(J) &= -2 = \lambda_1 + \lambda_2 < 0 \\ \det(J) &= 1 - mq = \lambda_1\lambda_2 \end{aligned}$$

$$\mathrm{if} \begin{cases} mq < 1\text{: the equilibrium is stable} \\ mq > 1\text{: the equilibirum is a saddle} \end{cases}$$

At the saddle point, the system possesses two real eigenvalues, one neg-
ative $-\lambda_s$ and one positive λ_u. The linearized system can be written,

$$\begin{aligned} \dot{u} &= -\lambda_s u + O(u^2, uv, v^2) \\ \dot{v} &= \lambda_u v + O(u^2, uv, v^2) \end{aligned} \tag{4.2}$$

with u and v the eigenvectors corresponding to $-\lambda_s$ and λ_u. At the sad-
dle point, they correspond to the tangent approximation of the stable
and unstable manifold of the saddle point. At the first order, the rate of
convergence to the saddle in the stable manifold is given by $e^{-\lambda_s t}$ while
the escape rate is governed by $e^{\lambda_u t}$.

We define the ratio τ:

$$\tau = \frac{\lambda_s}{\lambda_u} \tag{4.3}$$

This ratio locally quantifies the time-scale separation between a fast at-
traction to the saddle in the stable manifold and a slow repulsion in the
unstable manifold.

Figure 4.3 shows the phase portrait of the system 4.1 for a value of γ
corresponding to a saddle with a large τ. Due to the time-scale separa-
tion at the saddle point, trajectories (dark blue and light grey curves)
that start in the vicinity of the stable manifold (green line) converge in

the fast time-scale to a neighborhood of the saddle point. They escape the saddle in the slow time-scale, resulting in a long transient latency. Eventually, they converge to one of the two stable equilibria.
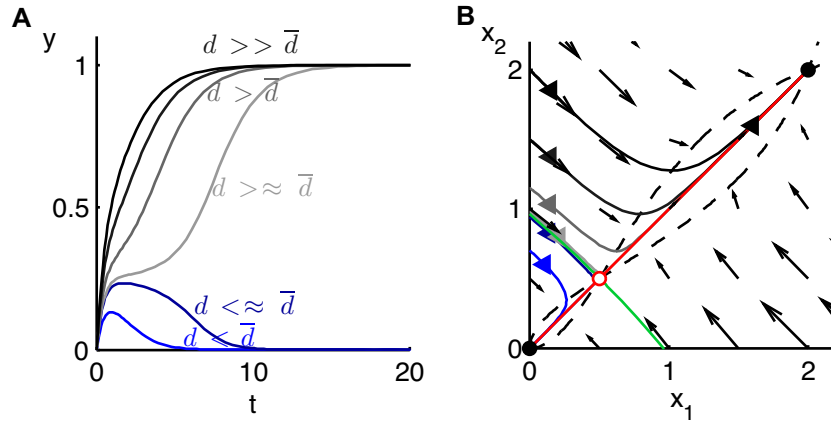
Figure 4.3: Latencies induced by a time-scale separation at the saddle point. The figure shows trajectories for initial conditions at an increasing distance of the separatrix (A). The corresponding trajectories are depicted in the phase plane (B). Trajectories starting close to the separatrix are delayed by the saddle point. The quantity d describes the strength of an impulse signal that modifies the initial condition of the system while $\bar{d}$ is the lowest signal strength necessary to trigger the switch, see section 4.2.1.

4.2.1 Latencies

A saddle point with a large τ induces transient latencies in the switch. This mechanism is a simple way to create switches with input-strength dependent latencies. As an illustration, we consider an input-output version of the system 4.1:

$$\begin{aligned} \dot{x} &= -x + F(x) + Bu(t) \\ y &= Cx \end{aligned} \tag{4.4}$$

with $x = [x_1\ x_2]^T$, $B = [0\ d]^T$, $d \in \mathbb{R}$, $C = [1\ 0]^T$, $F(x) = [\mathrm{sat}(x_2)\ \mathrm{sat}(x_1)]^T$ and $x_0 = [0\quad 0]^T$, i.e the system is initially in the 'off' state.

We analyze the effect of short duration (pulse-like) inputs, modeled for simplicity by a Dirac function, i.e $u(t) = \delta(t)$. These inputs represent an instantaneous change in the state of the system such as a modification of the initial concentrations of the system. If the signal strength d is greater than a particular threshold $\bar{d}$, the system switches from the 'off' state to the 'on' state (i.e from decision 1 to decision 2) see Figure 4.3 A where the output has been normalized. The threshold $\bar{d} \in \mathbb{R}_0^+$ is the minimum input necessary to trigger the switch. The 'off' state corresponds to $y = 0$ and the 'on' state to $y = 1$. If $d < \bar{d}$, the system returns to the 'off' state and no switch occurs. The switch occurs when the transient signal is strong enough to push the system state beyond the separatrix in the phase plane. The switching time depends on the signal strength. Figure 4.3 B shows the corresponding trajectories in the phase plane. The time-scale separation at the saddle point forces trajectories that approach the stable manifold to rapidly converge to a neighborhood of the saddle point from which they slowly escape, causing the delay. This results in a mechanism of input-strength dependent latencies with latencies particularly long for inputs close to the threshold, $\bar{d}$.
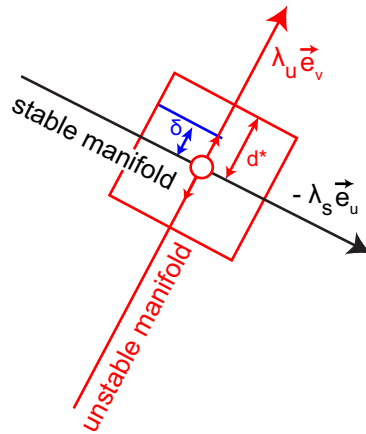
Figure 4.4: Local analysis at the saddle point, see (4.2) and the text below.

The duration of these latencies can be estimated by integrating the linearized system (4.2), we get:

$$u(t) = u(0)e^{-\lambda_s t}$$
$$v(t) = v(0)e^{\lambda_u t} \tag{4.5}$$

Trajectories are attracted by the saddle point at a speed $e^{-\lambda_s t}$ in the direction of the vector tangent to its stable manifold ($\overrightarrow{e}_u$). They escape the saddle at a speed $e^{\lambda_u t}$ following the direction tangent to the unstable manifold ($\overrightarrow{e}_v$). When, at the saddle point, the ratio τ (4.3) is large, i.e. $\lambda_s >> \lambda_u$, trajectories fast converge to the unstable manifold of the saddle and then slowly escape along this manifold resulting in latencies in the switch. In this case, the scalar motion on this unstable manifold is sufficient to quantify the latencies.

The decision-time or escape-time τ_d is defined as the time to reach a distance $d^* > 0$ of the saddle point in the direction, $\overrightarrow{e}_v$ of the tangent approximation of the unstable manifold, see Figure 4.4. The expression,

$$v(t) = v(0)e^{\lambda_u t} \tag{4.6}$$

characterizes the escape rate from the saddle in this direction. We get for an initial condition at a distance $v(0) = \delta$ of the separatrix (stable manifold),

$$\frac{v(\tau)}{v(0)} = \frac{d^*}{\delta} = e^{\lambda_u \tau_d}, \quad d^* > \delta > 0 \tag{4.7}$$

$$\tau_d = \frac{1}{\lambda_u} \ln \frac{d^*}{\delta} \tag{4.8}$$

The value of d^* being fixed, the duration of delays is inversely proportional to λ_u and scales logarithmically with the ratio $\dfrac{d^*}{\delta}$.

4.2.2   Reversibility

An important consequence of latencies and delayed decision making is illustrated in Figure 4.5. In this picture, the effect of a small reverting input is compared on two different systems. The first one is a switch
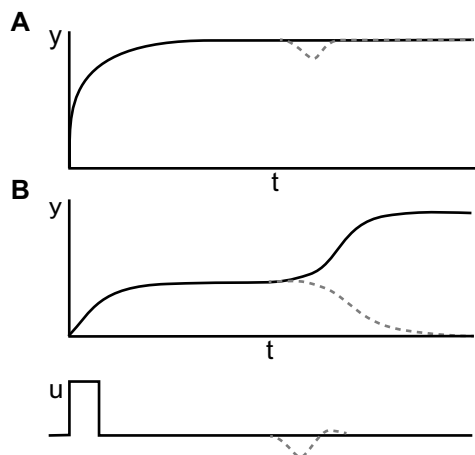
Figure 4.5: Effect of small reverting perturbations on a switch either presenting no latency (A) or presenting a long transient latency (B) close to the saddle point. For this last one, a small perturbation is likely to revert the switch. This is a schematic representation of a phenomenon discussed on published biological models in Chapter 6.

without latencies while the second one presents long latencies induced by the saddle point. By contrast to the first system which does not present latencies, a small perturbation can revert the switch in the second system with latencies. As the system remains close to the saddle point and thus to the separatrix during the intermediate phase, a small input perturbation can easily revert the switching decision. This is illustrated by the grey dashed signals. Therefore, such delayed decision making system is very sensitive to reverting perturbations during this intermediate phase. Such a property could have biological significance in a signalling mechanism as it will be illustrated in Chapter 6.

4.3 The saddle node bifurcation

'The saddle-node bifurcation is the basic mechanism by which fixed points are created and destroyed. As a parameter is varied, two fixed points move toward each other, collide, and mutually annihilate (Strogatz, 1994).' At a saddle node bifurcation, only one eigenvalue crosses the imaginary axis, i.e only one eigenvalue has a zero real part (see

the general definition of a saddle node bifurcation in Guckenheimer and Holmes (1983), also discussed in Chapter 5). In this thesis, we consider the typical saddle node bifurcation where a stable equilibrium disappears when it collides whit a saddle point. In planar models, this situation corresponds to a situation where, at the bifurcation, the system possesses one eigenvalue with a negative real part and one eigenvalue with a zero real part.

A large τ occurs when $\lambda_u << \lambda_s$. This situation is typically encountered in the vicinity of co-dimension one bifurcations such as saddle node bifurcation of the saddle point with a stable equilibrium. Indeed, the positive eigenvalue $\lambda_u > 0$ at the saddle point can be made as small as desired by pushing the system closer to the saddle node bifurcation while the negative eigenvalue at the saddle point, $-\lambda_s$, remains strictly negative.

To illustrate the effect of saddle node bifurcation on the switch, we consider the input-output version of the system studied in the previous section, see system 4.4 but with step inputs, i.e $u(t) = \mathcal{H}(t)$. Figure 4.6 depicts trajectories for increasing values of d. Step inputs affect the nullclines and equilibria of the system. The switch is triggered when the signal strength d is strong enough to push the system beyond a bifurcation point. At the switching threshold $\bar{d}$ (i.e the minimum value of the input signal to trigger the switch), the stable equilibrium merges with the saddle point in a so-called saddle-node bifurcation, the positive eigenvalue λ_u vanishes and the ratio τ is infinite. For $d > \bar{d}$, only the excited state remains. When $d \gtrapprox \bar{d}$, there is a bottleneck created by the proximity of nullclines where the dynamics is slowed down. Even if the saddle point has disappeared, the *ghost saddle* delays trajectories (Strogatz, 1994). The decision-time is mainly determined by the escape time from this bottleneck.

The effect of a ghost saddle is a phenomenon well characterized in system dynamics, (Strogatz, 1994). To illustrate this phenomenon, we introduce the system:

$$\dot{x} = x^2 + k, \quad k \in \mathbb{R} \tag{4.9}$$

As it will be introduced in the next chapter, this system corresponds to
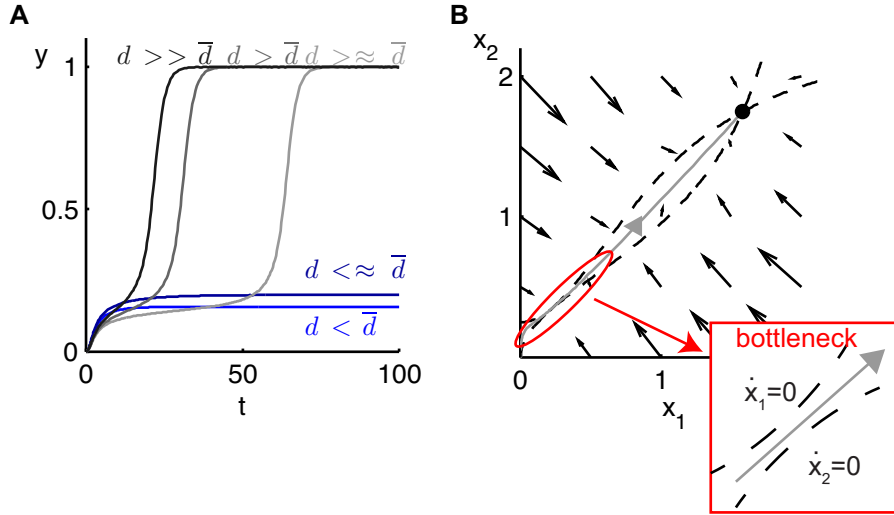
Figure 4.6: Switches with input-strength dependent latencies. Effects of a step input.

the normal form of a saddle node bifurcation. For $k < 0$, the system has two equilibria given by $x = \pm\sqrt{-k}$, one is stable (black dot) and one unstable (white dot), see Figure 4.7. For $k = 0$, the two equilibria merge in a saddle node bifurcation (black-white dot). For $k > 0$, the system has no equilibria and $\dot{x} = x^2 + k$ is always positive, the system escapes to infinity. The parameter k controls the distance to the saddle point.

If $k > 0$, the solutions will escape to infinity. However, the escape time can be particularly long. This escape time or decision time from the interval (x_0, x_{thresh}) can be computed by:

$$\tau_d = \int_{x_0}^{x_{\text{thresh.}}} x^2 + k \ dt = \frac{1}{\sqrt{k}}\text{atan}(\frac{x}{\sqrt{k}})|_{x_0}^{x_{\text{thresh.}}}$$

with $x_0, x_{\text{thresh}} \in \mathbb{R}$ and $x_0 < x_{\text{thresh}}$.
The time for x to go from $-\infty$ to $+\infty$ ($x_0 = -\infty$ and $x_{\text{thresh}} = +\infty$,) is then given by:

$$\tau_d = \frac{\pi}{\sqrt{k}}$$

that is the classical escape time from a bottleneck (Strogatz, 1994).
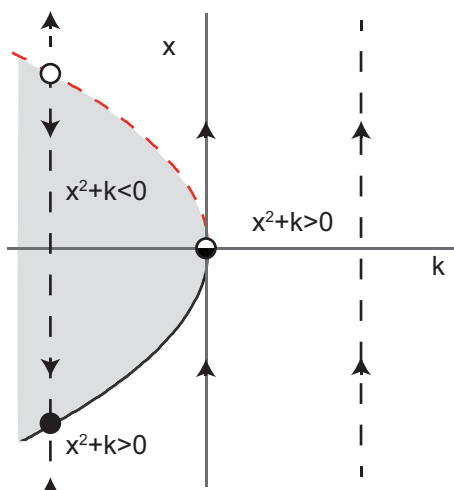
Figure 4.7: Normal form of a saddle node bifurcation: $\dot{x} = x^2 + k$

When the system is close to the saddle node, k is close to zero and the escape time is particularly long.

4.3.1   Latencies and reversibility

The previous paragraph showed that the time to escape from a bottleneck created by a ghost saddle is fixed by the distance to the saddle node bifurcation, k. Thanks to this type of bifurcation, the biological process can implement a new mechanism of delayed-decision making for constant inputs that modify the equilibria of the system. As for the mechanism presented previously, the system presents an input threshold corresponding to the strength of the signal necessary to push the system at the bifurcation point. The duration of latencies is then a decreasing function of the distance to this threshold i.e. of the distance to the bifurcation point. For these type of inputs, when the process has been triggered, it can only be reverted by constant inputs that will push back the system in the bistable regime.

4.3.2   Remarks

In Section 4.1, we highlighted a mechanism to create input-strength dependent latencies based on impulse signals. However, this mechanism

relies on the presence of a system with a large τ, a situation typically encountered in the vicinity of a saddle node bifurcation. What happens to this mechanism when the system is pushed beyond the bifurcation point?

$$
\begin{aligned}
\dot{x} &= -x + F(x) + Bu(t) + Dp(t) & (4.10) \\
y &= Cx & (4.11)
\end{aligned}
$$

where $B = [0\ d]^T, d \in \mathbb{R}$, $u(t) = \delta(t)$, $D = [0\ \alpha]^T, \alpha \in \mathbb{R}$ and $p(t) = \mathcal{H}(t)$ with $\mathcal{H}(t)$, the classical Heaviside step function representing a constant input production term. When $\alpha = 0$, the system is bistable and we observe latencies in the decision making process, see Figure 4.3 in Section 4.2. For $\alpha = 0.2$, the saddle point disappears trough a saddle-node bifurcation. Despite the absence of a saddle point, see Figure 4.8 A-B drawn for $\alpha = 0.25$, one still observes the latency-induced decision. The phenomenon disappears as the system moves further away from the bifurcation point, see Figure 4.8 C-D where $\alpha = 1.5$. The mechanism persists beyond the saddle node because of the ghost saddle. Therefore, latencies induced by impulse signals can still be observed beyond the bifurcation point., i.e even if the system is no longer bistable.

The distinction between impulse and step inputs deserves further discussion. When talking about step signals we talk about increasing a quantity which will be conserved in the system or applying a constant signal to the system. This situation typically occurs if we consider that a cell is immersed in a medium where the concentration of inducer remains constant. Impulse signals represent a modification in an initial concentration which is not conserved in the system, for example the injection of some protein which can be degraded by the cell. However this simple distinction hides some complexity. For example a step input of a fixed duration could be considered as either an impulse signal or a constant input depending on the time-scale of the decision-making process with respect to the length of the input signal.

4.4   Parametric sensitivity

Sensitivity analysis is a standard tool to quantify the effect of parameter variation on the system behavior. Local sensitivity analysis is routinely
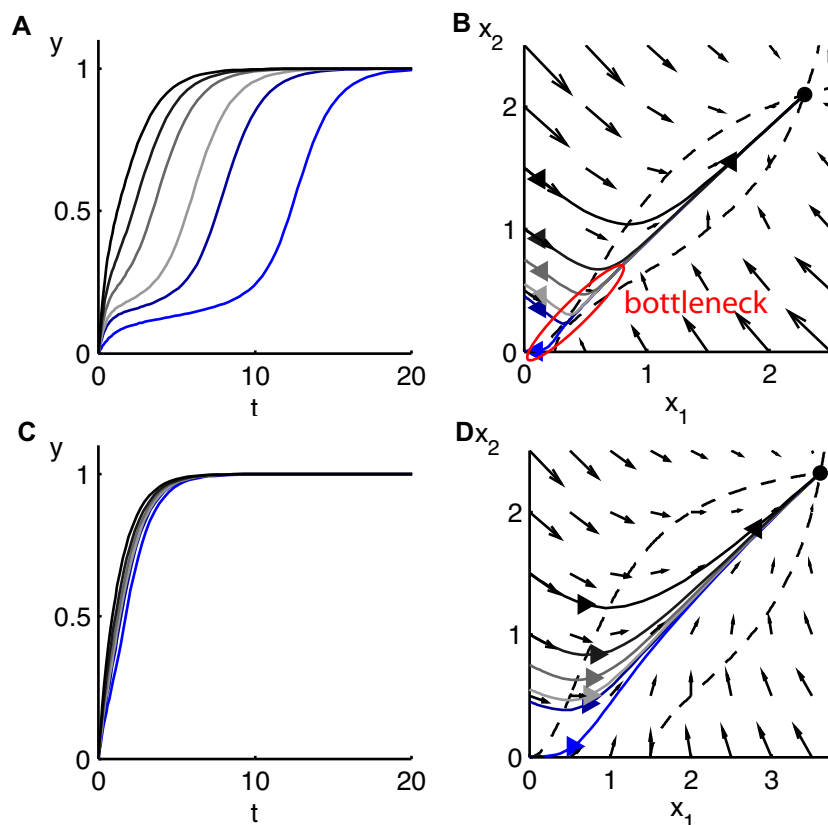
Figure 4.8: Figures (A-B) and (C-D) show the switch is modified by adding a step input $p(t)$ to the switch described by (4.4) and depicted on Figure 4.3. (A-B) $\alpha = 0.25$, only the 'off " state remains while the value of α is close to the bifurcation point $\alpha_s = 0.2$. The saddle point has disappeared but its ghost creates a similar delay. One can still observe switches with input-strength dependent latencies. (C-D) $\alpha = 1.5$, both the bottleneck and the switches with delays disappear.

applied around stable fixed points. Here, we propose to compute the local sensitivity analysis at the saddle point. For a hyperbolic steady states, the local sensitivity at the steady state $x_0 \in \mathbb{R}^n$ for a set of nominal parameters $p = p_0 \in \mathbb{R}^m$ can by computed by (Ingalls, 2008;

Turányi, 1990),

$$S \;=\; -\left.\frac{\partial f(x,p)}{\partial x}\right|^{-1}_{x=x_0,p=p_0} \left.\frac{\partial f(x,p)}{\partial p}\right|_{x=x_0,p=p_0}, \qquad (4.12)$$

or, its normalized version for a steady state x_0 with nonzero entries

$$\bar{S} \;=\; -\mathrm{diag}(x_0)^{-1} \left.\frac{\partial f(x,p)}{\partial x}\right|^{-1}_{x=x_0,p=p_0} \left.\frac{\partial f(x,p)}{\partial p}\right|_{x=x_0,p=p_0} \mathrm{diag}(p) \quad (4.13)$$

with $\mathrm{diag}(x_0)^{-1} \in \mathbb{R}^{n\times n}$ and $\mathrm{diag}(p) \in \mathbb{R}^{m\times m}$.

For each parameter, p_j, $j = 1\ldots m$, we compute the cumulated sensitivity given by the scalar:

$$\bar{s}_{p_j} = \sum_{i=1}^{n} |\bar{S}_{ij}| \qquad (4.14)$$

where $|\bar{S}_{ij}|$ is the absolute value of the element (i,j) of the matrix $\bar{S}$. The row vector $\bar{s}_p = [\bar{s}_{p_1},\ldots,\bar{s}_{p_m}] \in \mathbb{R}^{1\times m}$ collects the cumulated sensitivities for each parameter. The idea is that, by identifying the parameters which affect the saddle point, we will be able to identify parameters that control the switch performance. This sensitivity analysis will be performed in Chapter 6.

4.5 Noise sensitivity

As introduced in Chapter 3, biological systems are subject to different sources of noise. When the level of species is sufficiently large but not large enough to be described by ordinary differential equation, the diffusion approximation is a simple way to account for random perturbations. The diffusion approximation allows to represent the system as a set of stochastic differential equations (SDE). Let us consider a noisy version of the system 4.1.

$$\dot{x} = \mathrm{sat}(x) + \epsilon\xi(t), \quad x \in \mathbb{R}^2 \qquad (4.15)$$

with $\xi(t)$ a vector valued random process of zero mean and $\epsilon > 0$ small. The components of this vector are independent. Each component corresponds to an independent identically distributed random variable. We

consider that $\xi(t)$ is a Wiener process (Arnold, 1974).

Let us consider the mechanism by which impulse signals create input-dependent delays. As this mechanism of delays strongly depends on the local effects of the saddle point, a reasonable question is to see if these delays can still be observed in the presence of small noise. The problem of computing the escape time from a saddle point subjected to small random perturbations has been studied in (Kifer, 1981; Stone and Holmes, 1990). In particular, for random perturbations starting on the local stable manifold of a hyperbolic saddle point, the escape time scales as:

$$\frac{1}{\lambda_u}|\ln \epsilon| \tag{4.16}$$

see, (Kifer, 1981). Increasing ϵ will therefore decrease the time spent close to the saddle. However the relation is logarithmic. This means that for small λ_u, delays will still been observed in the presence of noise. The relation of Kifer (1981) is for an initial condition on the stable manifold of the saddle. The problem is solved with an initial distribution around this stable manifold in (Stone and Holmes, 1990). However, this problem is analytically solved for heteroclinic attractors under the restricting hypothesis of the orthogonality of eigenvectors at the saddle point.

In addition, these results do no include the effect of an initial distance to the separatrix. In order to test these effects, we simulated numerically the system,

$$dx_1 = [-x_1 + \text{sat}(x_2)]dt + \epsilon dW_1$$
$$dx_2 = [-x_2 + \text{sat}(x_1)]dt + \epsilon dW_2 \tag{4.17}$$

with dW_1 and dW_2, two independent Wiener processes of zero mean, i.e $< dW_{1,2} >= 0$ and $< dW_{1,2}^2 >= dt$ where $< \cdots >$ denotes expectation. ϵ is the root mean square noise level. Numerical simulation is based on an Euler-Maruyama scheme, see Appendix A.

Figure 4.9 shows the mean decision time in function of δ, the initial distance to the separatrix, for different values of ϵ (blue: $\epsilon = 1e^{-4}$, red: $\epsilon = 1e^{-3}$, black: $\epsilon = 1e^{-2}$). The mean decision time is defined as the mean time to reach a distance d^* of the saddle point in the direction of
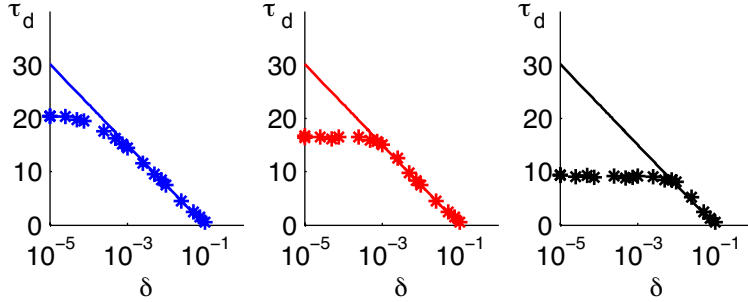
Figure 4.9: Mean decision time for a model of mutual activation for different values of ϵ (blue: $\epsilon = 1e^{-4}$, red: $\epsilon = 1e^{-3}$, black: $\epsilon = 1e^{-2}$). For large initial distance to the separatrix δ with respect to ϵ, the mean decision seems to follows the law predicted by the deterministic expression 4.8 (diagonal solid line). For small initial distance to the separatrix, the mean decision time is scaled by noise. It is a constant which depends on the value of ϵ as predicted by 4.16.

the eigenvector associated with the positive eigenvalue λ_u for an initial condition at a distance δ from the stable manifold of the saddle (like in the deterministic setting, see Figure 4.4). The mean is computed over several realizations of the stochastic process for the same initial condition. The distance δ is computed as the classical euclidian distance in the direction of the vector tangent to the unstable manifold. In this analysis, we neglect the convergence to the unstable manifold and study initial conditions on the unstable manifold of the saddle. For each point, the decision time is computed by performing a mean of the decision time over 500 realizations of the stochastic process. The distance d^* is fixed to $d^* = 0.1$. As for the deterministic decision time predicted by the local analysis 4.8, the mean decision time of the stochastic system decreases with the initial distance to the separatrix, δ. For large values of δ with respect to ϵ, the mean decision time follows the law predicted by the deterministic analysis, see 4.8 and the diagonal solid lines in Figure 4.9. When δ is small with respect to the noise, the decision time is scaled by the noise. In this later case, the mean decision-time seems to be a constant, which is fixed by the value of ϵ as predicted by 4.16 for initial conditions on the stable manifold, i.e $\delta = 0$.

The problem of estimating how noise affects the decision-making process in the vicinity of a saddle node bifurcation will be briefly discussed in Chapter 5.

4.6 Global analysis of the phase plane

Recently, a new method has been proposed to draw the isostables of a equilibrium (Mauroy et al., 2013). For a given equilibrium, 'the isostables are the sets of points that approach the same trajectory when they converge toward the fixed point'. Isostables are equally spaced in time, i.e a trajectory intersects the isostables with a constant time interval. This method is applied to the system (4.1) for a value of γ corresponding to a large ratio τ, see Figure 4.10 where isostables have kindly been computed by A. Mauroy. The isotables of the excited state (the stable equilibrium with non-zero concentrations) are depicted in black while isostables of the resting state (the stable equilibrium with zero concentrations) are depicted in blue. Isostables are almost parallel to the stable manifold of the saddle and they are particularly dense in the vicinity of the stable manifold of the saddle reflecting the decrease of the system speed close to the separatrix. Qualitatively, this global analysis provides the same information than that our local analysis at the saddle point. In this system with a large τ, trajectories are delayed in the vicinity of the saddle point as illustrated by the high density of isostables in the vicinity of the separatrix. There is a fast attraction to the unstable manifold in a direction parallel to the stable manifold as illustrated by the shape of isostables almost parallel to the separatrix.

4.7 Conclusion

In bistable models, the saddle point is a key ruler of the switch. Because it lies at the frontier between basins of attraction of equilibria, this point is a good candidate for a local analysis of the decision-making process in the phase plane. Like a mountain pass between two valleys, the saddle point is located on the shortest path to switch from one attractor to the other. In addition, its stable manifold acts as a natural threshold which
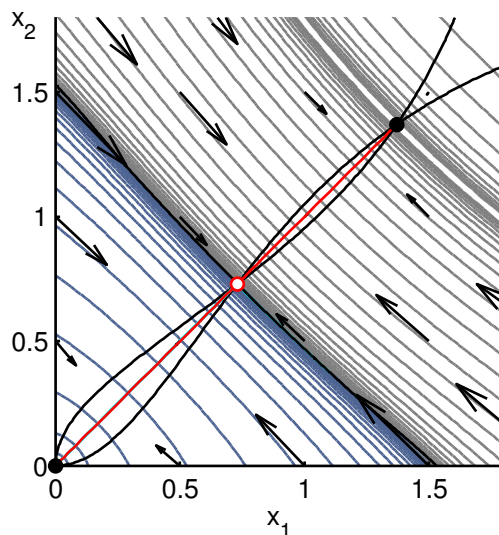
Figure 4.10: Isostables of a the system 4.1 for a value of γ corresponding to a large τ. The figure has been drawn from the numerical results kindly provided by A. Mauroy.

filters out small perturbations.

When the system presents a time-scale separation at the saddle point, properties such as latencies or transient reversibility, are likely to be observed. This time-scale separation is captured by a high ratio τ of eigenvalues at this point. For these systems with a fast convergence to the unstable manifold of the saddle, the sensitivity of the decision-time is estimated by computing the escape time from the saddle point. This latency depends on the positive eigenvalue of the system at the saddle, the initial distance to the separatrix and the noise strength. In systems with large τ, small noise is likely to perturb the decison-making process because the system presents long transients close to the separatrix, where perturbations are able to revert the switch.

A high ratio τ naturally occurs in the vicinity of a saddle node bifurcation. In this case, the switching performance is strongly affected by the distance to the bifurcation point and the global system behavior is very

sensitive to the parametric perturbations which control the distance to this bifurcation. Therefore, identifying parameters which control this distance is not only a way to study static performance criteria of the switch but also its dynamical properties such as the decision-time and the reversibility.

All the considerations of this chapter have been drawn for a planar model. An important issue is to know whether this type of behaviors can still be observed for high-dimensional models. Indeed, our goal is to identify simple ways to design switches with a given property even when the dimension of the system is not limited to the typical dimension of a network motif. Is it possible to observe latencies in high dimensional systems? Can we generalize the ratio τ? What does this ratio capture in high dimensional models? Is it a simple way to link the dynamic and the static properties of the system such as for the lower dimensional analysis? These questions will be addressed in Chapter 5 and results will be illustrated on three models of the literature in Chapter 6.

A local analysis method
for high-dimensional models of bistability

This chapter extends the measures and concepts introduced in the previous chapter to n-dimensional models. We generalize the ratio τ. The link between the system dynamics and the proximity to a bifurcation is rigorously justified by the Center manifold theory. This theory allows the reduction of a n-dimensional system to a simple one-dimensional equation called normal form when the system operates close to a codimension one bifurcation. This equation can be used to get insight on the decision-making process.

5.1   Localization of the saddle point

Localizing steady states in a high-dimensional system of nonlinear differential equations is not a straightforward task because it requires finding the roots of the algebraic equation $f(x) = 0, x \in \mathbb{R}^n$. The peformance of numerical root finding algorithms is usually local, that is, roots are easily found numerically provided that a good initial guess is known. For stable steady-states of a bistable system, a few simulations of the differential equation are sufficient to provide good initial guesses since simulations will converge to one of the two stable equilibria. In a similar way, simulations initialized in the vicinity of the stable manifold of the saddle point will have a long transient near the saddle point, especially if there is a strong time-scale separation, thereby providing good initial guess for the root finding algorithm. Because the stable manifold of the saddle is a separatrix of the two basins of attraction, initializing a simula-

tion near the stable manifold is achieved by picking a state variable that clearly distinguishes the two stable states (this choice is often suggested by biology) and by applying a bisection procedure to identify an initial condition close to the separatrix. In this thesis, we used Matlab's `ode15s` for simulating the differential equations and Levenberg-Marquardt option in the `fsolve` algorithm for solving the algebraic equations.

5.2   Local stability analysis

Let,

$$\dot{x} = f(x) \quad x \in \mathbb{R}^n \tag{5.1}$$

describe an n-dimensional bistable dynamical system having two stable equilibria. We assume that the two stable equilibria are connected by a heteroclinic orbit through a saddle point, x_0.

The local stability of an equilibrium point, x_0 is computed by linearizing the differential equation around that point to obtain the Jacobian matrix

$$J \quad = \quad \left. \frac{\partial f(x)}{\partial x} \right|_{x=x_0} \tag{5.2}$$

and calculating the eigenvalues and corresponding eigenvectors of J. A saddle point has eigenvalues with both positive and negative real parts. We assume that the saddle point is hyperbolic, i.e. it has no eigenvalues with zero real part. In addition, we assume that the system only possesses one real positive eigenvalue $\lambda_u > 0$. We will see later that this hypothesis is natural for bistable models.

At the saddle point:

$$\lambda_u = \lambda_1 > 0 > \text{Re}(\lambda_2) = -\lambda_s > \cdots > \text{Re}(\lambda_n)$$

From the stable manifold theorem (Guckenheimer and Holmes, 1983), the eigenvector associated with the positive eigenvalue λ_1 provides the tangent approximation of the unstable manifold at saddle point, that is also the heteroclinic trajectory connecting the two stable states, while the remaining eigenvectors span an hyperplane tangent to the stable manifold, that is the hypersurface separating the basins of attraction of

the two stable sates. We generalize the two-dimensional definition of the ratio (4.3) by defining

$$\tau = \frac{\lambda_s}{\lambda_u}$$

a high ratio meaning a strong time-scale separation. As $\lambda_u \to 0$ and the other eigenvalues remain finite, the ratio τ becomes infinite. Center manifold theory can be applied to study the dynamics of the system.

5.3 Center manifold theory

Center manifold theorem is a tool to reduce the state space which need to be considered when analyzing bifurcations of a given type. This theorem characterizes the local behavior of solutions near a bifurcation and allows to reduce the dynamics of complex nonlinear systems to a simple ordinary differential equation called normal form. Therefore, this tool is particularly interesting to describe the local behavior of complex nonlinear systems. Theoretical results presented in this section are extracted from Guckenheimer and Holmes (1983) and Kuznestov (2004).

We introduce the center manifold theorem following the formulation of Kuznestov (2004). We suppose that the system,

$$\dot{x} = f(x), x \in \mathbb{R}^n, \tag{5.3}$$

has an equilibrium at $x_0 = 0$ which is not hyperbolic. We assume that the Jacobian matrix of the system, J computed at this point has n_- eigenvalues with $\text{Re}(\lambda) < 0$, n_0 eigenvalues with $\text{Re}(\lambda) = 0$, and n_+ eigenvalues with $\text{Re}(\lambda) > 0$. Let, T^c, be the (generalized) eigenspaces of J associated with the union of the n_0 eigenvalues and $\phi(t)$ the flow associated to (5.3), then

Theorem 5.3.1. *(Centre manifold theorem as presented in Kuznestov (2004)) There is a locally defined smooth n_0-dimensional invariant manifold $W^c_{loc}(0)$ of (5.3), that is tangent to T^c at $x = x_0$. Moreover, there is a neighborhood U of x_0 such that if $\phi^t\, x \in U$ for all $t \geq 0 (t \leq 0)$, then $\phi_t x \to W^c_{loc(0)}$ for $t \to +\infty$ $(t \to -\infty)$. The manifold $W^c_{loc}(0)$ is called the center manifold.*

In the following part of the section, we only consider the case $n_+ = 0$. Indeed, as for the planar analysis and introduced in the next section, we only focus on co-dimension one bifurcations, such as saddle node bifurcations, where a stable equilibrium collides with a saddle point. Without loss of generality, we can always set $x_0 = 0$. Then the system (5.3) can be rewritten as follows:

$$\begin{aligned} \dot{x} &= Ax + f(x, z), \quad (x, y) \in \mathbb{R}^n \times \mathbb{R}^m \\ \dot{z} &= Bz + g(x, z) \end{aligned} \tag{5.4}$$

where A and B are $n \times n$ and $m \times m$ matrices whose eigenvalues have respectively, zero real parts and negative real parts, and f and g vanish at the origin. Since the center manifold is tangent to T^c, we can represent it as a (local) graph:

$$W^c = \{(x, z) | z = h(x)\}, \quad h(0) = Dh(0) = 0; \tag{5.5}$$

where $h : U \to R^m$ is defined on some neighborhood $U \in R^n$ of the origin. The projection of the vector field on $z = h(x)$ onto T^c gives:

$$\dot{x} = Ax + f(x, h(x)) \tag{5.6}$$

The solutions of (5.6) describes the flow of (5.4) restricted to W^c. By derivating 5.5 with respect to t, and noting $Dh(x) = [\partial h_i / \partial x_j]$, the Jacobian matrix of $h(x)$, we also get:

$$\dot{z} = Dh(x)\dot{x} = Dh(x)[Ax + f(x, h(x))] = Bh(x) + g(x, h(x))$$

or

$$N(h(x)) = Dh(x)[Ax + f(x, h(x))] - Bh(x) - g(x, h(x)) = 0 \tag{5.7}$$

with boundary condition

$$h(0) = Dh(0) = 0 \tag{5.8}$$

The center manifold can be computed by solving 5.7.

In order to reduce the system to its motion on the center manifold, we made the hypothesis that B has only negative eigenvalues. This condition ensures the attractivity of the center manifold. When λ_u goes to zero and the ratio τ becomes infinite, the system presents the conditions for a local attractive center manifold.

5.3.1   Normal forms and co-dimension one bifurcations

Thanks to the center manifold theorem, the behavior of a complex nonlinear system near a nonhyperbolic equilibrium (e.g., a bifurcation) can be studied locally by observing its restricted dynamics on its center manifold. The normal form procedure is a procedure which aims at simplifying the analytic expression of the vector field on the center manifold (Guckenheimer and Holmes, 1983). By an appropriate change of coordinate, the systems dynamics on the center manifold can be reduced to a canonical expression called normal form. Depending on the transversality conditions satisfied by the system, the dynamics on the center manifold is topologically equivalent to different normal forms.

Saddle node: If at the equilibrium $(x, \alpha) = (x_0, \alpha_0)$,

$$
\begin{aligned}
f_x(x_0, \alpha_0) &= 0 \\
f_\alpha(x_0, \alpha_0) &\neq 0 \\
f_x^2(x_0, \alpha_0) &\neq 0
\end{aligned}
\tag{5.9}
$$

where $f_x(x_0, \alpha_0)$ is the partial derivative of $f(x, \alpha)$ with respect to x computed at $(x, \alpha) = (x_0, \alpha_0)$, $f_\alpha(x_0, \alpha_0)$ is the partial derivative of $f(x, \alpha)$ with respect to α computed at $(x, \alpha) = (x_0, \alpha_0)$ and $f_x^2(x_0, \alpha_0)$ is the second partial derivative of $f(x, \alpha)$ with respect to x computed at $(x, \alpha) = (x_0, \alpha_0)$.

The dynamics on the center manifold is described by the normal form,

$$
\dot{x} \;\; = \;\; \alpha - x^2 \quad (\textit{saddle-node})
$$

For small $\alpha > 0$, the system possesses two equilibria, one is stable while the other is an unstable (saddle if $n \geq 2$) point. At $\alpha = 0$, these two equilibria merge in a saddle node bifurcation. For $\alpha < 0$, there is no equilibrium. There are other types of bifurcations associated to different transversality conditions, we introduce the trans-critical bifurcation.

Trans-critical bifurcation: If at the equiibrium $(x, \alpha) = (x_0, \alpha_0)$,

$$
\begin{aligned}
f_x(x_0, \alpha_0) &= 0 \\
f_\alpha(x_0, \alpha_0) &= 0 \\
f_{\alpha x}(x_0, \alpha_0) &\neq 0 \\
f_x^2(x_0, \alpha_0) &\neq 0
\end{aligned}
\tag{5.10}
$$

The bifurcation is a trans-critical bifurcation and the motion on the center manifold is described by,

$$
\dot{x} = \mu x - x^2 \quad (transcritical)
$$

The system possesses two equilibria for any value of α, one is stable and the other unstable (saddle if $n \geq 2$). The two points exchange stability at the bifurcation. This situation typically occurs if, due to some symmetries, the system possesses an equilibrium whatever the value of the parameter.

5.4   Bistable models and center manifold theory

Many n-dimensional bistable models have a geometry that straightforwardly generalizes the geometry of a planar bistable model: two stable equilibria and a saddle point with $n - 1$ attractive directions and one repulsive direction. The separatrix between basins of attraction of these equilirbia is a $n - 1$ dimensional manifold in the state-space. On this manifold must lie a saddle point. The Jacobian matrix of the system computed at the saddle point presents $n - 1$ negative eigenvalues associated with this separatrix, the stable manifold and 1 positive eigenvalue, λ_u associated with the unstable manifold that is the heteroclinic orbit that connects the equilibria.

As the system approaches a saddle node bifurcation in which one of the two attractors disappears, the positive eigenvalue λ_u goes to zero and the other eigenvalues remain strictly negative As all the non vanishing eigenvalues remain negative, the condition of stability of the center manifold is automatically satisfied and the system dynamics can be reduced to a one dimensional normal form describing its motion on the center

manifold. The motion on this center manifold is slow in the vicinity of the bifurcation resulting in latency in the convergence to the remaining stable attractor. These latencies depends on the distance of the system to the bifurcation.

Center manifold theory is a mathematical tool to traduce the intuitions formulated in Chapter 4 and extend them to any high-dimensional model. In this chapter, we linked the possibility to create switches with latencies, to the presence of a high ratio τ. The center manifold theorem provides a link between these notions. We should emphasize that latencies are induced by a local property, i.e. a saddle node bifurcation. Therefore, nothing imposes that the system is really presenting two stable attractors, and latencies could be observed for other types of systems presenting a saddle point with a large τ. However, the conditions of stability and presence of a center manifold are naturally satisfied by bistable models. We will see in Chapter 8 that these considerations are important.

Center manifold theory can also be applied to stochastic systems (Boxler, 1989).

5.5 Center manifold and normal forms for stochastic systems

A stochastic version of the center manifold theory has been proposed by Boxler (1989). More recently, a normal form procedure has been proposed to separate slow and fast modes in stochastic dynamical systems (Roberts, 2008) and simplify multiscale nonlinear dynamics. Interestingly, stochastic center manifold theory has been recently applied to the problem of computing the escape rates in a stochastic system with multiple time-scales (Forgoston and Schwartz, 2009).

In their work, Forgoston and Schwartz proposed two procedures to compute the stochastic center manifold. The naive procedure consists in computing the deterministic center manifold and add a noise vector to the right side of the equation describing the motion on this center manifold. The second procedures relies on the construction of a stochastic normal form that reduces the order of the system but also separates

slow and fast processes as proposed in Roberts (2008). Although this procedure is more accurate, it is particularly difficult to implement in practice. Moreover, Forgoston et al. showed that, 'because the noise effects occur at such a high order, the correction to the stochastic (naive) result is minimal (Forgoston and Schwartz, 2009).'

Let us assume that following a similar procedure to the ones proposed in Forgoston and Schwartz (2009); Roberts (2008), the system dynamics of a stochastich system can be reduced to its motion on its stochastic center manifold. We focus on the saddle node bifurcation. The problem of studying the noisy normal form:

$$\dot{x} = x^2 + k + \sqrt{2D}\xi(t) \tag{5.11}$$

where the parameter D denotes the noise intensity, and the gaussian white noise $\xi(t)$ obeys the autocorrelation function $< \xi(t), \xi(t + \tau) >= \delta(\tau)$, has been studied in Lindner et al. (2003). In this latter paper, the normal form is studied to estimate the mean escape time and coefficient of variation of a TypeI neuron described by the one-dimensional θ-model.

Let us study the normal form (5.11).

if $k < 0$ The system possesses a saddle point and a stable equilibrium. For weak noise, $D << |\beta|^{\frac{3}{2}}$,

$$< \tau_d >= \frac{\pi}{\sqrt{|k|}}\exp\left[\frac{4|k|^{\frac{3}{2}}}{3D}\right]$$

This is the Kramer's escape rate for the potential $U(x, k) = -\dfrac{x^3}{3} - kx$ (Kramers, 1940).

if $k > 0$ In particular, for weak noise $D^{\frac{2}{3}} << k$, the distribution of the passage time can be approximated by a normal distribution whose mean and variance are given by:

$$\tau_d = \frac{\pi}{\sqrt{k}} \tag{5.12}$$

$$< \tau_d^2 >= \frac{3D\pi}{4k^{\frac{5}{2}}}$$

The coefficient of variation is then given by:

$$CV = \frac{\sqrt{< \tau_d^2 >}}{< \tau_d >} = \sqrt{\frac{3D}{4\pi}} k^{-\frac{3}{4}} \tag{5.13}$$

The coefficient of variation is the inverse of the signal to noise ratio.

5.6 Conclusion

Phenomena introduced in planar models of bistability have their counterpart in high-dimensional bistable models. Center manifold theory provides a mathematical framework that allows the study of these phenomena in high-dimensional, possibly stochastic systems. Generally, bistable models present a particular structure with a separatrix and a one-dimensional unstable manifold. Because of this particular structure, phenomena such as reversibility and latencies are likely to be observed in these systems for large τ. This situation typically occurs when the system is close to a bifurcation. With regard to the analysis presented in this chapter and in the previous one, a local analysis of the saddle point should help to quantify the switch performance. In particular, the design of a bistable model could be based on specifications of its saddle point.

Robustness and performance
in dynamical models of cellular switches

From the theoretical analysis of Chapters 4 and 5, we learned that saddle points and saddle nodes are key rulers of the decision-making process in bistable models. This section presents a local analysis of three published models of deterministic cellular switches. The analysis is first applied to a small model of the apoptotic switch proposed by Eißing et al. (Eissing et al., 2004), then to a larger model of the apoptotic switch by Schliemann et al. (Schliemann et al., 2007) and finally to a model of long term potentiation proposed by Aslam et al. (Aslam et al., 2009). Because in all these three models, the switch is triggered by a transient signal (pulse-like), we apply our analysis at the saddle point. The local analysis sheds light on the mechanism governing the switch between stable steady-states and is used to quantify the robustness of the process to parametric perturbations. The results are compared with results from non local analyses.

6.1 Apoptosis

As introduced in Chapter 1, apoptosis, the cellular death is characterized by the activation of specific enzymes called effector capsases which participate to the dismantlement of the cell (Elmore, 2007; Green and Evan, 2002; Wolf and Green, 1999). Caspases, present in a latent form in the cell cytosol are activated by proteolysis, i.e the cleavage of chemical bounds in the protein. Activation of effector caspases can be initiated through several pathways (Elmore, 2007; Green and Evan, 2002; Wolf

and Green, 1999). The intrinscic pathway relies on the formation of pores in the outer membrane of mitochondria leading the release of particular signalling proteins including cytochrome c and Smac/DIABLO in the cytosol (Saelens et al., 2004). The cytochrome c binds to other proteins to form the apoptosome, a complex which recruits and triggers the activation of initiator which in turn activate effector caspases (Hill et al., 2004). The permeabilization of the outer membrane is regulated by proteins of the Bcl-2 family (Cory and Adams, 2002).

The activation of the extrinsic pathway is triggered by the fixation of specific ligands to proteins called death receptors. These death receptors are members of the tumor necrosis factor (TNF) receptor gene superfamily (Locksley et al., 2001). By the formation of a specific complex called DISC (death inducing signalling complex), proteins are recruited to activate the initiator Caspase 8 which in turn activates the effector Caspase 3 (Kischkel et al., 1995; Scaffidi et al., 1999).

In the first section of this dissertation, we illustrated how the switch in effector caspases has been at the origin of the concept of switch in apoptosis. Let us recall the characteristics of the switch in the light of the previous chapters. The main characteristics of the apoptotic switch are reviewed in Spencer and Sorger (2011).

Experiments at the single cell level have revealed that the activation of effectors caspases is an all-or-none phenomenon (Rehm et al., 2002; Tyas et al., 2000). At the population level, the response is graded (Hentze et al., 2002; Scaffidi et al., 1998). This graded response can be explained in term of the variability in the timing the cell triggers the switch. Recent experiments have shown that this variability does not seem to have a genetic origin but conversely to rely on the differences in initial concentration of proteins present in the cell (Spencer et al., 2009). These properties are consistent with the presence of a bistable switch in the apoptotic process. Indeed, in bistable models, the presence of a threshold is natural. Because the stable manifold of the saddle acts a separatrix in the state space, the systems presents two behaviors which are robust to small perturbations. The switch can be triggered either by an input sufficiently large to make the system cross the separatrix or sufficiently large and long to induce a bifurcation of the resting state as

illustrated with the saddle node bifurcation. Bistable model have the additional property to induce variable latencies whose length depends on the strength of the input. These latencies are induced by a slow escape from the saddle point in its unstable manifold. This property is not only robust but enhanced in the vicinity of bifurcations of the resting state where the positive eigenvalue of the saddle λ_u vanishes, and the dynamics of the decision-making process is governed by the system dynamics on the center manifold. In the vicinity of these bifurcations, the vector field is small making the system very sensitive to perturbation and noise. Therefore, it is likely to observe variability in the switching time in a population of cells. This variability results in a graded response at the level of a population.

Whether bistability is essential or not to the apoptotic switch is a hypothesis which is still debated (Albeck et al., 2008). Furthermore, in bistable models, the bistability has been attributed to various steps in the apoptotic process (Bagci et al., 2006; Chen et al., 2007; Eissing et al., 2004; Legewie et al., 2006). Our goal in this section is not to identify the physiological cause of the switch in effector caspases. Rather, we try to show that the general principles discussed theoretically in the previous chapter are really encoded in models of the literature. In particular, we illustrate the role played by the saddle point and saddle node bifurcations in the switch dynamics. Our results show that a simple local analysis at the saddle point of these model can be used to estimate the global performance and robustness of the switch and identify parameters which are likely to modify the switch behavior.

6.1.1 8-dimensional model

The model of Eißing (Eissing et al., 2004) is a model of 8 ordinary differential equations with 19 kinetic parameters describing the activation of effector caspases in the exrtinsic pathway. In this model, the activation of the initiator caspase C8 is enhanced through a positive feedback loop with the effector caspase C3, see Figure 6.1. In this model, two inhibitors of apoptosis IAP and CARP can link to caspases to avoid apoptosis.

Eißing et al proposed an input-ouput version of the model. The input

affects the concentration of activated initiator caspases $C8^*$ while the ouput is related to the concentration of activated effector caspases $C3^*$. In the present analysis, the input signal directly acts on the number of initiator caspases that become activated ($C_8 \rightarrow C_8^*$) rather than an extra inflow of active initiator caspases. This slight modification with respect to Eissing et al. (2004) has been chosen to better describe the effect of a pro-apoptotic signal but the same results hold for the original input. For nominal parameter values, the system exhibits three steady-states with non-negative concentrations, two stable points corresponding to life and death and a saddle point, see Table 6.1. We can notice that concentrations at the stable life equilibrium are very close to concentrations at the saddle point. For impulse signals above 75 mol/cell, the cell switches from life to death. These results agree with the analysis of Bullinger (2005). For inputs above the threshold, the cell presents a delay before the switch. This delay depends on the strength of the input signal, see Figure 6.2 where the output, i.e the number of molecules of activated caspase 3, C3* has been normalized. The output is equals to zero in the unexcited state and equals to one in the exited state.
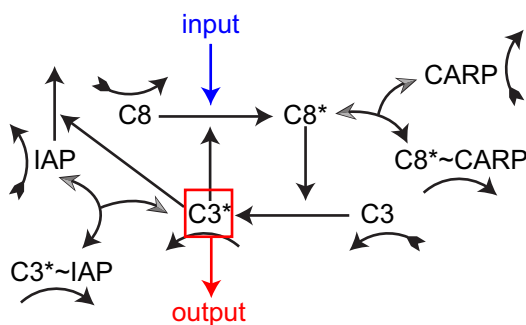
Figure 6.1: Model of Eißing. In response to a pro-apoptotic input signal, initiator caspases C8 become activated and activate the effector caspase C3. Activated C3, C3*, activate C8 in return through a positive feedback loop. Inhibitors CARP and IAP bind to C8* and C3* to prevent apoptosis.

	x_{life}	x_{saddle}	x_{death}
C8*	0	0.4900	74380
C3*	0	0.3900	5162
C3*−IAP	0	34.2400	2999
IAP	40000	39550	264
C8	130000	129870	9132
C3	21000	20850	19
CARP	40000	39492	21
C8*−CARP	0	40	3457

Table 6.1: Concentrations at equilibria for the model of Eissing et al. (2004) in molecules per cell.

Local analysis at the saddle point

The model of Eißing (see Appendix A.1) linearized at the saddle point has one real positive eigenvalue λ_1, and 7 negative ones $\lambda_2 \ldots \lambda_7$. The ratio, τ between the slowest negative eigenvalue $-\lambda_s$ and the positive one, λ_u is high (≈ 10), see Table 6.2. As illustrated on Figure 6.3, trajectories which start close to the separatrix corresponding to the switching threshold converge to the vicinity of the saddle point before slowly escaping along the unstable manifold of the saddle to asymptotically reach one of the two stable equilibria, see Figure 6.3. The slow escape from the saddle produces a mechanism of input-strength dependent latencies as it was previously observed on the two dimensional system. Long transients are reflected by the small value of λ_u at the saddle with respect to the other eigenvalues at this point and the high ratio τ.

$-\lambda_s$	λ_u	τ
-0.0011	1.08e-04	9.9897

Table 6.2: Model of Eißing: Eigenvalues and ratio τ

The cumulative sensitivity $\bar{s}_p$ computed at the saddle point shows that the saddle is insensitive to the parameters k_4, k_5 and k_6 (see Appendix A.1), the ones controlling the degradation of free activated caspases C3* and C8* and the active degradation of the inhibitor IAP by C3*, see Appendix A.1. This local sensitivity analysis is compared with the
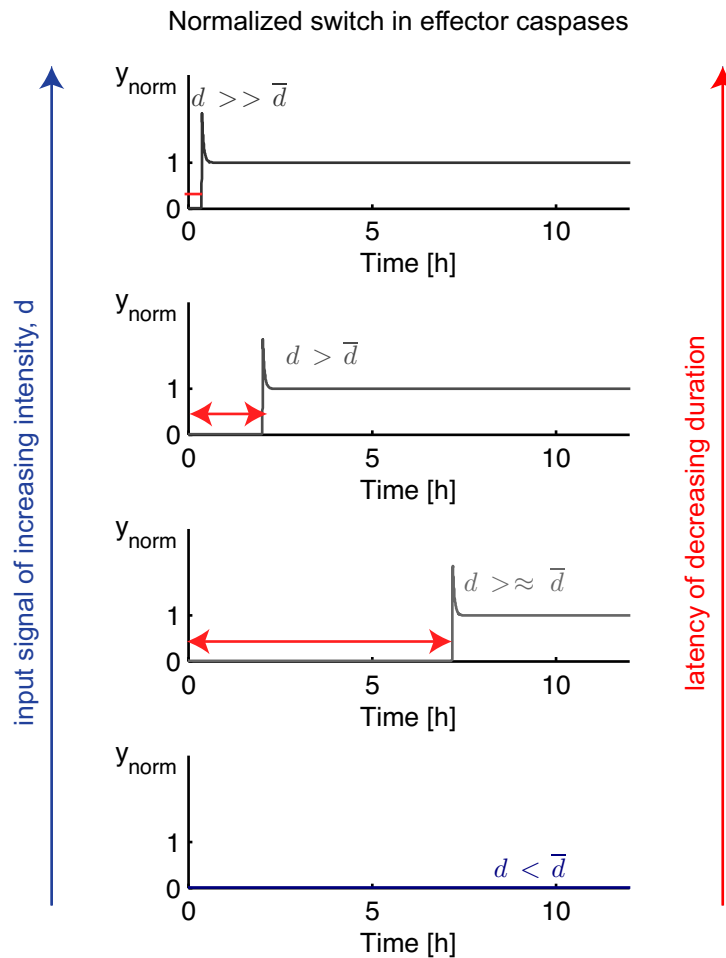
Figure 6.2: Input-strength dependent latencies in the model of EIßing. For inputs above the threshold $\bar{d}$, the system switches to the death state characterized by a high concentration of effector caspases. Trajectories have been normalized such that the concentration of $C3^*$ equals zero in the life state and equals one in the death state. Trajectories are depicted for inputs corresponding to an increasing percentage of the threshold (input = 0.5 (blue), 1.05 , 1.1 and 1.5 times the switching threshold). The latency is long for inputs close to the threshold and then is shortened as the input signal increases.
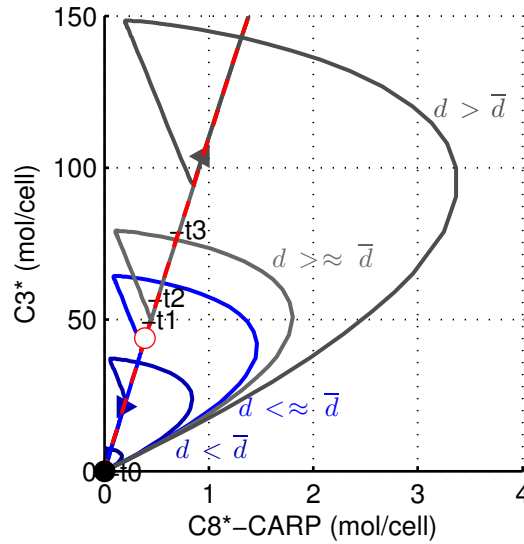
Figure 6.3: Two-dimensional projection of state space trajectories in a 8-dimensional model of apoptosis proposed by Eissing et al. (2004). Trajectories starting close to the stable manifold of the saddle point quickly converge to the neighborhood of the saddle where there are delayed before converging to the excited state leading to latencies in the decision making process.

result of a non local robustness analysis, the DOR analysis proposed by (Ma and Iglesias, 2002) and introduced in Chapter 3. The degree of robutsness (DOR) of a bistable model with respect to a particular parameter $k > 0$ (all remaining parameters being fixed) is defined by the expression (3.1), i.e.:

$$\text{DOR} = 1 - \max\left\{\frac{k_{\min}}{k}, \frac{k}{k_{\max}}\right\} \tag{6.1}$$

where $(k_{\min}, k_{\max}) \subseteq (0, \infty)$ denotes the range of bistability. A degree close to one means that the system is very robust to parameter k and a degree close to zero means that it is very sensitive to this parameter. For the model of Eißing, we computed the range of bistability for each parameter by drawing the corresponding diagram of bifurcation with the

software XPP-AUT (Ermentrout, 2002).

This analysis shows that the system is particularly robust to the parameters k_4, k_5 and k_6, thus to the ones with low sensitivities at the saddle point. Conversely, the bistability is not robust to parameters with high sensitivities. The good match between both analyses reveals the predictive power of the local sensitivity analysis at the saddle point to estimate the robustness of the bistable behavior. Interestingly, the three insensitive parameters control the degradation of free caspases suggesting that free caspases are not involved in the death decision making process. Instead, the slow dynamics at the saddle point are mostly governed by inhibitors.
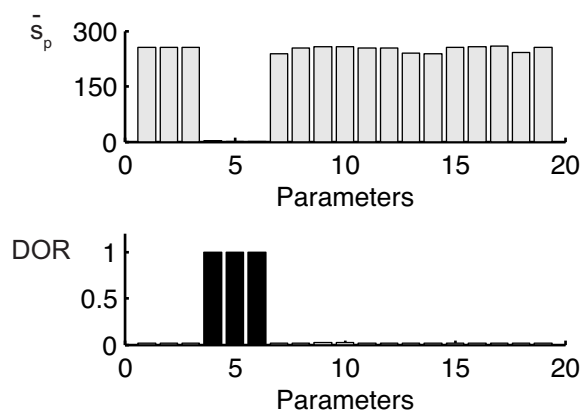
Figure 6.4: Model of Eissing et al: comparison between local sensitivity analysis and DOR analysis. Results of the local sensitivity analysis matches the results of the DOR analysis: parameters with a low sensitivity at the saddle point have a high degree of robustness (DOR) (black) while parameters with a high sensitivity have a low DOR (light gray). Parameters are represented by their rank in the table A.1.

Figure 6.5 is a comparison of the local sensitivity analysis when performed at the stable life (top), saddle (center) and stable death (bottom) equilibria. The life state has null concentrations making impossible the normalization of sensitivities by the concentrations at this state. In order to overcome this problem and compare sensitivities between them, we normalized the sensitivities not by concentrations at each equilibrium

but by the maximal concentration between all these three equilibria. Therefore the normalization is the same for each equilibrium. This sensitivity measure is called $\tilde{s}_p$. Results are depicted on Figure 6.5. By contrast to the local sensitivity analysis at the saddle (center), local sensitivity analyses at stable equilibria (top and bottom) fail to capture the robustness of the switch. Comparison with the results of diagrams of bifurcation (not shown) reveals that the life state is an equilibrium of the system whatever the values of the parameters. The stability of this equilibrium changes when it meets the saddle in a trans-critical bifurcation, making the system switch to the death state for arbitrarily small perturbations.
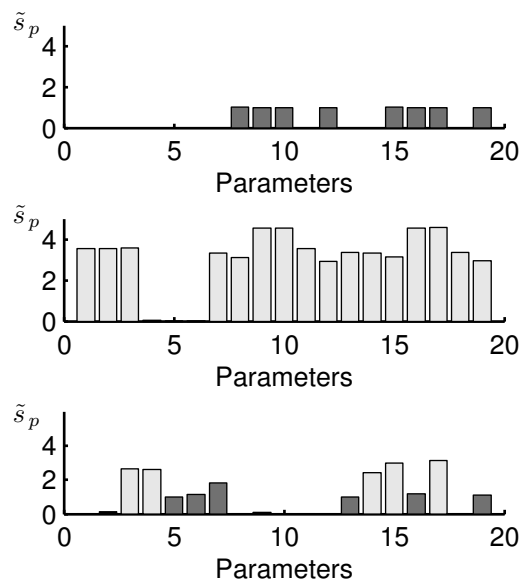
Figure 6.5: Model of Eissing et al: local sensitivity analysis at equilibria. Sensitivities are normalized by the maximal concentrations observed at steady-state. The analysis is performed at the life stable equilibrium (up), the saddle point (center) and the death life state (down). The sensitivity analysis at the life stable equilibria (up) fails to capture the sensitivity of the switch to a given set of parameters including the parameters which control the positive feedback loop between the activated Caspase 3* and Caspase 8* and the sensitivity to IAP (see the comparison of the DOR analysis for parameters k_1, k_2, k_3). The sensitivity at the death equilibrium (bottom) does not capture the sensitivity to degradation of inactivated Caspase 3, Caspase 8 and the IAP and CARP inhibitors (see parameters k_8 to k_{12}).

6.1.2 37-dimensional model

The model by Schliemann et al. is a large model of apoptosis (Schliemann et al., 2007) describing the pro- and anti-apoptotic signaling pathways induced by the stimulation with the cytokine TNF, see Figure 6.6. On the one hand, TNF enhances the activity of NF-κB, an important transcription factor for anti-apoptotic proteins. On the other, TNF internalizes and then activates the initiator caspase Caspase 8, which is part of a positive feedback loop of mutual activation of Caspase 8, Caspase 3 and Caspase 6. In the input-output version of the system, the input modifies the initial concentration of TNF while the output is chosen as the concentration of activated Caspase 3.

For nominal parameter values, see Appendix A.1, the model has a total of 37 states and is also bistable with a saddle point having only one positive eigenvalue, which furthermore is the smallest one in absolute values, see Figure 6.7 and Table 6.3. The ratio τ is less pronounced here, approximatively a factor two.

The switch is delayed for impulse inputs close to the input threshold, see Figure 6.9 for simulations with various input intensities around the threshold level $\bar{d}$. The delayed decision making is particularly pronounced for inputs slightly above the threshold, where the latency is quite significant (about one day). This is well predicted by the local analysis which shows that the positive eigenvalue at the saddle point is particularly small with respect to the magnitude of other eigenvalues at the linearization (Figure 6.7). Visualizing the trajectories in the state space (Figure 6.8) illustrates the importance of the saddle point and of its unstable manifold. Inputs close to the transition threshold result in trajectories that first converge to the proximity of the saddle point before diverging along the unstable manifold. Because of a smaller τ value than in the model of Eißing, the convergence is less pronounced for inputs not very close to the threshold.

$-\lambda_s$	λ_u	τ
-5.6e-05	2.6e-05	2.2

Table 6.3: Model of Schliemann: Eigenvalues and ratio τ

Figure 6.6: Pro and anti-apoptotic signaling pathways in the model of Schliemann et al. The picture has be redrawn from Schliemann et al. (2007) in accordance with the terms of the Creative commons attribution license.

Figure 6.11 shows the relative sensitivities at saddle point. As the saddle presents zero concentrations at steady-state, we use two methods of normalization. The first one consists in computing $\bar{s}$ and summing sensitivities on non-zero steady states (Figure 6.10) and the second one is the $\tilde{s}$ sensitivity introduced previously (Figure 6.11). Let us remark that, in this case, if a concentration is null for every steady-state, it is replaced by its maximal concentration over a trajectory.

Figure 6.7: Magnitude of the eigenvalues of the Jacobian matrix computed at the saddle point in Schliemann et al. (2007), the stable ones are depicted in black while the unstable one is depicted in red. The inlet zooms in on the three slowest eigenvalues.

For the two methods, the general qualitative picture is similar. In both cases, the linearized system is particularly sensitive to the parameters controlling the degradation of NFκB and the transcription, degradation and translation of I$\kappa\beta\alpha$ and to reactions which involve the caspases and their inhibitors while it is quite robust to parameters controlling the reactions that govern the binding of the ligand to the receptor. Softwares such as XPP-AUT have difficulties to handle a 37 dimensional model. Instead, we estimated the DOR manually by perturbing one parameter at a time and checking that the system is still bistable through numerical simulation, i.e by checking numerically that the system still possesses two stable equilibria. The DOR analysis correlates well with the sensitvities depicted on Figure 6.10. Almost all the parameters (all except the parameters 6 and 7 related to NFκB) presenting a light gray histogram, i.e histograms associated with parameters having a large sensitivity at saddle point have a $DOR \leq 0.75$. At the opposite, black histograms, associated with parameters presenting a low sensitivity at saddle point have a $DOR \geq 0.95$. The parameters with the lowest degree of robustness are associated to reactions associated with the positive feedback loop between initiator and effector caspases ($DOR \leq 0.5$). As for the model of Eißing, sensitivity analysis at the saddle point is a good predictor of the robustness of the bistable behavior. The comparison with the sensitivities at the stable steady-state shows that, as for the model of Eissing, this measures does not capture the sensitivity to the positive feedback loop between Caspase 3 and Caspase 8 (see parameters related to caspases in 6.12). This is not really surprising in the sense that the model has a similar positive feedback loop to the model of Eißing which
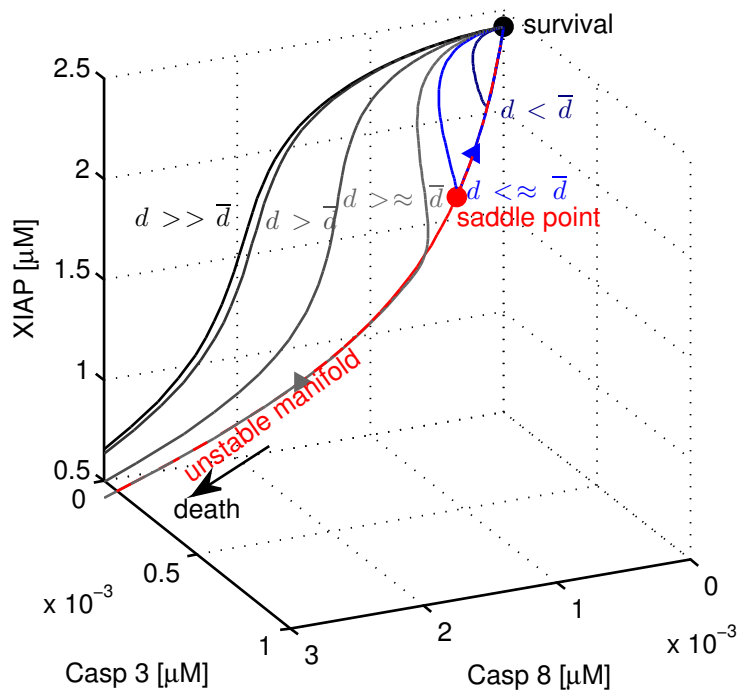
Figure 6.8: Three-dimensional projection of state space trajectories in a 37-dimensional model of apoptosis proposed by (Schliemann et al., 2011). Output trajectories for impulse inputs, slightly below (light blue curve), slightly above (light grey curve), above (dark grey curve) and significantly above (black curve) the decision making threshold, $\overline{d}$. Trajectories passing close to the saddle point are delayed. Trajectories follow the unstable manifold of the saddle point (red dashed curve) before reaching the survival or the death state.

is embedded in a higher dimensional model. The local sensitivity analysis at the saddle suggests an essential role for caspases and inhibitors in the control of the switch from life to death in agreement with a recent analysis of the system based on experimental data (Schliemann et al., 2011). Also the sensitivity analysis seems to give interesting results on the parametric robustness of the bistable behavior, it would

require further investigation. For example, we could test the effect of the normalization on the sensitivity of the system.

Figure 6.9: Input-strength dependent latencies in the model of Schliemann et al. For inputs above the threshold $\bar{d}$, the system switches to the death state characterized by a high concentration of activated effector caspases. Trajectories have been normalized such that the concentration of activated effector caspases equals zero in the life state and equals one in the death state. Trajectories are depicted for inputs corresponding to an increasing percentage of the threshold (input = 0.5 (blue), 1.05, 1.1 and 1.5 times the switching threshold). The latency is long for inputs close to the threshold and then is shortened as the input signal increases.

Figure 6.10: Sensitivity analysis at saddle point for the model of apoptosis proposed by Schliemann et al. (Schliemann et al., 2007). The parameters have been divided in three sets. The first one includes the parameters controlling the reactions involving the binding of TNF to receptor, the second one the parameters controlling the activity of NF-κB and the last one the parameters linked to the reactions governing caspases and their inhibitors. The sensitivity is normalized by the non-zero concentrations at the saddle point.
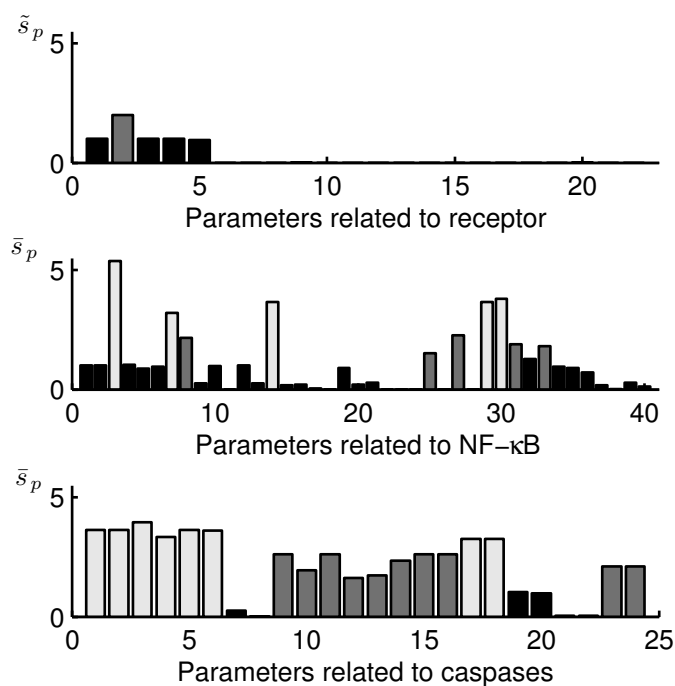
Figure 6.11: Sensitivity analysis at saddle point for the model of apoptosis proposed by Schliemann et al. (Schliemann et al., 2007). The parameters have been divided in three sets. The first one include the parameters controlling the reactions involving the binding of TNF to receptor, the second one the parameters controlling the activity of NF-κB and the last one the parameters linked to the reactions governing caspases and their inhibitors. The sensitivity is normalized by the maximal concentration at the three equilibria.
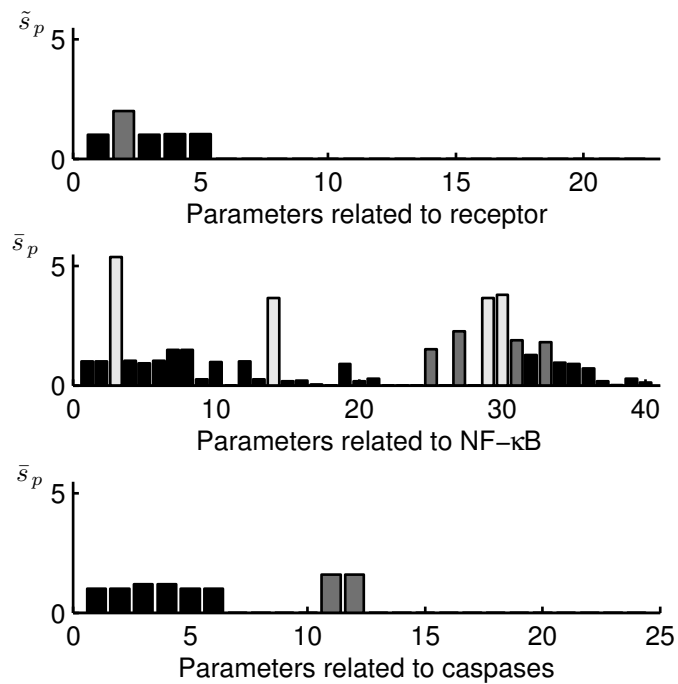
Figure 6.12: Sensitivity analysis at the life equilibrium for the model of apoptosis proposed by Schliemann et al. (Schliemann et al., 2007). The parameters have been divided in three sets. The first one include the parameters controlling the reactions involving the binding of TNF to receptor, the second one the parameters controlling the activity of NF-κB and the last one the parameters linked to the reactions governing caspases and their inhibitors. The sensitivity is normalized by the maximal concentration at the three equilibria.

6.2   Model of long-term potentiation

This section shows the results of our local analysis to a model of long term potentiation proposed by Aslam et al. (Aslam et al., 2009). Long term potentiation (LTP) describes the long-lasting increase in synaptic strength described in learning and memory processes (Frey and Morris, 1997). Aslam et al. proposed a model of late LTP (L-LTP) in agreement with experimental data where long term potentiation is achieved thanks to the presence of a bistable switch resulting from the molecular loop between the kinase (α-CaMKII) and the translation regulation factor (CPEB1), see Figure 6.13. The protein α-CaMKII can be in one of three states: inactive (X), active (X^A) and phosphorylated (X_p^A). When active and phosphorylated, α-CaMKII phosphorylates CPBE1 which in return initiates the translation of a new α-CaMKII protein. This creates a positive feedback leading to a fast increase of the total concentration of α-CaMII. For biologically plausible parameters values (see Appendix A), the 10-dimensional ODE model is bistable. The induction of L-LTP is modeled by a brief pulse (10 seconds), which transiently increases the basal level of $(Ca^{2+})_4$-CaM. For weak pulses, the system returns to the initial steady state corresponding to low concentration of total CaMKII. For stronger pulses, the system switches to the other steady state and the total concentration of CaMKII increases to approximately twice its basal level, see Figure 6.14 where the output has been normalized.

We numerically found a saddle point and computed the eigenvalues of the Jacobian matrix at this point, see Figure 6.15 and Table 6.4. All the eigenvalues are real with $\lambda_u > 0$, the slowest eigenvalue. As for the models of Eißing and Schliemann, the unstable manifold of the saddle point is one-dimensional. The ratio τ is smaller than for the model of Eißing but sufficient to ensure the local attractivity of the unstable manifold and observe latencies in the switch for inputs close to the threshold, see Figure 6.14.

$-\lambda_s$	λ_u	τ
-0.0013	4.04e-04	3.3

Table 6.4: Model of Aslam: Eigenvalues and ratio τ
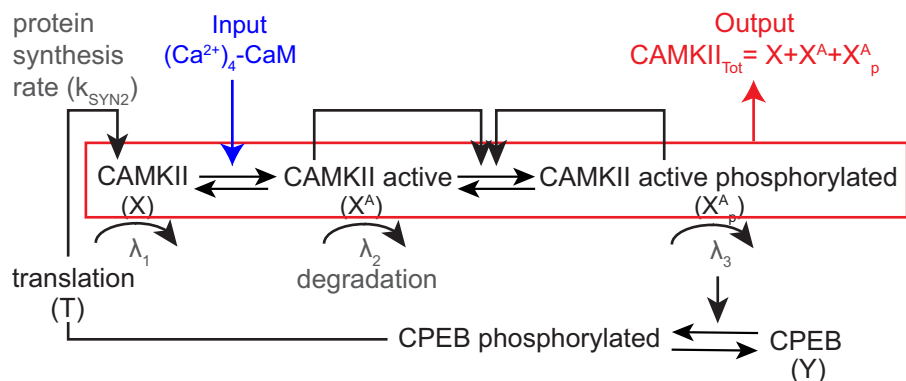
Figure 6.13: Model of Aslam et al. The model describes the positive feedback loop between the protein α-CaMKII and the translation factor CPEB1. The protein α-CaMKII can be in one of three states: inactive (X), active (X^A) and phosphorylated (X^A_p). When active and phosphorylated, α-CaMKII phosphorylates CPBE1 which in turn can initiate the translation of a new α-CaMKII protein (Aslam et al., 2009)

.

The local sensitivity analysis at the saddle point correlates well with the degree of robustness: parameters with high sensitivities have a low degree of robustness while parameters with low sensitivities have a high degree of robustness, see Figure 6.16[1].

We looked at the effect of a parametric perturbation on the switch. We chose a set of parameters with different sensitivities at the saddle point and perturbed one parameter at a time. Then we computed the new switching threshold $\bar{d}$ and simulated the system for increasing inputs above this new threshold $\bar{d}$. Simulations show that both the switching threshold and the delay durations are mostly affected by the sensitive parameters at the saddle point, such as the basal level of $(Ca^{2+})_4$-CaM (parameter 22) and the rate of activation of CaMKII k_1 (parameter 1), see Figure 6.17. By contrast, the switch is insensitive to modification of the protein synthesis rate kSYN2 (parameter 20).

---

[1]The relative sensitivity of parameters 27 and 28 is not shown as these parameters are equals to zero in the nominal model
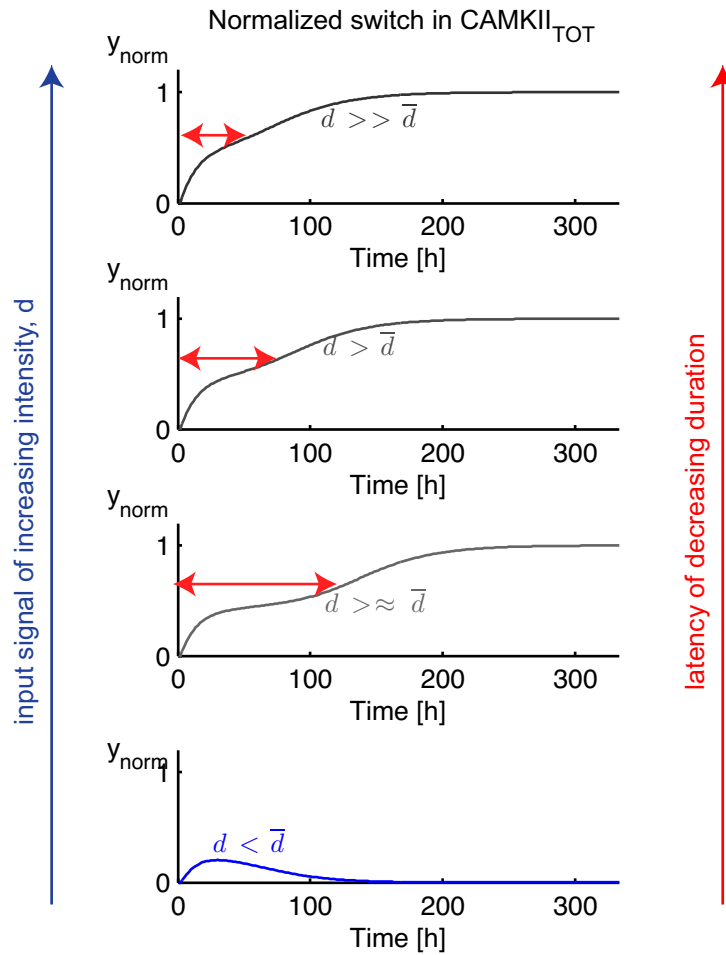
Figure 6.14: Latencies in the model of Aslam et al. (2009).

As previously illustrated in dimension 2, delayed decision making is enhanced close to a saddle node bifurcation where the ratio τ is generally high. In the model of Aslam, the ratio τ is not so large. We decided to test the system's behavior when we increase the ratio τ. This is illustrated by modifying the initial value (control) of parameters $(Ca^{2+})_4$-CaM, kSYN1, k_1 and putting them close to their value at bifurcation, $(Ca^{2+})_4$-CaM$_c$, kSYN1$_c$, k_{1c}, see Figure 6.18. As predicted by our analysis, the mechanism of delayed-decision making is enhanced
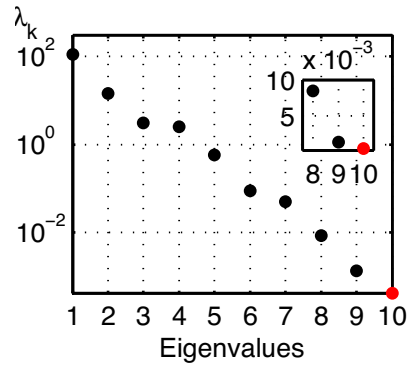
Figure 6.15: Magnitude of the real part of the eigenvalues of the Jacobian matrix computed at the saddle point for the model of Aslam et al. (2009) : the stable ones are depicted in black while the unstable one is depicted in red. The inlet zooms in on the three slowest eigenvalues.
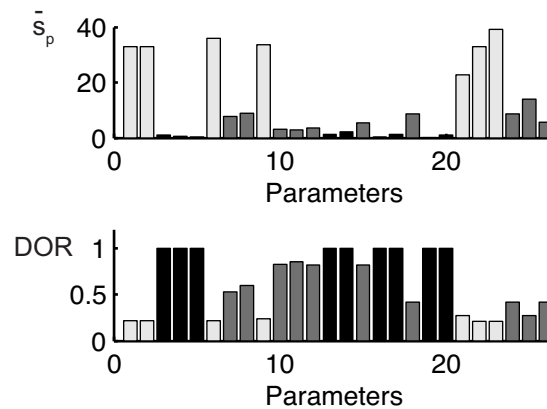
Figure 6.16: Model of Aslam et al: comparison between local sensitivity analysis and DOR analysis. Results of the local sensitivity analysis matches the results of the DOR analysis: parameters with a low sensitivity at the saddle point have a high degree of robustness (DOR) (black) while parameters with a high sensitivity have a low DOR (light gray).

when a parameter is pushed close to a value corresponding to saddle node bifurcation. This illustrates the possible trade-off between a switch with input-dependent latencies and robustness.
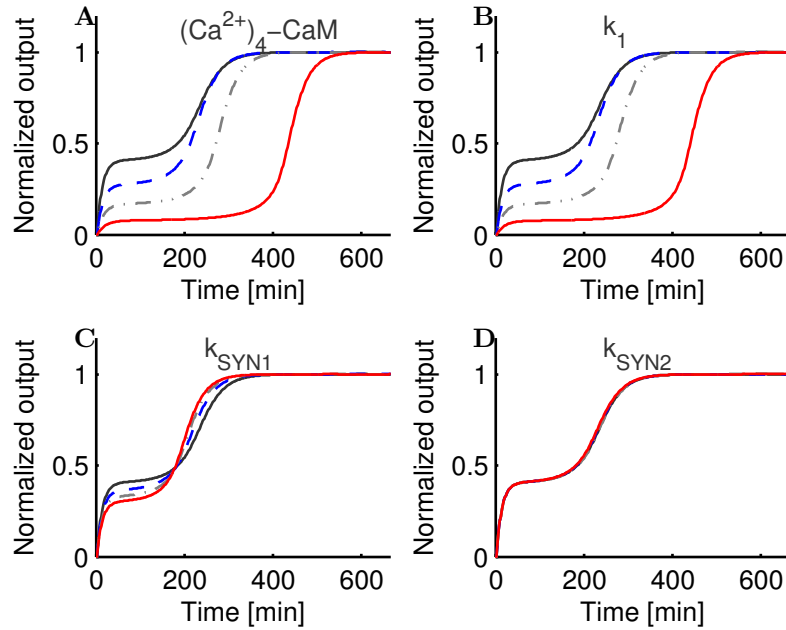
Figure 6.17: Parameter perturbation of the model of Aslam et al. Aslam et al. (2009). (A)-(D) The switching is depicted for nominal values of the parameters (black curve), 10 % of parameter perturbation (blue dashed curve), 20 % (gray dashed-dotted curve) and 30 % of variation (red curve). The system is simulated for an input slightly above the threshold, i.e $d = 1.01\bar{d}$, where the threshold $\bar{d}$ is recomputed for each parameter perturbation. (A) $(Ca^{2+})_4$-CaM (parameter 22), (B) k_{SYN1} (parameter 18), (C) k_1 (parameter 1) and (D) k_{SYN2} (parameter 20). Both the switching threshold and time are affected by perturbation of parameters $(Ca^{2+})_4$-CaM and k_1. In contrast, the switching threshold and time are insensitive to a perturbation of parameter kSYN2.
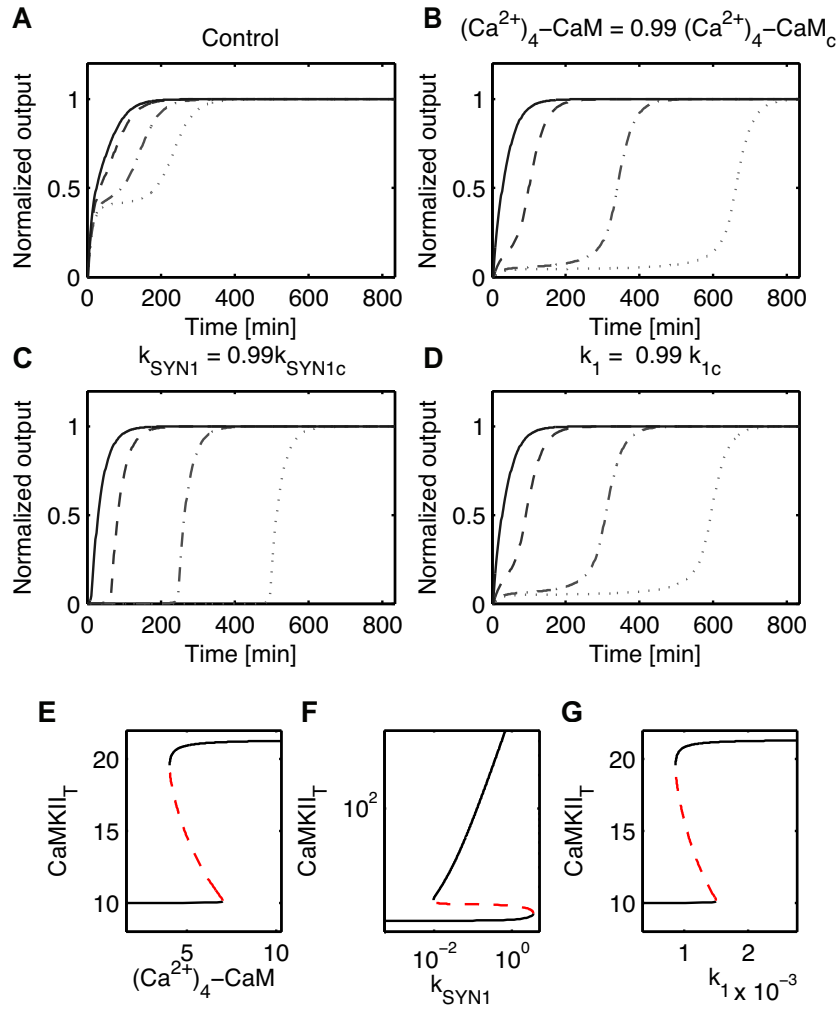
Figure 6.18: Influence of the distance to a bifurcation on the switching for the model of Aslam et al. Aslam et al. (2009). (A)-(D) Switching responses for the Aslam model for different input intensities d, above the threshold $\overline{d}$: $d = 1.01\overline{d}$ (dotted line), $d = 1.1\overline{d}$ (dashed-dotted line), $d = 2d$ (dashed line), $d = 10d$ (solid line). (A) Nominal model. (B)-(D) Perturbed models with single parameter set to 0.99 of its upper bifurcation value. (E)-(G) Bifurcation diagrams for the parameters $(Ca^{2+})_4$-CaM, k_{SYN1} and k_1. (B) and (E) $(Ca^{2+})_4$-CaM, (C) and (F) k_{SYN1}, and (D) and (G) k_1.

6.3   Conclusion

Sensitivity analysis is routinely applied to systems linearized around a stable equilibrium point in order to test the parametric robustness of the model. Here, we studied the sensitivity around an unstable equilibrium point to analyze the parametric robustness of a bistable decision process. Performing a local analysis around an unstable equilibrium point may seem of little relevance since it does not correspond to an experimental condition. However, it was shown in Chapter 4 and 5 that the saddle point is a key ruler of the transient behavior of bistable decision processes and has a central position in diagrams of bifurcations. In addition, the theoretical analysis predicts that the decision-making process is well described by the dynamics of the system on the one-dimensional slow unstable or center manifold when its attractivity is sufficient to force trajectories to pass close to the saddle point. As discussed in Chapter 5, this condition should be naturally satisfied by bistable models working close to a co-dimension one bifurcation of the saddle point with the resting state such as saddle node bifurcations.

We analyzed three previously published models of bistable switches and compared our results with results of non local methods such as diagrams of bifurcation and numerical simulations. For the three models, results of the local sensitivity analysis are good predictors of the results obtained with the non local methods. Local sensitivity analysis allowed us to identify the parametric perturbations that are the most likely to destroy the switch. In particular, in both models of apoptosis and for the set of nominal parameters proposed by original authors, the apoptotic switch is particularly sensitive to the parameters controlling positive feedback such as the parameters controlling the positive feedback loop between activated initiator Caspase 8 and effector Caspase 3. This result is in agreement with previous analyses of the models which identified the complexes caspases-inhibitors as key rulers of the decision making process (Bullinger, 2005; Eissing et al., 2005). Our analysis also reveals that the simple mechanism to create switches with latencies introduced in dimension 2 is robust and implemented in higher dimensional models of the litterature. In apoptosis, recent experiments suggest that the variability in the duration of the latent period has a non-genetic origin and depends on the protein levels in the cell (Spencer et al., 2009).

These results are well captured by the proposed mechanism where the variability of the delay depends on the initial concentration of enzymes involved in the death process and the way trajectories are attracted and then repulsed by the saddle point.

A striking feature of the proposed analysis is that it captures important properties of bistable switches models beyond one important hypothesis of this chapter, i.e the assumption of a switch induced by impulse signals. Because of the ghost effect of the saddle point, our analysis in the vicinity of a saddle-node bifurcation applies beyond the bifurcation, that is, to models that are monostable and contain no saddle. This situation typically occurs when a step signal is sufficiently strong to make the system cross a bifurcation. For both impulse signals and step signals, the slow escape from the (ghost) saddle results in latencies in the switch, a phenomenon which is well illustrated by the small (or vanishing) value of the positive eigenvalue at the saddle with respect to the magnitude of other eigenvalues in the system.

The mechanism of delayed decision making has strong biological relevance because it is related to potential reversibility. In the state space, the long latency period of delayed decision takes place close to the separatrix of the basins of attraction. As a consequence, small perturbations have the ability to revert the switch during the entire latency period. This potential of reversibility might be particularly relevant for the long term potentiation model of Aslam. The importance of the model lies in its ability to reproduce experimental results, in particular to account for the different effects of applying inhibitors during the induction or the maintenance phase of L-LTP: if applied during the induction of L-LTP, protein synthesis inhibitors can block L-LTP but they do not reverse the potentiation when applied during the maintenance phase of L-LTP (Fonseca et al., 2006; Frey and Morris, 1997). Moreover blocking the αCaMKII activity stops the L-LTP induction phase but not the maintenance phase (Malinow et al., 1989; Otmakhov et al., 2004). These observations are completely consistent with our explanation that small perturbations can revert the decision during the latency period, i.e close to the saddle point in the state space, but not once the system has reached one of the two equilibria.
The results of this chapter have appeared in Trotta et al. (2010, 2012).

<div align="right">

Chapter 7

</div>

Organizing singularities

In this chapter we introduce the concept of organizing singularities. We highlight how singularities, locally organize bistability both in statespace and in parameter space. First we introduce the hysteresis singularity and show how this singularity provides a natural route to bistability in biological models. Then, we introduce the winged-cusp, a singularity that will be used to extend the concept of bistability to a switch between a stable equilibrium and a stable limit cycle.

7.1   Lessons learnt from the first part of the thesis

The first part of the thesis showed that despite the nonlocal nature of switches, important measures of performance are well characterized by a local analysis at the saddle point. The high ratio τ quantifies the timescale separation at the saddle and can be used as a likelihood measure of observing phenomena such as latencies or transient reversibility. A high ratio τ naturally occurs in the vicinity of co-dimension one bifurcations of the saddle point with the resting state. This means that a small perturbation is likely to push the system beyond the bifurcation point. Local sensitivity analysis at the saddle point is a simple way to identify the parametric perturbations which are the most likely to push the system beyond these bifurcations as supported by our comparison of sensitivity analysis with non-local methods of robustness on several models of the literature. However, in many bistable models, the switch through a saddle node bifurcation triggered by a constant input is a natural way to operate. This is not taken into account by our local sensitivity analysis because it involves non linear perturbations in the

parameter space. A better way of defining the robustness of a bistable switch for these bistable models, would be to mimic our use of a local tool to capture a non local phenomenon not only in the state space but also in the parameter space. This means that we would like to identify isolated points of high relevance in the parameter space. In this chapter, we introduce singularity theory and show how this theory can be used to deal with this problem.

7.2 A short introduction to singularity theory

The goal of this chapter is not to provide a full description of singularity theory but to extract concepts and methods which can be used in the analyzing of biological switches. Singularity theory is presented in Golubitsky and Schaeffer (1985).

The theory of singularity studies the problem of bifurcations in models with multiple parameters. By performing a particular reduction called the Lyapunov Schmidt reduction, the problem can be reduced to studying how the solutions of a single scalar equation,

$$g(x, \lambda) = 0, \quad x, \lambda \in \mathbb{R} \tag{7.1}$$

varies with the parameter λ. The variable x represents the state of the system while λ is the bifurcation parameter. The set of pairs (x, λ) satisfying 7.1 is called the *bifurcation diagram. Singular points* satisfy $g(x^*, \lambda^*) = \partial_x(x^*, \lambda^*) = 0$.

Definition 7.2.1. *A universal unfolding of $g(x, \lambda)$, is a parametrized family of functions $G(x, \lambda, \alpha)$, where α lies in the unfolding parameter space R^k, such that*

- *$G(x, \lambda; 0) = g(x, \lambda)$*

- *Given any $p(x)$ and a small $\mu > 0$, one can find an α near the origin such that the two bifurcation problems $G(x, \lambda; \alpha) = 0$ and $g(x, \lambda) + \mu p(x) = 0$ are qualitatively equivalent.*

- *k is the minimum number of unfolding parameters needed to reproduce all perturbed bifurcation diagrams of $g(x, \lambda)$. k is called the codimension of $g(x, \lambda)$.*

Following Golubitsky and Schaeffer (1985), we introduce the concept of *organizing center*.

Definition 7.2.2. *The notion of organizing center is used to describe an equation which occurs in a model for certain values of the parameters such that the universal unfolding of this equation generates many or all the bifurcations diagrams occurring in the physical problem.*

Unfolding parameters change the qualitative bifurcation diagram of $G(x, \lambda, \alpha) = 0$. In this theory, a distinction can be made between bifurcation and unfolding parameters. The methods impose a structure on the parameter space that can be useful to get a deeper understanding of the problem. Moreover, this method allows to get a quasi-global description of the model by performing a local analysis (Golubitsky and Schaeffer, 1985).

7.3 The hysteresis singularity

Let us consider the scalar equation:

$$g(x, \lambda) = 0 \tag{7.2}$$

and assume that (7.2) presents a singularity at $(x, \lambda) = (x_0, \lambda_0)$, i.e,

$$g(x_0, \lambda_0) = g_x(x_0, \lambda_0) = 0 \tag{7.3}$$

if in addition,

$$g_x^2(x_0, \lambda_0) = 0 \tag{7.4}$$

with,

$$\begin{aligned} g_\lambda(x_0, \lambda_0) &\neq 0 \\ g_x^3(x_0, \lambda_0) &\neq 0 \end{aligned} \tag{7.5}$$

then $g(x, \lambda)$ has a co-dimension 1 hysteresis singularity (Golubitsky and Schaeffer, 1985),

$$g(x, \lambda) = x^3 - \lambda \tag{7.6}$$

with universal unfolding,

$$G(x, \lambda, \alpha) = x^3 - \lambda + \alpha x \tag{7.7}$$

Figure 7.1 shows the solution of 7.7 for different values of the bifurcation parameter γ and the unfolding parameter α. The singularity occurs at $\alpha = 0$. For $\alpha > 0$, the system is monostable. For $\alpha < 0$, two saddle-node bifurcations appear. The system has two stable equilibria and a saddle point for a specified range of the bifurcation parameter λ. The distinction between the bifurcation and the unfolding parameter is important. When $\alpha > 0$, the system can not be bistable whatever the value of λ. Therefore, identifying an hysteresis singularity and the corresponding unfolding parameter in a model where bistability is suspected is a way to identify the mechanism that gives rise to the bistable behavior in the system.
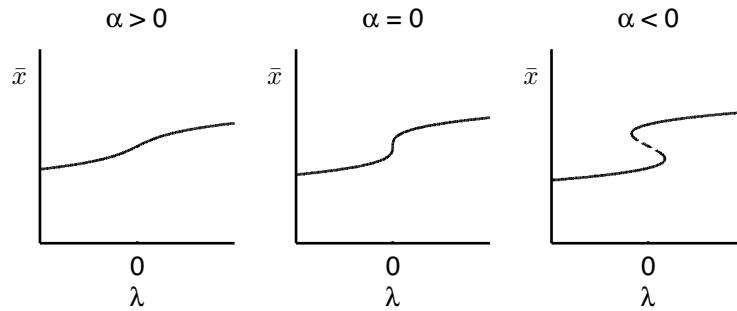
Figure 7.1: Hysteresis singularity.

7.3.1 Hysteresis singularity in the model of Griffith

Consider the model of Griffith introduced in Chapter 2 with a constant input u,

$$
\begin{aligned}
\dot{m} &= -am + \frac{e^m}{K + e^m} + u = -am + \mathrm{sat}(e) + u \\
\dot{e} &= -be + m \\
y &= e
\end{aligned}
\tag{7.8}
$$

Let us analyze the static properties of the system. By posing $\dot{m} = 0$ and $\dot{e} = 0$, we get the static relation:

$$
bay = u + \mathrm{sat}(y)
$$
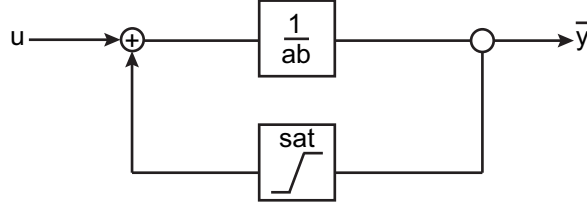
Figure 7.2: Block digram for the model of Griffith

which is described by the block diagram 7.2.

Defining $\gamma = ab$, the singularity conditions yields :

$$
\begin{aligned}
g(u, y) &= \gamma y - u - \text{sat}(y) &&= 0 \\
g_y &= \gamma - \partial_y \text{sat}(y) &&= 0 \\
g_{y^2} &= -\partial_{y^2}^2 \text{sat}(y) &&= 0
\end{aligned}
\tag{7.9}
$$

and

$$
g_u = -1 \neq 0 \tag{7.10}
$$

Replacing sat by its polynomial expression, we get for the conditions 7.9:

$$
\begin{aligned}
g_{(u, y)} &= \gamma y - u - \frac{y^2}{K + y^2} &&= 0 \\
g_y &= \gamma - \frac{2yK}{(K + y^2)^2} &&= 0 \\
g_{y^2} &= -\frac{2K(3y^4 + 2Ky^2 - K^2)}{(K + y^2)^4} &&= 0
\end{aligned}
\tag{7.11}
$$

The third condition in (7.11) imposes that the singularity occurs for a value of y^* corresponding to the inflexion point of $sat(y)$, y^*. Assuming $K > 0, y^* \geq 0$, we get,

$$
y^{*2} = \frac{-K \pm \sqrt{K^2 + 3K^2}}{3} \tag{7.12}
$$

which has two real solutions for $K > 0$. In this particular example, we fix $K = 1$. The only physical solution for y^* is $y^* = \frac{\sqrt{3}}{3}$.

At $y = y^*$, the second condition in (7.11) yields, $\gamma = \partial_y \text{sat}(y)|y = y*$, i.e the parameter γ should be equal to the slope of the *sat* function at $y = y^*$, γ_s,

$$\gamma_s = \frac{2Ky^*}{(K + y^{*2})^2} \tag{7.13}$$

Replacing y^* by $\frac{\sqrt{3}}{3}$ in our example with $K = 1$, we get $\gamma_s = \frac{3\sqrt{3}}{8}$.

By posing $\alpha = \gamma - \gamma_s$ in the first condition of 7.11, we get the input-output relation curve depicted on Figure 7.3. The parameter α is the unfolding parameter while the parameter u is the control parameter. To be bistable, it is required that $\alpha < 0$, i.e $\gamma = ab < \gamma_s = \frac{3\sqrt{3}}{8}$ and γ_s represents the slope of the saturation function at y^*, i.e at the inflexion point.

In the model of Griffith (Griffith, 1968), this slope increases with the level of cooperativity while a and b represents respectively the rates of degradation of the mRNA and the protein. If the product of the rates of degradation is too high with respect to the level of cooperativity, the system will only show one stable steady-sate for each value of the input u. Conversely, if the degradation is slow with respect to the level of cooperativity, the system will exhibit bistability for a given set of inputs.

For $\alpha < 0$, the system presents two branches of stable equilibria connected through a branch of saddle points. For α slightly below 0, we can notice that the input value corresponding to the saddle node bifurcation of the resting state (lower branch) is very close to $u = 0$. The singularity condition imposes the presence of an inflection point in the feedback of the protein on the mRNA. This inflection point can be achieved if the feedback is sigmoid, i.e if it implies a cooperative mechanism, or a Hill function with $n \geq 2$ as it was already stated by Griffith (Griffith, 1968).

7.3.2 Hysteresis singularity and switch robustness

The theory of singularity deals with multi-parametric systems. However, all the parameters are not considered as being equal in the system. This concept is clearly illustrated by the hysteresis singularity. At the beginning of this section, we discussed the fact that the definition of
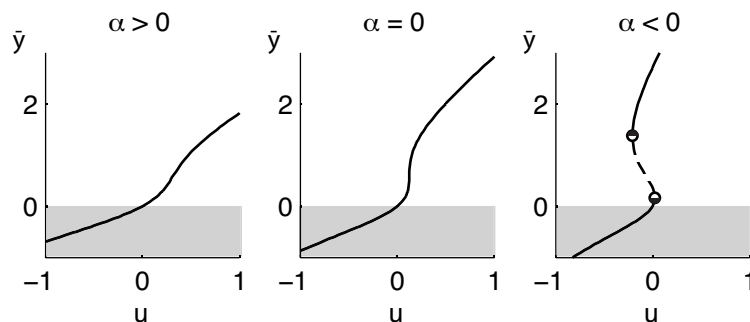
Figure 7.3: Hysteresis singularity in the model of Griffith

robustness is not suited for systems where the switch is triggered by an input moving the system from one-side to the other of a local bifurcation of the resting state. The example of the hysteresis singularity shows that is it possible to provide a different definition of robustness. Indeed, if u is the input of the system, identifying the distance of an unfolding parameter to the hysteresis singularity is a way to estimate the robustness of the switch. Indeed, if the unfolding parameter becomes positive, the system exhibits monostability for any value of the input and looses its capacity to encode a two-dimensional all-or-none decision-making process.

In the model of Griffith, the singularity theory predicts that the system is monostable if the degradation of proteins is sufficiently strong with respect to the cooperative behavior. In order to test if this prediction is a general principle, we tested the effect of increasing the parameter λ in the model of Aslam, i.e the parameter controlling the degradation of the different forms of CaMKII. Results show that if this parameter is increased, the system switches from bistability to monostability (Figure 7.4).

7.4 The winged cusp

Singularity theory not only allows to 'localize' the analysis of the switch in the parameter space. It also provides a way to generalize our analysis of decision-making processes to more general forms of bistability.
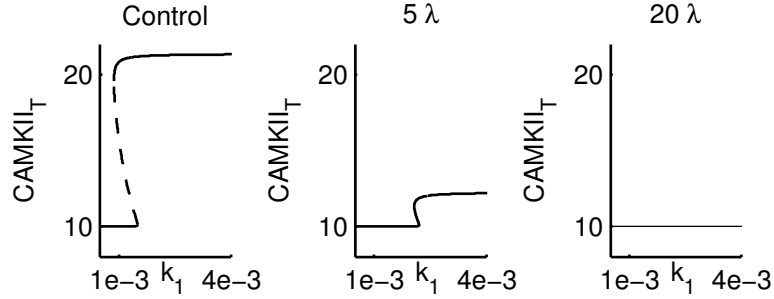
Figure 7.4: Effect of increasing the rate of degradation of in the model of Aslam. When the degradation is to strong the system only possesses one stable steady-state whatever the value of the bifurcation parameter k_1.

We have just seen that the hysteresis singularity organizes a switch between two stable equilibria. In exactly the same way, the recent paper (Franci et al., 2013a) shows that the cusp singularity organizes a switch between a stable equilibrium and a stable limit cycle. Postponing to the next chapter the relevance of this switch, we briefly review the cusp singularity theory (Golubitsky and Schaeffer, 1985).

Let us consider the scalar equation:

$$g(x, \lambda) = 0 \tag{7.14}$$

and assume that 7.14 presents a singularity at $(x, \lambda) = (x_0, \lambda_0)$, i.e,

$$g(x_0, \lambda_0) = g_x(x_0, \lambda_0) = 0 \tag{7.15}$$

if in addition,

$$\begin{aligned} g_\lambda(x_0, \lambda_0) &= 0 \\ g_{x,\lambda}(x_0, \lambda_0) &= 0 \\ g_x^2(x_0, \lambda_0) &= 0 \end{aligned} \tag{7.16}$$

with $g_{x,\lambda}$, the partial derivative of g with respect to λ and then with respect to x, and,

$$\begin{aligned} g_\lambda^2(x_0, \lambda_0) &\neq 0 \\ g_x^3(x_0, \lambda_0) &\neq 0 \end{aligned} \tag{7.17}$$

then equation 7.14 presents a cusp singularity (Golubitsky and Schaeffer, 1985):

$$g = x^3 + \lambda^2 \tag{7.18}$$

with the universal unfolding,

$$G(x, \lambda, \alpha, \beta, \gamma) = x^3 + \lambda^2 + \gamma\lambda x + \beta x + \alpha \tag{7.19}$$
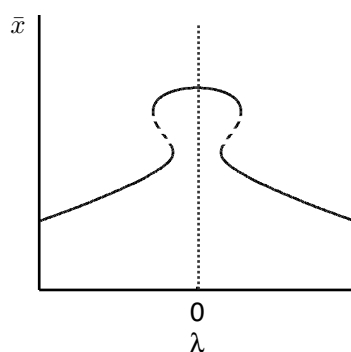
Figure 7.5: Winged cusp

The winged cusp presents a particular shape, it looks like two hysteresis singularities which meet for some parameter value. In the left half plane, the increase in the parameter λ, increases the value of the equilibrium while for the right half-plane, an increase of the parameter λ, decreases the equilibrium value. The effect of the parameter λ is non-monotone.

7.5   Conclusion

Singularity theory is a local tool to isolate points of high relevance in the state and parameter space. This theory provides a framework to extend our local analysis in the state space to a local analysis in the state space and the parameter space. Singularity theory provides an interesting setting to study bistability. This framework naturally highlights the mechanisms that gives birth to a bistable behavior such as a positive feedback loop coupled to ultrasensitivity. In addition, singularities organize bistability. Hysteresis singularity organizes bistability between two stable steady-states, while the cusp singularity organizes a switch between a stable steady-state and a stable limit cycle as it will

be illustrated in the next chapter on a model of neuronal excitability (Franci et al., 2013a), see Figure 7.6.
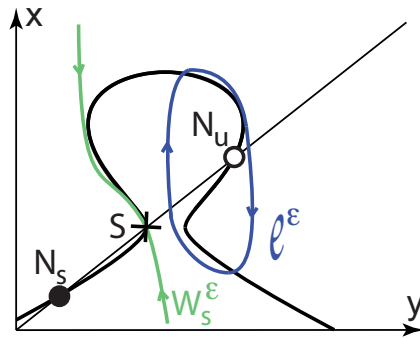
Figure 7.6: A cusp singularity organizing a switch between a stable steady-state and a stable limit cycle. Figure from Franci et al. (2013a)

Chapter 8

First spike latency in spiking neurons

This chapter studies the first spike latency in models of neuronal excitability. Thanks to the concepts developed in the previous chapters, we show that first spike latencies rely on a particular type of neuronal excitability called regenerative excitability. Based on the theoretical analysis of Chapter 5, we propose some tools to quantify the information encoded by the first spike latency in these models.

The material presented in this chapter is a joint work with Dr. Alessio Franci, INRIA-Lille.

8.1 First spike latency in single neurons

At the level of a single neuron, the first spike latency corresponds to the time between the reception of an excitatory input and the generation of the first action potential. This latency depends on several electrical and chemical processes including the propagation of the electric signal along the neuron axon and the (in)activation of postsynaptic currents (Axmacher and Miles, 2004). These postsynaptic currents specific of the type of neuron studied, are particularly important for the control of the first spike latency (Axmacher and Miles, 2004; Fricker and Miles, 2000; Molineux et al., 2005). In particular, the hyperpolarizing K^+ current of Type A has been identified as a key ruler of the first spike latency in several neurons including spiny projection neurons of neostriatum and basal ganglia and cerebellar stellate cells (Anderson et al., 2010; Molineux et al., 2005). K^+ currents of Type A also regulate the firing of action potentials in CA1 pyramidal cells (Hoffman et al., 1997; Martina

et al., 1998), a particular neuron of hippocampus for which the robustness of the first spike latency has been tested experimentally (Axmacher and Miles, 2004; Fricker and Miles, 2000). In CA1 pyramidal cells, the first spike latency is sensitive to the strength of the excitatory input. For strong stimuli, latencies are short and robust, while there are long and variable for stimuli slightly above the firing threshold (Axmacher and Miles, 2004). They also strongly depend on the balance between inward and outward currents which flow trough the membrane close to the firing threshold (Axmacher and Miles, 2004).

Motivated by our previous work on latencies in cellular decision-making models, we would like to test if similar modeling principles could be applied to models of single spiking neurons. In particular, we would like to test the hypothesis that first spike latencies are induced by the proximity of a local saddle node bifurcation of the resting state, an hypothesis already suggested by previous studies (Izhikevich, 2007). In models of neuronal excitability, this hypothesis has mainly been investigated in theoretical small dimensional systems but poor attention has been paid to the real implementation of this mechanism in high-dimensional conductance-based models. In this chapter, we investigate the following questions. Is a saddle node bifurcation a sufficient condition to observe first spike latencies? Is this mechanism robust in high-dimensional models? What are the possible physiological explanations for this mechanism?

8.2 First spike latency in planar reductions

In 1963, Hodgkin and Huxley were awarded the Nobel Prize for their work on neuronal excitability (Hodgkin and Huxley, 1952). By studying the axon of a giant squid, they identified the mechanisms at the origin of the generation of action potentials in excitable cells. They proposed to model the neuron membrane as a RC-circuit. The membrane voltage (V) is governed by:

$$C\dot{V} = \sum I_{ion} + I \tag{8.1}$$

where $\sum I_{ion}$ represents the sum of the ionic currents which flow through the neuron membrane and I is the external current applied to the neuron.

Each ionic current obeys Ohm's law;

$$I_{ion} = -\bar{g}_{ion}(V - E_{ion})$$

The key assumption of this model is that conductances of the ion channel are voltage dependent. The model of Hodgkin and Huxley includes two ion channels that are voltage-dependent, a sodium channel (Na^+) and a potassium channel (K^+). Gating variables are associated to each one of these channels, the Na^+ has an activating (m_{Na+}) and and inactivating gating variable (h_{Na+}), the sodium channel only presents an activating variable (n_{K+}). Later, it was discovered that these gating variables capture the average stochastic opening and closing of voltage-dependent ion channels (Hille, 1984). Therefore, the model has four variables ($V, m_{Na+}, h_{Na+}, n_{K+}$).

$$
\begin{aligned}
C\dot{V} =& -\bar{g}_K n^4(V - E_K) - \bar{g}_{Na}m^3 h(V - E_{Na}) \\
& - \bar{g}_L(V - E_L) + I \\
\tau_m(V)\dot{m} =& m_\infty(V) - m \\
\tau_h(V)\dot{h} =& h_\infty(V) - h \\
\tau_n(V)\dot{n} =& n_\infty(V) - n
\end{aligned}
$$

where C is the membrane capacity, $C = 1\mu F/cm^2$ and $-\bar{g}_L(V - E_L)$ represents the current of ions that flow through the leakage channels.

$$x_\infty(V) = \frac{\alpha_x(V)}{\alpha_x(V) + \beta_x(V)}$$

and

$$\tau_x(V) = \frac{1}{\alpha_x(V) + \beta_x(V)}$$

x	$\alpha_x(V)$	$\beta_x(V)$
m	$(2.5 - 0.1V)/\left[\exp(2.5 - 0.1V) - 1\right]$	$4\exp(-V/18)$
n	$(0.1 - 0.01V)/\left[\exp(1 - 0.1V) - 1\right]$	$0.125\exp(-V/80)$
h	$0.07\exp(-V/20)$	$1/\left[\exp(3 - 0.1V) + 1\right]$

x	$E_x(mV)$	$g_x(mS/cm^2)$
Na	115	120
K	-12	36
L	10.6	0.3

During an action potential, the activation of sodium channels follows almost immediately the variation of potential while the sodium inactivation and the potassium activation are much slower. Because of this time-scale separation between fast variables (V, m_{Na^+}) and slow variables (h_{Na^+}, m_{K^+}), this model can easily been studied mathematically.

8.2.1 Fast model reduction

Fast models rely on the assumption that the voltage dynamics and the activation of Na^+ channels is fast with respect to the activation of K^+ channels and the inactivation of Na^+ channels. In these models, these two slow variables are treated as parameters (Keener and Sneyd, 2009).

$$
\begin{aligned}
C\dot{V} =& -\bar{g}_K n_0^4 (V - E_K) - \bar{g}_{Na} m^3 h_0 (V - E_{Na}) \\
& -\bar{g}_L(V - E_L) + I \\
\tau_m(V)\dot{m} =& m_\infty(V) - m
\end{aligned}
\tag{8.2}
$$

The phase plane of the fast model is depicted on Figure 8.1. The fast-model is a typical E-E model such as the toy model introduced in Chapter 4. In this system, the voltage produces a positive feedback loop on the opening of sodium channels which in turn increase the voltage. For parameters values corresponding to physiological conditions, the system is bistable. When a current I is applied to the neuron, the V-nullcline is pushed right. For sufficiently strong I, the resting state merges with the saddle point in a saddle node bifurcation. For inputs close to the threshold, there is a bottleneck where trajectories are delayed.

Can fast models account for first spike latencies? These models are only valid for small t and V. Once the action potential has been initiated, the values of n_0 and h_0 increase modifying the phase portrait of the system. This model is not able to describe the system dynamics on the
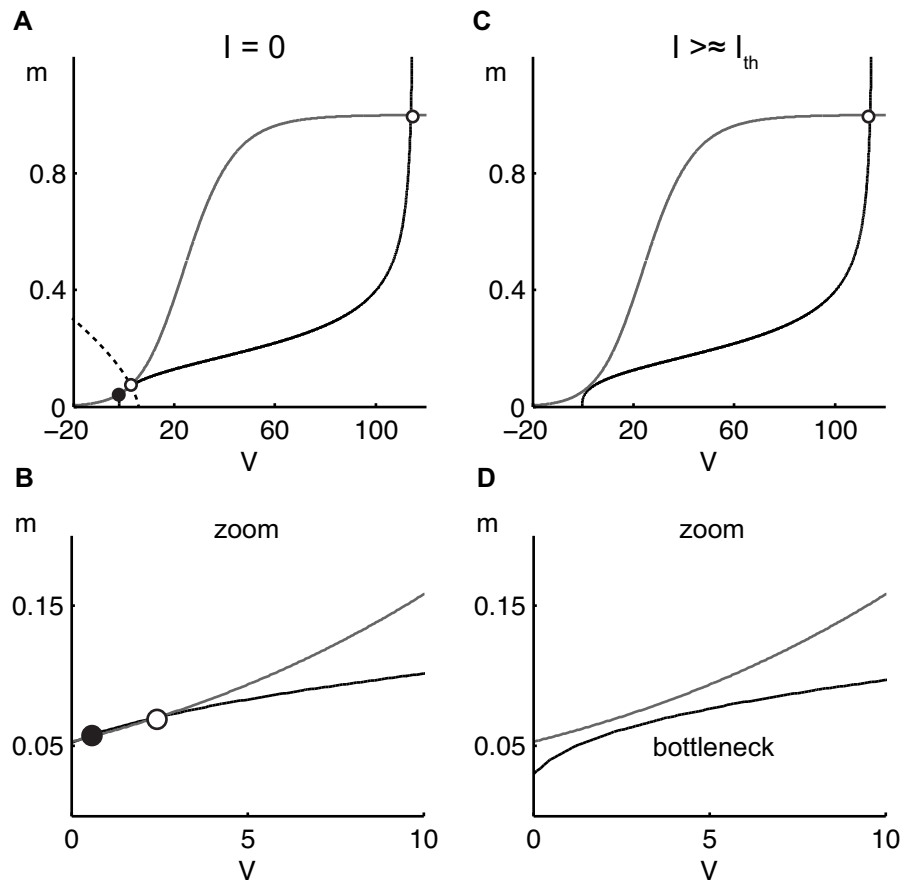
Figure 8.1: Bistability in the fast model reduction of Hodgkin and Huxley. For $I = 0$ (A-B) , the system has three equilibria, a stable equilibrium, a resting state and a unstable equilibrium. For $I = I_{th}$, the saddle point and the resting state merge in a saddle node bifurcation. For I, slightly above the switching threshold, the system presents a bottleneck because of the ghost saddle point (C-D).

time-scale of one entire or more than one action potentials. Therefore,
it is no suited to capture first spike latencies.

8.2.2   Hysteresis and cusp in the fast model

The fast model is only valid for fixed values of the parameters n_0 and
h_0. What does happen when these variables increase following the ap-
plication of a step of current? Figure 8.2 A shows the effect of increasing
the parameter n_0, in the phase portrait of the fast model. When this
parameter increases, the V-nullcline is pushed left. Because K^+ ions es-
cape from the intracellular medium, the potential decreases. The static
input-output relationship between n and V presents the typical hystere-
sis curve depicted on Figure 8.2 B. An increase in the value of n_0 results
in an decrease in the static voltage response.
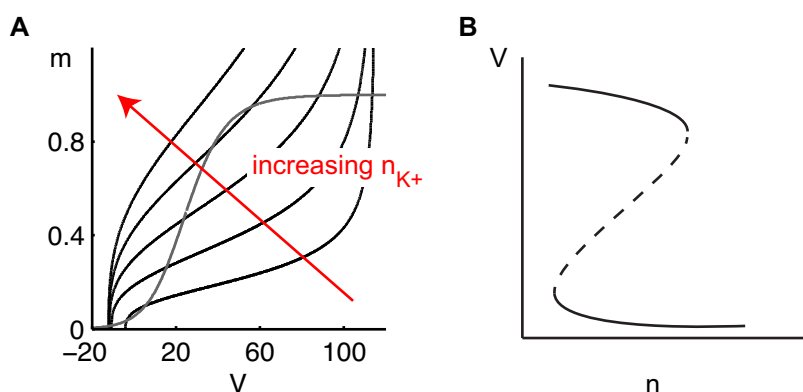
Figure 8.2: Effect of increasing n in the fast model of Hodgkin and
Huxley.

The model of Hodgkin and Huxley works admirably well to describe the
generation of action potentials. However, this neuron only includes two
types of voltage-dependent channels, Na^+ and K^+ channels. With the
development of electrophysiology, numerous channels have been shown
to regulate the neuron excitability (Hille, 1984). In particular calcium
channels play a critical role in this process (Tsien, 1983). Calcium chan-
nels have a slow activation. Therefore the activation of these channels
can be treated as a parameter in the fast model reduction, in the same

way as potassium:

Adding a calcium current in the HH model leads to:

$$CV̇ = - \bar{g}_K n_0^4 (V - E_K) - \bar{g}_{Na} m^3 h_0 (V - E_{Na})$$
$$- \bar{g}_L (V - E_L) - \underbrace{\bar{g}_{Na} m_{Ca,0} (V - E_{Ca})}_{I_{Ca}} + I \qquad (8.3)$$
$$\tau_m(V)\dot{m} = m_\infty(V) - m$$
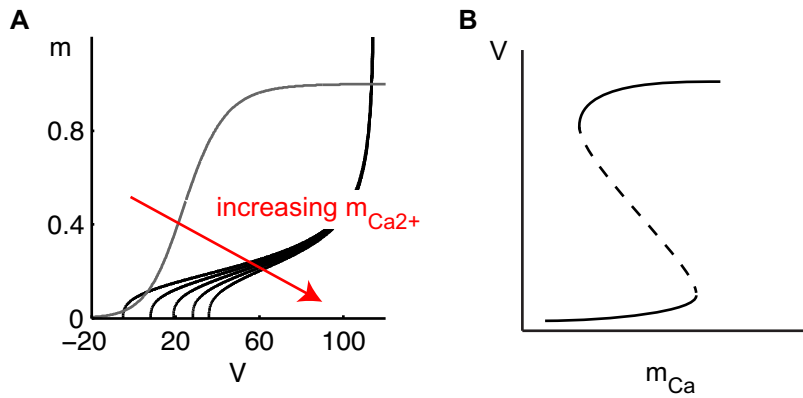
Figure 8.3: Effect of increasing $m_{Ca,0}$ in the fast model of Hodgkin and Huxley + calcium.

Let us assume, that during an action potential, calcium channels can open following a depolarization of the neuron. The effect of increasing the parameter $m_{Ca,0}$ is depicted in Figure 8.3. As for the parameter n, the static input-output relation between the voltage and m_{Ca} is a hysteresis curve. However, in this case an increase in the value of m_{Ca} results in an increase in the static voltage response.

Figure 8.4 is a schematic representation of the possible effect of increasing both the parameter $m_{Ca,0}$ and the parameter n in the Hodgkin and Huxley model with calcium. We obtain the winged-cusp introduced in Chapter 7. The winged-cusp translates the fact that the effect of slow gating variables on the equilibrium potential is non-monotone. It captures the balance between the two hysteresis responses depicted on
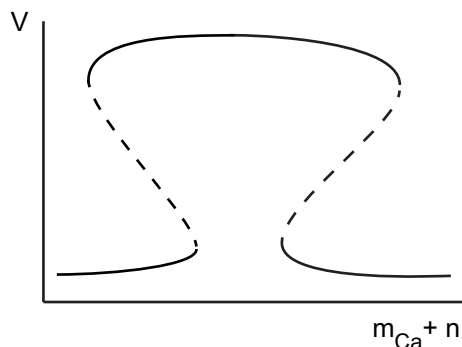
Figure 8.4: Effect of increasing simultaneously $m_{Ca,0}$ and n in the fast model of Hodgkin and Huxley + calcium by fitting a static (linear) relationship between $m_{Ca,0}$ and n.

Figures 8.2 and 8.3. This situation is typically encountered when two slow variables as m_{Ca} and n are aggregated in a single variable as it is performed in slow-fast planar model reductions.

8.2.3   Slow-fast planar models

A common reduction based on time-scale separation that is valid on a longer time-scale, is the slow-fast model reduction. In this reduction, it is assumed that fast gating variables such as m_{Na^+} instantaneously follow the variation of potential (V) so that they can be represented by their steady-state approximation $m_{Na^+_\infty(V)}$. Slow gating variables are assumed to have the same time-scale and are gathered in one single variable n. The resulting system is a two-dimensional slow-fast model.

In the classical slow-fast reduction of the Hodgkin and Huxley model, such as the FitzHugh-Nagumo model (FitzHugh, 1955), the V-nullcine presents a cubic shape and the n-nullcline is a monotone increasing function of the voltage. The cubic shape of the V-nullcline is due to the bistability of the fast subsystem, it captures the hysteresis in Section 8.2.2. Indeed, in the fast model, n is a bifurcation parameter producing the typical hysteresic curve discussed in Chapter 7. A slow fast model is typically described by:

$$C\dot{V} = \quad V - \frac{V^3}{3} - n + I$$
$$\dot{n} = \quad \epsilon\left(n_\infty(V) - n + n_0\right)$$

$$(8.4)$$

If we want to capture the mirror hypothesis brought by the combined activation of potassium and calcium channels, we need a different phase portrait. This motivates the novel phase portrait (Franci et al., 2013b),

$$\dot{V} = \quad V - \frac{V^3}{3} - n^2 + I$$
$$\dot{n} = \quad \epsilon\left(n_\infty(V) - n + n_0\right)$$

$$(8.5)$$

where $n_0 > 0$ and $n_\infty(V)$ is the standard Boltzman activation function:

$$n_\infty(V) := \frac{a}{1 + e^{-bV}} \quad a, b > 0$$

Here, the V-nullcline corresponds to the unfolding the winged-cusp, $G(-V, -n, I, 1, 0)$ introduced in Chapter 7. What is the meaning of this particular shape? We saw in the previous paragraph that the shape of the V-nullcline is determined by the steady-state approximation of the fast system for each value of n. The regenerative phase portrait is bistable for appropriate parameter values. It is a bistability between a stable equilibrium and a limit cycle.

Let us introduce the concepts of restorative and regenerative slow gating variables (Drion et al., 2012; Franci et al., 2013b). A restorative gating variable is a variable which produces a negative feedback on the membrane potential close to the resting state: a small depolarization of the membrane increases the value of the gating variable which in turns leads to an hyperopolarization of the membrane. Typically, a restorative variable describes the activation (inactivation) of an outward (resp. inward) current of positive ions. Recovery variables n and h of the Hodgkin-Huxley model are restorative because they respectively represent the activation of an outward K^+ current and the inactivation of an inward Na^+ current. A regenerative gating variable produces a positive feedback on the membrane potential close to the resting state: a small depolarization of the membrane increases the value of the gating variable which in turns leads to a larger depolarization of the membrane.
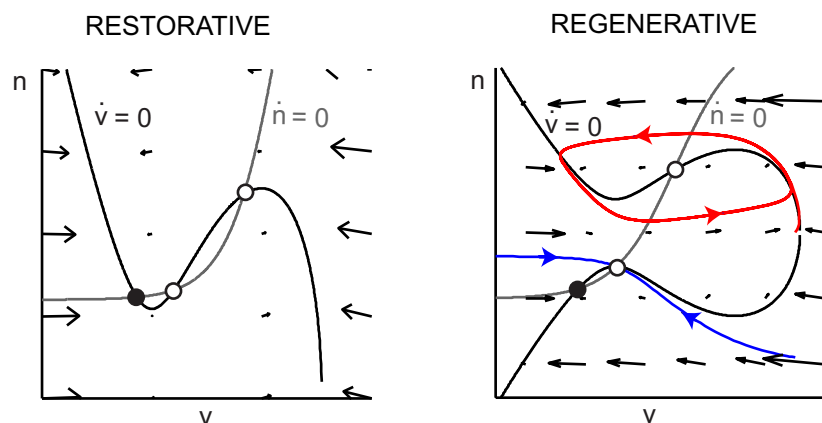
Figure 8.5: Comparison between restorative and regenerative phase portraits. For suitable values of the applied current I, the regenerative phase portrait presents both a stable equilibrium (black dot) and a stable limit cycle (red curve). The basins of attraction of these attractors are separated by the stable manifold (blue curve) of the saddle (white center dot).

RESTORATIVE	REGENERATIVE
h_{Na^+}, n_{k+}	$m_{Ca^{2+}}$
negative feedback on potential	positive feedback on potential

Table 8.1: Classification of slow gating variables (HH+Ca^{2+}) in function of their effect on the membrane potential close to the resting potential

Typically, a regenerative gating variable models the activation (inactivation) of an inward (resp. outward) current of positive ions. This type of gating variables often represents the slow activation of a calcium channel.

In the model of Hodgkin and Huxley, all the slow gating variables are restorative. Therefore, they all produce a negative feedback on the potential. The static relation between n and the voltage is monotone resulting in the hysteresis curve depicted in Figure 8.2. When the system presents both restorative and regenerative slow channels, the static relation between n and V depends on the balance between the negative feedback of restorative variables and the positive feedback from regen-

erative variables. This static relation no longer monotone results in the new hysteresis of Figure 8.4.

8.2.4 Latencies in restorative and regenerative phase portraits

In the restorative phase portrait, a saddle node bifurcation is a saddle node bifurcation on invariant circle (SNIC) under the presence of a timescale separation between the voltage dynamics and the slow variable n (Figure 8.6). This bifurcation results in a mechanism of low frequency coding. In fact, it corresponds to a situation where the fast subsystem is just beyond the saddle node bifurcation when the slow n variable is at equilibrium. This mechanism essentially relies on the bistability of the fast model. However, there is no hysteresis nor bistability in the slow-fast model. Therefore, there is no mechanism to ensure the memory and latency found in bistable models.

In sharp contrast, the regenerative phase portrait exhibits a robust first spike latency. This latency results from the switch of the stable resting state to the stable limit cycle through a saddle node bifurcation. In this case, the mechanism is induced by the bistability of the slow model. The regenerative model shares the characteristics of bistable models illustrated in the previous part of the thesis. It is a rest-and-spike dynamical decision-making process, characterized by a hysteresis response, a memory and a latency.

In the Appendix A, the reader can find the mathematical conditions to observe a saddle node in both the restorative and regenerative phase portraits, these conditions support the present analysis.

8.3 First-spike latency in conductance-based models

A general $n-$dimensional conductance based model describes the dynamics of the neuron membrane potential in function of the time and the external current applied to the neuron $I(t)$. The neuron membrane
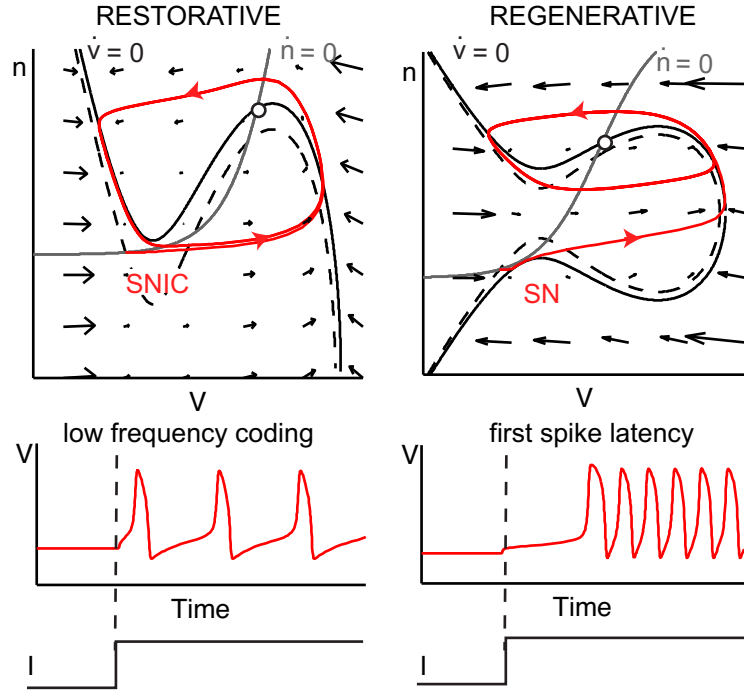
Figure 8.6: Comparison of the effect of a step current slightly above the firing threshold in restorative and regenerative phase portraits depicted in Figure 8.5. In the restorative phase portrait, the system loses stability through a saddle node on invariant circle (SNIC) bifurcation and the neuron shows a low frequency. In the regenerative phase portrait, the system undergoes a saddle node (SN) bifurcation and the neuron shows a first spike latency before firing at a high frequency.

dynamics is described by the general model:

$$CV̇ \quad = \quad \sum_k I_k(t) + I(t) \tag{8.6}$$

$$\tau_i \, \dot{x}_i \quad = \quad x_{\inf_i}(V - V_0) - x_i, \quad i = 1 \ldots n - 1 \tag{8.7}$$

where $\sum_k I_k(t) = \sum_k g_k(x)(V - E_k)$ is the sum of the ionic currents through ion channels and $x_{\inf_i}$ are are strictly monotone increasing sigmoids (Franci et al., 2013b). The strength of each ionic current ($I_k(t)$) is determined by the membrane conductance to this specific ion (g_k) and

RESTORATIVE	REGENERATIVE
h : Na^+ inactivation	b: K_A^+ inactivation
n: K^+ activation	
a : K_A^+ activation	
negative feedback on potential	positive feedback on potential

Table 8.2: Classification of slow gating variables for the model of Connor and Stevens (1971) in function of their effect on the membrane potential close to the resting potential.

the Nernst potential of this ion (E_k). Conductances (g_k) are function of the state of the gating variables represented by the vector **x** and describing the permeability of the membrane to these specific ionic currents.

8.3.1 Model of Connor and Stevens

We consider the model introduced in Connor and Stevens (1971), recently studied in Barreiro et al. (2012). This model is of particular interest because it includes a K^+-current of type A, i.e a hyperpolarizing potassium current particularly important for first spike latencies (Molineux et al., 2005). The strength of this current is controlled by the conductance g_A. In response to membrane depolarizations, this current is slowly inactivated, decreasing the flow of potassium which can exit from the neuron, i.e the source of hyperpolarization. Therefore the inactivation of this channel produces a positive feedback on the potential. Close to the resting potential, the variables n_{K^+} (potassium activation) and $n_{K^+,A}$ (potassium of type A inactivation) have the same time-scale (Figure 8.7). It should be noted that we used the parameters proposed by Ermentrout and Terman (2010). However, in the original models of Connor and Stevens (1971), the inactivation of potassium channels is much slower, we will discuss this difference later.

Bistability in the model of Connor and Stevens

Previous studies have shown that the model of Connor and Stevens presents a Hopf bifurcation for low values of g_A and a SNIC bifurcation if g_A is increased. By modifying this conductance, the neuron switches
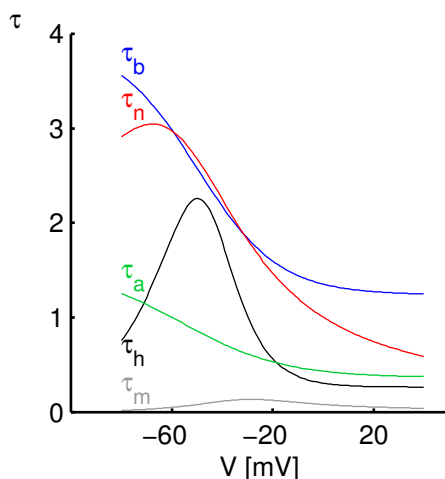
Figure 8.7: Time constants in the model of Connor and Stevens with parameters from Ermentrout and Terman (2010): activation of Na$^+$ currents channels (τ_m), inactivation of Na$^+$ currents channels (τ_h), activation of K$^+$, A currents channels (τ_a), inactivation of K$^+$, A currents channels (τ_b) and activation of K$^+$ currents channels (τ_n). For values of the potential close to the resting potential $V \approx -60mV$, the inactivation of K$^+$, A currents channels (τ_b) and activation of K$^+$ currents channels (τ_n) have the same time-scale.

from type II to type I excitability. As illustrated in the previous paragraph, the two sources of positive feedback on the potential are the activation of sodium channel and the inactivation of K_A^+ channels. While the activation of sodium channel is fast, the inactivation of potassium channels of Type A is slow. Potassium channels of type A are a source of regenerativity in the neuron. The planar analysis predicts that by increasing the value of g_A, i.e by increasing the strength of regenerative slow channels with respect to the strength of restorative slow variables, the neuron exhibits first spilke latencies and bistability. Figure 8.8 shows the firing of a single neuron for values of g_A corresponding to Type I excitability, i.e intermediate values of g_A and high values of g_A. During the first 50 ms, the neuron potential is fixed slightly below the firing threshold. At time $t = 50$, a step input, slightly above the firing threshold is applied to the neuron. For intermediate values of g_A, the neuron

fires at low frequency. At high values, the neuron presents a long latency before firing at high frequency. At $t = 150$ ms, the current is reset to its initial value. While for intermediate values of g_A, the potential instantaneously returns to the resting potential, for high values of g_A the neuron still fires action potentials. In this last case, the neuron exhibits a bistable behavior. As predicted by the planar analysis, a high level of regenerativity induces both first spike latency and bistability.
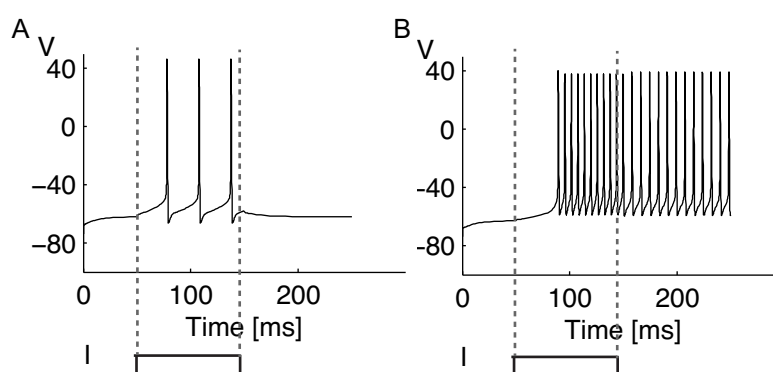
Figure 8.8: Model of Connor and Stevens: effect of a step input close to the firing threshold for intermediate values of ($gA = 48$) and high values of g_A ($gA = 200$). In both model, the current is initially fixed at a value slightly below the firing threshold . At 50 ms, a small step input is applied during 100 ms and then the current to I_0. When the neuron show low frequency coding and no bistability for small values of g_A (A), it exhibits both first spike latency and bistability for high values of g_A (B).

Local sensitivity at saddle node

A local analysis for g_A high and a value of current corresponding to the firing threshold, shows that the system posses a saddle node bifurcation at this point. Indeed, only one eigenvalue is equals to zero for this input. We performed a sensitivity analysis close to the saddle node bifurcation. We fixed the current slightly below the firing threshold and simulate the system to get the resting state close to the saddle node bfiurcation. Then we applied sensitivity analysis at this point (the stable one) as

defined in Section 4.4 in Chapter 4. Results show that the system is particularly sensitive to the g_A conductance, see Figure 8.9, close to the saddle node bifurcation. In other words, the first spike latency is particularly sensitive to this parameter.

Noise sensitivity

In vitro, neurons typically receive input spikes from thousands of other neurons. In practice, it is not possible to take into account all these spike arrivals. A simple strategy is to focus on a subset of neurons and treat spikes from other neurons as a source of noise. Under the diffusion approximation, these random stochastic input arrivals can be approximated by a gaussian noise term is added to the equation describing the neuron voltage (Gerstner and Kistler, 2002). The neuron voltage is described by a stochastic differential equation:

$$C\dot{V} = \sum I(V, n_i) + I(t) + \sqrt{2D}\xi(t) \tag{8.8}$$

with D, the noise intensity and $\xi(t)$ a gaussian white noise.
The first spike latency can be characterized by determining the mean first passage time of 8.8, $<T>$. The sensitivity of the first spike latency to noise for a given input current I is then determined by the coefficient of variation. This coefficient, often used in neurosciences Gerstner and Kistler (2002), represents the inverse of the signal to noise ratio and is given by :

$$CV = \frac{\sqrt{<\Delta T^2>}}{<T>}$$

with $<\Delta T^2>$, the variance of the first spike latency.

Our analysis predicts that both the mean and the coefficient of variation varies as a power law of the distance to the saddle node bifurcation. In Figure 8.11, we fitted the mean first spike latency and coefficient of variation with respectively : $T_{\text{mean}} = \alpha \Delta I^{-\frac{1}{2}}$ and $CV = \beta(D)\Delta I^{-\frac{3}{4}}$. Results seem to fit the model. However, our analysis should require a true model validation. In addition, we limited ourselves to small noise to be in the condition of the theoretical analysis but this results in low variance in the first spike latency. Therefore, these preliminary results should be interpreted cautiously.
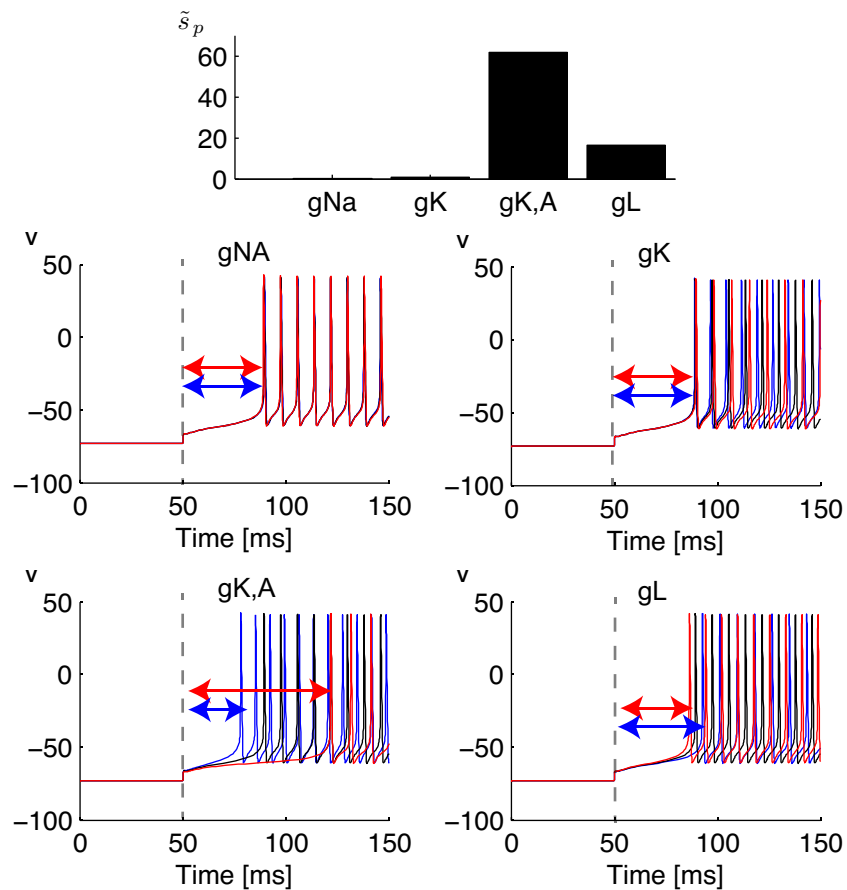
Figure 8.9: First spike latency sensitivity for the model of Connor and Stevens $g_A = 150$. Cumulative sensitivities are computed at the resting state for a value of the current $(I = 50)$ slightly below to the switching threshold $(I = 5.60)$.
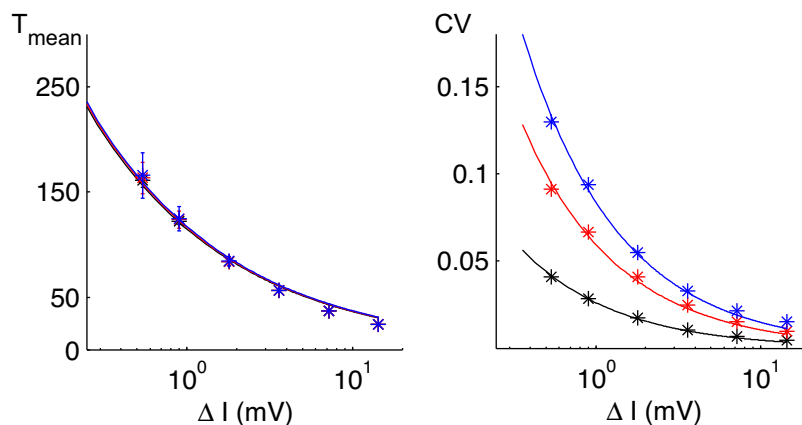
Figure 8.10: Mean first spike latency and coefficient of variation for the model of Connor and Stevens (1971). Results are depicted for different noise intensities, $\sigma = \sqrt{2D}$ with $D=0.1$(black), $D=0.5$(red), $D=1$(blue).
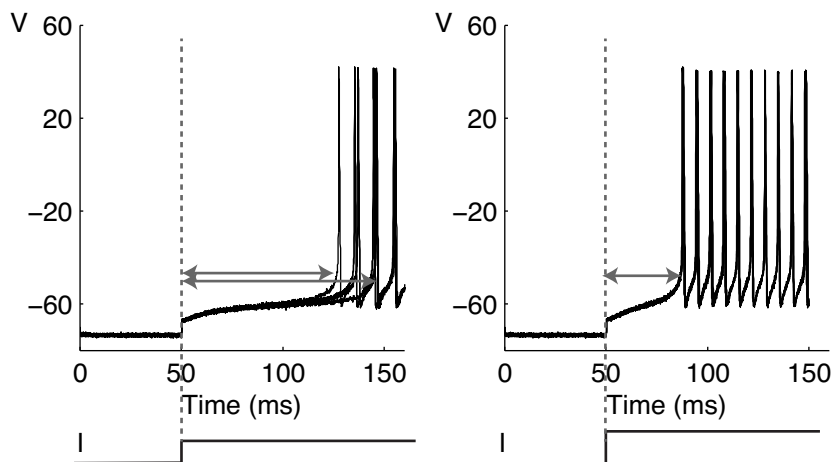
Figure 8.11: $D = 1$, $in = 0.025$ and $In = 0.1$

8.4 Conclusion

It was previously suggested that saddle node bifurcations can lead to a mechanism of first spike latency in models of neuronal excitability. In the first part of the thesis, we showed that latency was indeed used an

important function of biological switches to create input-dependent delays. Motivated by these results, we investigated the behavior of planar models corresponding to formal slow-fast reductions of higher dimensional conductance-based models. Our analysis reveals that first spike latencies are indeed observed for neurons presenting regenerative slow channels. In the presence of these channels and for appropriate values of the applied current I, the model is bistable in the slow time-scale, that is a stable equilibrium and a stable limit cycle coexist. This analysis is confirmed in the study of a high-dimensional conductance-based model. In Chapter 5, it was demonstrated that latencies naturally occur in bistable models when the resting state and the saddle point merge in a saddle node bifurcation. In planar bistable models, the proximity to a saddle node bifurcation can either results from the bistability of the fast system leading to a SNIC bifurcation and low-frequency coding or to the bistablility of the slow system resulting in first spike latencies. The bistability of the slow system is possible thanks to the presence of a positive feedback loop between the voltage and the (in)activation of slow gating variables.

8.4.1   Bistability in neuronal models

As illustrated in the first part of this thesis, bistability is an ubiquitous component of biological models. As illustrated throughout this thesis, a pervasive source of bistability in biological models is the positive feedback loop around sharp (sigmoid like) transitions. In the Hodgkin and Huxley model, the only source of positive feedback close to resting potential is the activation of fast Na^+ gating channels. As a consequence, bistability is generally associated with the fast-subsystem in planar models of neuronal excitability. However, the zoo of ion channels which are today known to regulate neuronal excitability (Gerstner and Kistler, 2002; Hille, 1984) provides many more sources of positive feedback. As illustrated by the model of Drion et al. (2012), sodium channels are not the only channels to produce a positive feedback on the neuron membrane. For example, calcium channels are a prominent source of positive feedback close to the resting potential. Activation of calcium channels is slow with respect to the activation of sodium channels resulting in the possible bistability of the slow model. In this case, bistability does not occur between two stable equilibria but between a stable equilibrium

and a stable limit cycle. It is organized by a cusp singularity instead of a hysteresis singularity. The analysis of the model of Connor and Stevens (1971) shows that potassium channels of Type A are another important source of regenerativity. Because these channels slowly inactivate close to the resting potential, they induce first spike latencies in the neuron.

In planar models of neuronal excitability, bistability is often associated to a sub-critical Hopf bifurcation (Izhikevich, 2007). This alternative source of bistability is not considered in this thesis because it does not persist in the physiologically meaningful situation of fast-slow systems. See (Franci et al., 2013b) for a more extensive discussion. Yet, bistability is a mechanism observed in several experimental studies (Hahn and Durand, 2001; Heyward et al., 2001; Lechner et al., 1996; Lee and Heckman, 1998; Williams et al., 2002) and that seems to have particular functional implications (Baldissera et al., 1994; Gruber et al., 2002).

8.4.2 First spike latency coding

Could the first spike latency be a neuronal code? A good code is a code which is robust but also able to encode information. Our analysis predicted that first spike latency scale as $T = k^{\alpha}, \alpha = \frac{-1}{2}$, with k the distance to the saddle node. This relation persists under small perturbations of the voltage dynamics. The coefficient of variation, which represents the inverse of the signal to noise ratio scales with a factor $k^{-0.75}$. This means that high signal to noise ratios are observed far from the saddle node bifurcation. However, in this range of currents, the latency is less sensitive to a variation of current as illustrated by the decrease in the slope of the current-mean first spike latency curve in Figure 8.11 A. Therefore, if this code is possible, it relies on a trade-off between sensitivity and robustness fixed by the distance to the bifurcation.

<div align="right">

Chapter 9

</div>

Conclusion and perspectives

This dissertation is devoted to the study of performance and robustness of biological switches. In our analysis, bistable switches are presented as decision-making processes. Because these decision-making processes are temporal processes, they deserve a dynamical analysis. The study focuses on three different cellular processes, apoptosis the controlled cell death, first spike latency in neurons and long term potentiation, a phenomenon underlying synaptic plasticity. In these three processes, the cell has to face a decision, to die or not to die in apoptosis, to spike or not to spike in the neuron, to remember or to forget in long term potentiation (Chapter 1).

Our historical survey of the literature (Chapter 2) showed how the concept of switch translates to bistability in mathematical models. On the other hand, it highlighted how the notion of switch evolved from a simple nonlinear static input-output relation to a dynamical process where phenomena such as latencies and reversibility are important issues. In bistable models, a stable attractor is associated to each decision. These bistable models do not only implement a binary (static) choice, they implement a dynamical decision-making process which has memory.

Our definition of performance and robustness for biological switches relies on the study of the system away from stable steady-states, i.e. in the transient behavior characterizing the switch between two stable operating conditions (Chapter 3). We emphasized that the performance and robustness of bistable models is currently studied by means of extensive numerical simulations, because of the apparent mismatch between

mathematical analysis tools mainly based on local analysis of the system around a stable steady-state and the non local nature of decision-making.

In this thesis, we proposed a different approach. We considered the switch as a process rather than a set of trajectories and identify the key rulers of this process in both the state and parameter spaces (Chapters 4, 5, 7). The saddle point is a key ruler of the phase portrait, always found with the right time-scale separation in the neighborhood of saddle-node bifurcations (Chapters 4 and 5) and singularities are associated to critical change of behavior in both the state and parameter spaces (Chapter 7). There is an interplay between these local rulers and the system's dynamics. At bifurcations such as saddle nodes, a local analysis reveals the sensitivity of the system to small inputs and perturbations. Around that point of high-sensitivity, the decision-making process can easily be reverted or slowed down, it becomes sensitive to the external world. At singular points not only the linear part of the system vanishes but also its quadratic term in the normal form. A local analysis around these particular points suggests that they organize much of the global phenomenon.

We have shown that the proposed analysis is not only valid for small dimensional models such as small network motifs but can be extended to high-dimensional systems. This is justified by a theoretical analysis (Chapter 5) and illustrated on high-dimensional models of the literature (Chapter 6). The decision-making process depends on how trajectories are attracted to and then pushed away from the saddle point. When the system is close to a bifurcation, the repulsion is slow leading to latencies in the decision.

With singularity theory (Chapter 7), we showed than a local analysis in both the state and parameter space can help at understanding the behavior of biological switches. Positive feedback loops coupled to ultrasensitive mechanisms are natural conditions for bistability in this mathematical framework.

In the light of the first seven chapters, we studied in the last part of the thesis the first spike latency in models of neuronal excitability. Results show that the first spike latency is not a mere property of systems with

a saddle node bifurcation (as previously presented in the literature) but rather a constitutive property of bistable models. This bistability comes from the positive feedback of slow regenerative channels on the membrane potential close to the resting state. We proposed some tools to quantify the robustness of the first spike latency in both a deterministic and simple stochastic setting.

By studying models of various processes, we pointed out that the same principles can be used to encode dynamical phenomena in very different cellular processes. Both the latencies observed in apoptposis and the first spike latency in single neurons are captured by the same mathematical concepts, revealing the added value of an abstract framework for the analysis of biological switches.

Perspectives and future work

This dissertation suggests a number of physiological hypotheses that could be studied in further research. In particular, the presence of dynamical phenomena such as latencies could be used by the cell as check point mechanisms where the system integrates a collection of small inputs before taking a decision. The system, insensitive to small perturbation becomes, during a given window of time, sensitive to small perturbations and inputs. This mechanism could explain how processes that should be robust to small perturbations could be finely controlled, once the cell has triggered a decision-making process. The link between bistability in neuronal models and first spike latency is an another hypothesis that should require careful experimental investigations.

In the first part of the thesis, we briefly introduced the fact that bistable models can be used at different-scales and represent collective decision-making processes. We think that future work could be carried out in this direction. In addition, our study mainly focused on unicellular models, it would be interesting to explore how our results extend to a population of cells.

From a mathematical point of view, the analysis of normal forms and bifurcation in the presence of noise seems an interesting topic to explore.

Further research would be required to study the interplay between local noisy systems and global properties of the decision-making process. This type of study could be particularly interesting for neurons.

Our analysis reveals the importance of time and fluctuations in the study of biological systems. These concepts have been studied in thermodynamics in the context of chemical reactions. Thermodynamics is clearly missing in the present analysis and it would be interesting to consider this field in further work.

In this dissertation, we studied the problem of performance and robustness of biological switches. It turned out that the problem was much richer than expected. Understanding biological systems requires to integrate fields as diverse as chemistry, physics, control, mathematics and physiology. All these fields have to to deal with constraints imposed by the particular structure of biological systems, their variability and multiscale properties. The study of biological systems offers new challenges to all these disciplines

Appendix A

Appendix

A.1 Implementation of models

Model of Eissing et al. We re-implemented the 8-dimensional model of Eißing et al. (Eissing et al., 2004) in MATLAB based on the description provided in Bullinger (2005). In this model, the interactions among species are governed by the law of mass action, and are represented by,

$$
\begin{aligned}
C8^* + C3 &\xrightarrow{k_{+1}} C8^* + C3^* \\
C8 + C3^* &\xrightarrow{k_{+2}} C8^* + C3^* \\
C3^* + IAP &\xrightarrow{k_{+3}} C3^* \sim IAP \\
C3^* \sim IAP &\xrightarrow{k_{-3}} C3^* + IAP \\
C3^* + IAP &\xrightarrow{k_{+4}} C3^* \\
C8^* + CARP &\xrightarrow{k_{+11}} C8^* \sim CARP \\
C8^* \sim CARP &\xrightarrow{k_{-11}} C8^* + CARP
\end{aligned}
$$

$$
\begin{aligned}
C8^* &\xrightarrow{k_{+5}} \\
C3^* &\xrightarrow{k_{+6}} \\
C3^* \sim IAP &\xrightarrow{k_{+7}} \\
\xrightarrow{k_{-8}} IAP &\xrightarrow{k_{+8}}
\end{aligned}
$$

$$\xrightarrow{k_{-9}} C8 \xrightarrow{k_{+9}}$$
$$\xrightarrow{k_{-10}} C3 \xrightarrow{k_{+10}}$$
$$\xrightarrow{k_{-12}} CARP \xrightarrow{k_{+12}}$$
$$C8^* \sim CARP \longrightarrow \xrightarrow{k_{+13}}$$

The table A.1 shows the values of parameters used for numerical simulations. These values correspond to nominal parameters values provided in Bullinger (2005).

1	$k_{+1} = 5.8\text{e-}5$	11	$k_{+11} = 0.0005$
2	$k_{+2} = 1\text{e-}5$	12	$k_{+12} = 0.001$
3	$k_{+3} = 0.0005$	13	$k_{+13} = 1.16\text{e-}2$
4	$k_{+4} = 0.0003$	14	$k_{-3} = 0.21$
5	$k_{+5} = 0.0058$	15	$k_{-8} = 464$
6	$k_{+6} = 0.0058$	16	$k_{-9} = 507$
7	$k_{+7} = 0.0173$	17	$k_{-10} = 81.9$
8	$k_{+8} = 0.0116$	18	$k_{-11} = 0.21$
9	$k_{+9} = 0.0039$	19	$k_{-12} = 40$
10	$k_{+10} = 0.0039$		

Table A.1: Model of Eißing: Parameter numbers and values (all in MIN^{-1})

Model of Schliemann et al.   At the time we began our analysis of the model, the model proposed in Schliemann et al. (2011) was still under revision. Therefore, our parameters and equations may vary slightly with respect to the model proposed in that paper. Here, we list all the reactions and parameters used in this model.

	Turnover Receptor	
1	TNFRcyt $\leftrightarrow$ TNFR	TNF-R1 transport into membrane
2	$\rightarrow$ TNFRcyt	TNFR production
3	TNFR $\rightarrow 0$	TNF-R1 degradation
4	$0 \leftrightarrow$ RIP	RIP turnover
5	TNF-TNFR $\rightarrow$	TNF-TNF-R1 degradation
6	TNFRC1 $\rightarrow$	TNFR-complex1 degradation
7	TNFRC2 $\rightarrow$	TNFR-complex2 degradation
8	TNFRC2-FLIP-FLIP $\rightarrow$	TNFRC2-FLIP-FLIP degradation
9	TNFRC2-FLIP-pCasp8 $\rightarrow$	TNFRC2-FLIP-pCasp8 degradation

Table A.2: Reactions governing the receptor turnover in a first version of Schliemann et al. (2011).

	Receptor	
10	TNF + TNFR ↔ TNF-TNFR	TNF-TNF-R1 binding and release
11	TNF-TNFR + RIP ↔ TNFRC1	TNF-R1-complex1 building
12	TNFRC1 + ↔ Cinterm1	Receptor internalisation step1
13	Cinterm1 ↔ Cinterm2	Receptor internalisation step2
14	Cinterm2 ↔ Cinterm3	Receptor internalisation step3
15	Cinterm3 ↔ TNFRC2	Receptor internalisation step4
16	TNFRC2 + pCasp8 + pCasp8 ↔ TNFRC2 + Casp8	Caspase-8 activation by TNFR-C2
17	TNFRC2 + FLIP + FLIP ↔ TNFRC2-FLIP-FLIP	FLIP recruitment to TNFR-C2
18	TNFRC2-FLIP-FLIP + IKK ↔ TNFRC2-FLIP-FLIP + IKKa	TNFR-C2 induced NF-κB activation
19	TNFRC2 + FLIP + pCasp8 ↔ TNFRC2-FLIP-pCasp8	FLIP-pCasp-8 heterodimers on TNFR-C2
20	TNFRC2-FLIP-pCasp8 + IKK ↔ TNFRC2-FLIP-pCasp8 + IKKa	TNFRC2-FLIP-pCasp8 induced NF-kappa B

Table A.3: Reactions governing the binding of the ligand to the receptor in a first version of Schliemann et al. (2011).

	TurnoverNF-kB	
21	$0 \leftrightarrow$ IKK	IKK turnover
22	$0 \leftrightarrow$ NFkB	NF-κB turnover
23	$0 \leftrightarrow$ FLIP	FLIP turnover
24	$0 \leftrightarrow$ XIAP	XIAP turnover
25	$0 \leftrightarrow$ A20	A20 turnover
26	IKKa $\rightarrow$	IKK* degradation
27	IkBa-NFkB $\rightarrow$	IκBα;-NF-κB complex degradation
28	NFkBnucl $\rightarrow$	nuclear NF-κB degradation
29	IkBat $\rightarrow$	IκBα; mRNA degradation
30	IkBa $\rightarrow$	free IκBα; degradation
31	IkBanucl $\rightarrow$	free nuclear IκBα; degradation
32	IkBa-NFkBnucl $\rightarrow$	nuclear IκBα;-NF-κB complex degradation
33	PIkBa $\rightarrow$	P-IκBa degradation
34	A20t $\rightarrow$	A20 mRNA degradation
35	XIAPt $\rightarrow$	XIAP mRNA degradation
36	FLIPt $\rightarrow$	FLIP mRNA degradation

Table A.4: Reactions governing the NFκB turnover in a first version of Schliemann et al. (2011).

	NF-kB	
37	IKK + TNFRC1 ↔ IKKa + TNFRC1	IKK activation by TNFRC1
38	IKKa ↔ IKK	IKK* inactivation / other phosphatases
39	A2 + TNFRC1 ↔ A20	TNFRC1 inactivation by A20
40	IkBa + NFkB ↔ IkBa-NFkB	IκBα; NF-κB association
41	IKKa + IkBa-NFkB ↔ IKK + NFkB + PIkBa	release and degradation of bound IκBα;
42	NFkB ↔ NFkBnucl	NF-κB N translocation
43	IKKa + IkBa ↔ IKK + PIkBa	phosphorylation of free IκBα;
44	NFkBnucl ↔ IkBat + NFkBnucl	IκBα; mRNA transcription
45	IkBat ↔ IkBa + IkBat	IκBα; translation
46	IkBa ↔ IkBanucl	IκBα; N translocation
47	IkBanucl NFkBnucl ↔ IkBa-NFkBnucl	IκBα; binding NF-κB in nucleus
48	IkBa-NFkBnucl ↔ IkBa-NFkB	IκBα;-NF-κB N-C export
49	NFkBnucl ↔ A20t + NFkBnucl	A20 mRNA transcription
50	A20t ↔ A20 + A2t	A20 translation
51	NFkBnucl ↔ XIAPt + NFkBnucl	XIAP mRNA transcription
52	XIAPt ↔ XIAP + XIAPt	XIAP translation
53	NFkBnucl ↔ FLIPt + NFkBnucl	FLIP mRNA transcription
54	FLIPt ↔ FLIP + FLIPt	FLIP translation

Table A.5: Reactions governing the reactions involving NFκB in a first version of Schliemann et al. (2011).

	Turnover Apoptosis	
55	0 ↔ pCasp8	Procaspase-8 turnover
56	0 ↔ pCasp3	Procaspase-3 turnover
57	0 ↔ pCasp6	Procaspase-6 turnover
58	Casp8 →	Caspase-8 degradation
59	Casp3 →	Caspase-3 degradation
60	Casp6 →	Caspase-6 degradation
61	XIAP-Casp3 →	XIAP-Caspase3 complex degradation
62	0 ↔ BAR	BAR turnover
63	BAR-Casp8 →	BAR-Caspase-8 complex degradation

Table A.6: Reactions governing the turnover of caspases and inhibitors in a first version of Schliemann et al. (2011).

	Apoptosis	
64	Casp8 + pCasp3 ↔ Casp8 + Casp3	Caspase-3 activation
65	Casp3 + pCasp6 ↔ Casp3 + Casp6	Caspase-6 activation
66	Casp6 + pCasp8 ↔ Casp6 + Casp8	Caspase-8 activation
67	XIAP + Casp3 ↔ XIAP-Casp3	XIAP-Caspase-3 complex formation
68	XIAP + Casp3 ↔ Casp3	XIAP degradation due to Caspase-3
69	XIAP-Casp3 ↔ XIAP	XIAP-Caspase-3 complex breakup
70	Casp3 + RIP ↔ Casp3	negative feedback loop Caspase-3 on C1
71	Casp3 + FLIP ↔ Casp3	FLIP degradation
72	BAR + Casp8 ↔ BAR-Casp8	BAR-Caspase-8 complex formation

Table A.7: Reactions governing the reactions between caspases and inhibitors in a first version of Schliemann et al. (2011).

1	$ka_1 = 0.001(\text{sec}^{-1})$	12	$kd_{10} = 1.134\text{e-}05\ (\text{sec}^{-1})$
2	$ka_2 = 3.226\text{e-}07\ (\mu M\text{sec}^{-1})$	13	$ka_{11} = 0.17\ (\mu M^{-1}\text{sec}^{-1})$
3	$ka_3 = 2.352\text{e-}02\ (\text{sec}^{-1})$	14	$ka_{12} = 5\text{e-}04\ (\text{sec}^{-1})$
4	$ka_4 = 5\text{e-}05\ (\mu M\text{sec}^{-1})$	15	$ka_{13} = 5\text{e-}04\ (\text{sec}^{-1})$
5	$kd_4 = 1\text{e-}04\ (\text{sec}^{-1})$	16	$ka_{14} = 5\text{e-}04\ (\text{sec}^{-1})$
6	$ka_5 = 2.352\text{e-}02\ (\text{sec}^{-1})$	17	$ka_{15} = 0.01\ (\text{sec}^{-1})$
7	$ka_6 = 5.6\text{e-}05\ (\text{sec}^{-1})$	18	$ka_{16} = 5.3216\text{e+}04\ (\mu M^{-2}\text{sec}^{-1})$
8	$ka_7 = 5.6\text{e-}05\ (\text{sec}^{-1})$	19	$ka_{17} = 1\text{e+}05\ (\mu M^{-2}\text{sec}^{-1})$
9	$ka_8 = 5.6\text{e-}05\ (\text{sec}^{-1})$	20	$ka_{18} = 4\ (\mu M^{-1}\text{sec}^{-1})$
10	$ka_9 = 5.6\text{e-}05\ (\text{sec}^{-1})$	21	$ka_{19} = 1000\ (\mu M^{-2}\text{sec}^{-1})$
11	$ka_{10} = 12600\ (\mu M^{-1}\text{sec}^{-1})$	22	$ka_{20} = 2\ (\mu M^{-2}\text{sec}^{-1})$

Table A.8: Model of Schliemann: Parameters related to receptor

1	$ka_{21} = 2\text{e-}05\ (\mu M\text{sec}^{-1})$	12	$ka_{27} = 1\text{e-}04\ (\text{sec}^{-1})$
2	$kd_{21} = 1\text{e-}04\ (\text{sec}^{-1})$	13	$ka_{28} = 3.3\text{e-}05\ (\text{sec}^{-1})$
3	$ka_{22} = 3\text{e-}06\ (\mu M\text{sec}^{-1})$	14	$ka_{29} = 3.3\text{e-}04\ (\text{sec}^{-1})$
4	$kd_{22} = 1\text{e-}04\ (\text{sec}^{-1})$	15	$ka_{30} = 1\text{e-}04\ (\text{sec}^{-1})$
5	$ka_{23} = 7.028\text{e-}07\ (\mu M\text{sec}^{-1})$	16	$ka_{31} = 3.3\text{e-}05\ (\text{sec}^{-1})$
6	$kd_{23} = 1\text{e-}04\ (\text{sec}^{-1})$	17	$ka_{32} = 3.3\text{e-}05\ (\text{sec}^{-1})$
7	$ka_{24} = 2.413\text{e-}04\ (\mu M\text{sec}^{-1})$	18	$ka_{33} = 1\text{e-}01(\text{sec}^{-1})$
8	$kd_{24} = 1\text{e-}04\ (\text{sec}^{-1})$	19	$ka_{34} = 3.3\text{e-}04\ (\text{sec}^{-1})$
9	$ka_{25} = 3\text{e-}06\ (\mu M\text{sec}^{-1})$	20	$ka_{35} = 3.3\text{e-}04\ (\text{sec}^{-1})$
10	$kd_{25} = 1\text{e-}04\ (\text{sec}^{-1})$	21	$ka_{36} = 3.3\text{e-}04\ (\text{sec}^{-1})$
11	$ka_{26} = 1\text{e-}04\ (\text{sec}^{-1})$		

Table A.9: Model of Schliemann: Parameters related to NFκ-b

22	$ka_{37} = 50 \ (\mu M^{-1}\mathrm{sec}^{-1})$	32	$kd_{46} = 5\mathrm{e}\text{-}04 \ (\mathrm{sec}^{-1})$
23	$ka_{38} = 0.02 \ (\mathrm{sec}^{-1})$	33	$ka_{47} = 0.1 \ (\mu M^{-1}\mathrm{sec}^{-1})$
24	$ka_{39} = 3.45 \ (\mu M^{-1}\mathrm{sec}^{-1})$	34	$ka_{48} = 0.001 \ (\mathrm{sec}^{-1})$
25	$ka_{40} = 0.2 \ (\mu M^{-1}\mathrm{sec}^{-1})$	35	$ka_{49} = 2.5\mathrm{e}\text{-}06 \ (\mathrm{sec}^{-1})$
26	$ka_{41} = 10 \ (\mu M^{-1}\mathrm{sec}^{-1})$	36	$ka_{50} = 0.5 \ (\mathrm{sec}^{-1})$
27	$ka_{42} = 1.67\mathrm{e}\text{-}04 \ (\mathrm{sec}^{-1})$	37	$ka_{51} = 3.333\mathrm{e}\text{-}07 \ (\mathrm{sec}^{-1})$
28	$ka_{43} = 1 \ (\mathrm{sec}^{-1})$	38	$ka_{52} = 6.25\mathrm{e}\text{-}02 \ (\mathrm{sec}^{-1})$
29	$ka_{44} = 5\mathrm{e}\text{-}07 \ (\mathrm{sec}^{-1})$	39	$ka_{53} = 4.4\mathrm{e}\text{-}07 \ (\mathrm{sec}^{-1})$
30	$ka_{45} = 0.8 \ (\mathrm{sec}^{-1})$	40	$ka_{54} = 3.275\mathrm{e}\text{-}02 \ (\mathrm{sec}^{-1})$
31	$ka_{46} = 2.5\mathrm{e}\text{-}03 \ (\mathrm{sec}^{-1})$		

Table A.10: Model of Schliemann: Parameters related to NFκ-b

1	$ka_{55} = 1\mathrm{e}\text{-}04 \ (\mu M\mathrm{sec}^{-1})$	13	$ka_{63} = 1\mathrm{e}\text{-}04 \ (\mathrm{sec}^{-1})$
2	$kd_{55} = 1\mathrm{e}\text{-}04 \ (\mathrm{sec}^{-1})$	14	$ka_{64} = 0.05 \ (\mu M^{-1}\mathrm{sec}^{-1})$
3	$ka_{56} = 2.5\mathrm{e}\text{-}05 \ (\mu M\mathrm{sec}^{-1})$	15	$ka_{65} = 0.05 \ (\mu M^{-1}\mathrm{sec}^{-1})$
4	$kd_{56} = 1\mathrm{e}\text{-}04 \ (\mathrm{sec}^{-1})$	16	$ka_{66} = 0.05 \ (\mu M^{-1}\mathrm{sec}^{-1})$
5	$ka_{57} = 2\mathrm{e}\text{-}07 \ (\mu M\mathrm{sec}^{-1})$	17	$ka_{67} = 1.2\mathrm{e}{+}06 \ (\mu M^{-1}\mathrm{sec}^{-1})$
6	$kd_{57} = 1\mathrm{e}\text{-}04 \ (\mathrm{sec}^{-1})$	18	$kd_{67} = 600 \ (\mathrm{sec}^{-1})$
7	$ka_{58} = 1\mathrm{e}\text{-}04 \ (\mathrm{sec}^{-1})$	19	$ka_{68} = 6 \ (\mu M^{-1}\mathrm{sec}^{-1})$
8	$ka_{59} = 1\mathrm{e}\text{-}04 \ (\mathrm{sec}^{-1})$	20	$ka_{69} = 5\mathrm{e}\text{-}05 \ (\mathrm{sec}^{-1})$
9	$ka_{60} = 1\mathrm{e}\text{-}04 \ (\mathrm{sec}^{-1})$	21	$ka_{70} = 0.5 \ (\mu M^{-1}\mathrm{sec}^{-1})$
10	$ka_{61} = 1\mathrm{e}\text{-}04 \ (\mathrm{sec}^{-1})$	22	$ka_{71} = 0.5 \ (\mu M^{-1}\mathrm{sec}^{-1})$
11	$ka_{62} = 9.446\mathrm{e}\text{-}07 \ (\mu M\mathrm{sec}^{-1})$	23	$ka_{72} = 1\mathrm{e}{+}06 \ (\mu M^{-1}\mathrm{sec}^{-1})$
12	$kd_{62} = 1\mathrm{e}\text{-}04 \ (\mathrm{sec}^{-1})$	24	$kd_{72} = 600 \ (\mathrm{sec}^{-1})$

Table A.11: Model of Schliemann: Parameters related to caspases

Model of Aslam et al. MATLAB codes for the model of Aslam et al. are available at `http://www.nature.com/msb/journal/v5/n1/suppinfo/msb200938_S1.html`. The table A.12 shows the values of parameters used for numerical simulations. These values correspond to nominal parameters values provided in Aslam et al. (2009).

Model of Connor and Stevens We used the model and parameters implemented by B. Ermentrout available at `http://www.math.pitt.edu/~bard/bardware/neurobook/allodes.html`. This model is drawn from the original

1	$k_1 = 1.106\text{e-}03$ ($\mu M^{-1}\text{sec}^{-1}$)	15	$k_{10} = 2.772$ ($\mu M^{-1}\text{sec}^{-1}$)
2	$k_{-1} = 14$ (sec^{-1})	16	$k_{-10} = 0.14$ (sec^{-1})
3	$k_2 = 0.0224$ ($\mu M^{-1}\text{sec}^{-1}$)	17	$k_{11} = 2.38$ (sec^{-1})
4	$k_{-2} = 0.028$ (sec^{-1})	18	$\text{kSYN1} = 1.624\text{e-}02$ ($\mu M^{-1}\text{sec}^{-1}$)
5	$k_3 = 0.021$ (sec^{-1})	19	$k_{-12} = 0.28$ (sec^{-1})
6	$k_4 = 1.4$ ($\mu M^{-1}\text{sec}^{-1}$)	20	$\text{k}SYN2 = 112$ (sec^{-1})
7	$k_{-4} = 1.7063\text{e-}02$ (sec^{-1})	21	BASAL $= 10$ (μM)
8	$k_5 = 0.0616$ (sec^{-1})	22	$(Ca^{2+})_4$-CaM (basal level) $= 5.144$ (A.U.)
9	$k_6 = 2.7496$ ($\mu M^{-1}\text{sec}^{-1}$)	23	P $= 2.214\text{e-}03$ (μM)
10	$k_{-6} = 0.28$ (sec^{-1})	24	T $= 0.05$ (μM)
11	$k_7 = 2.786$ (sec^{-1})	25	$\lambda_1 = \lambda_2 = \lambda_3 = 7.28\text{e-}04$ (sec^{-1})
12	$k_8 = 0.028$ ($\mu M^{-1}\text{sec}^{-1}$)	26	YT $= 10$ (μM)
13	$k_{-8} = 0.14$ (sec^{-1})	27	BASAL1 $= 0$ (μM)
14	$k_9 = 0.2520$ (sec^{-1})	28	BASAL2 $= 0$ (μM)

Table A.12: Model of Aslam: Parameter numbers and values

paper of Connor and Stevens (1971). Based on the ODE file of B. Ermentroutx, we implemented and simulate the model in MATLAB .

A.2 Numerical tools

Diagrams of bifurcations Diagrams of bifurcations for the model of Eissing et al. (2004) and Aslam et al. (2009) were drawn using the software XPP-AUT (Ermentrout, 2002).

Numerical simulations Numerical simulations of deterministic systems were performed using the numerical integration solver $ode15s$ in MATLAB. This solver has been chosen because its is performant for stiff problems. Switch models are stiff because they present slow modifications of variables before and after the switch and fast variations during the switch. Integrating the models with the classical solver $ode45$ will lead to particularly long times of integration.

Stochastic simulations were performed using the $sdodde$ solver in MATLAB.

A.3 Saddle node bifurcation in planar phase portraits

We present the conditions to obtain a saddle node bifurcation in the slow-fast model reductions presented in Chapter 8.

Conditions to observe a saddle node in the restorative model

Let us assume that that the system (8.4) posses a saddle node bifurcation at $(V, n) = (\bar{V}, \bar{n})$, we can compute the Jacobian matrix of the system at this point:

$$J = \begin{pmatrix} \dfrac{\partial \dot{V}}{\partial V} & \dfrac{\partial \dot{V}}{\partial n} \\ \dfrac{\partial \dot{n}}{\partial V} & \dfrac{\partial \dot{n}}{\partial n} \end{pmatrix} \Big|_{(\bar{V}, \bar{n})} = \begin{pmatrix} 1 - \bar{V}^2 & -1 \\ \epsilon\, m & -\epsilon \end{pmatrix}$$

where $m = \dfrac{\partial n_\infty(V)}{\partial V}\Big|_{(\bar{V}, \bar{n})}$, is the slope of the tangent to the n-nullcline at the saddle node.

At the saddle node bifurcation:

(i) $\det(J) = \dfrac{\partial \dot{V}}{\partial V}\dfrac{\partial \dot{n}}{\partial n} - \dfrac{\partial \dot{V}}{\partial n}\dfrac{\partial \dot{n}}{\partial V} = \epsilon[\bar{V}^2 - 1 + m] = \lambda_1 \lambda_2 = 0$

(ii) $\operatorname{Tr}(J) = \dfrac{\partial \dot{V}}{\partial V} + \dfrac{\partial \dot{n}}{\partial n} = 1 - \bar{V}^2 - \epsilon = \lambda_1 + \lambda_2 = \lambda_2$

By (i),

(iii) $\dfrac{\partial \dot{V}}{\partial V} = \dfrac{\partial \dot{V}}{\partial n}\dfrac{\partial \dot{n}}{\partial V}\dfrac{\partial \dot{n}}{\partial n}^{-1} \Leftrightarrow 1 - \bar{V}^2 = m$

By (ii) and (iii),

(iv) $\lambda_2 = m - \epsilon$

To get a saddle node bifurcation, we have to impose $\lambda_2 < 0$. Assuming $n_\infty(V)$ is a positive monotone increasing function of V, i.e $m > 0$, we get:

$$m \le \epsilon$$

A saddle node bifurcation with an attractive center manifold can only occur if the n-nullcline intercepts the V-nullcline with a slope smaller than ϵ. This means that the n-nullciline should be almost parallel to the V-axis in the phase plane and that the saddle-node bifurcation of the slow-fast model is very close to the minimum of the first branch of the cubic. In fact, for $\epsilon = 0$, the saddle-node bifurcation should correspond to the minimum.

Conditions to observe a saddle node in the regenerative model

Let us assume that that the system (8.5) posses a saddle node bifurcation at $(V, n) = (\bar{V}, \bar{n})$, we can compute the Jacobian matrix of the system at this point:

$$J = \begin{pmatrix} \dfrac{\partial \dot{V}}{\partial V} & \dfrac{\partial \dot{V}}{\partial n} \\ \dfrac{\partial \dot{n}}{\partial V} & \dfrac{\partial \dot{n}}{\partial n} \end{pmatrix} \Big|_{(\bar{V}, \bar{n})} = \begin{pmatrix} 1 - \bar{V}^2 & -2\bar{n} \\ \epsilon m & -\epsilon \end{pmatrix}$$

where $m = \dfrac{\partial n_\infty(V)}{\partial V} \Big|_{(\bar{V}, \bar{n})}$, is the slope of the tangent to the $n-$ nullcline at the saddle node.

At the saddle node bifurcation:

(i) $\det(J) = \dfrac{\partial \dot{V}}{\partial V} \dfrac{\partial \dot{n}}{\partial n} - \dfrac{\partial \dot{V}}{\partial n} \dfrac{\partial \dot{n}}{\partial V} = \epsilon[\bar{V}^2 - 1 + 2\bar{n}m] = \lambda_1 \lambda_2 = 0$

(ii) $\mathrm{Tr}(J) = \dfrac{\partial \dot{V}}{\partial V} + \dfrac{\partial \dot{n}}{\partial n} = 1 - \bar{V}^2 - \epsilon = \lambda_1 + \lambda_2 = \lambda_2$

By (i),

(iii) $\dfrac{\partial \dot{V}}{\partial V} = \dfrac{\partial \dot{V}}{\partial n} \dfrac{\partial \dot{n}}{\partial V} \dfrac{\partial \dot{n}}{\partial n}^{-1} \Leftrightarrow 1 - \bar{V}^2 = 2\bar{n}m$

By (ii) and (iii),

(iv) $\lambda_2 = 2\bar{n}m - \epsilon$

A saddle node is ensured by $\lambda_2 < 0$. Assuming $m > 0$ as in Franci et al. (2013b), the sign of λ_2 depends on the location of the saddle node in the phase plane:

- $\bar{n} > 0$: $\lambda_2 = 2\bar{n}m - \epsilon$. For the center manfiold to be attractive, m should be small, i.e $O(\epsilon)$.

- $\bar{n} < 0$ $\lambda_2 = 2\bar{n}m - \epsilon$. $\lambda_2 < 0$ for any value of ϵ.

The condition $\bar{n} > 0$ typically describes the upper branch of the V-nullcline. This branch is similar to the V-nullcine of the classical slow-fast restorative planar reduction. The condition $\bar{n} < 0$ corresponds to the lower branch of the V-nullcline associated with regenerative excitability.

Bibliography

J. G. Albeck, J. M. Burke, S. L. Spencer, D. A. Lauffenburger, and P. K. Sorger. Modeling a snap-action, variable-delay switch controlling extrinsic cell death. *PLoS Biol*, 6(12):e299, 2008.

U. Alon. *An Introduction to Systems Biology: Design Principles of Biological Circuits*. Chapman & Hall/CRC mathematical biology and medicine series, 2006.

U. Alon. Simplicity in biology. *Nature*, 446(7135):497, 2007.

D. Anderson, W. H. Mehaffey, M. Iftinca, R. Rehak, J. D. T. Engbers, S. Hameed, G. W. Zamponi, and R. W. Turner. Regulation of neuronal activity by Cav3-Kv4 channel signaling complexes. *Nat Neurosci*, 13(3): 333–7, 2010.

L. Arnold. *Stochastic differential equations: theory and applications*. Wiley, NY, 1974.

N. Aslam, Y. Kubota, D. Wells, and H. Z. Shouval. Translational switch for long-term maintenance of synaptic plasticity. *Mol Syst Biol*, 5:284, 2009.

N. Axmacher and R. Miles. Intrinsic cellular currents and the temporal precision of EPSP-action potential coupling in CA1 pyramidal cells. *J Physiol*, 555(Pt 3):713–25, 2004.

E. Z. Bagci, Y. Vodovotz, T. R. Billiar, G. B. Ermentrout, and I. Bahar. Bistability in apoptosis: roles of bax, bcl-2, and mitochondrial permeability transition pores. *Biophys J*, 90(5):1546–59, 2006.

N. Bagheri, J. Stelling, and F. J. Doyle, 3rd. Quantitative performance metrics for robustness in circadian rhythms. *Bioinformatics*, 23(3):358–64, 2007.

G. Balázsi, A. van Oudenaarden, and J. J. Collins. Cellular decision making and biological noise: from microbes to mammals. *Cell*, 144(6):910–25, 2011.

F. Baldissera, P. Cavallari, and F. Dworzak. Motor neuron 'bistability'. A pathogenetic mechanism for cramps and myokymia. *Brain*, 117 (Pt 5):929–39, 1994.

N. Barkai and S. Leibler. Robustness in simple biochemical networks. *Nature*, 387(6636):913–7, 1997.

A. K. Barreiro, E. L. Thilo, and E. Shea-Brown. A-current and type I/type II transition determine collective spiking from common input. *J Neurophysiol*, 108(6):1631–45, 2012.

S. Basu, Y. Gerchman, C. H. Collins, F. H. Arnold, and R. Weiss. A synthetic multicellular system for programmed pattern formation. *Nature*, 434(7037):1130–4, 2005.

M. Bentele, I. Lavrik, M. Ulrich, S. Stößer, D. W. Heermann, H. Kalthoff, P. H. Krammer, and R. Eils. Mathematical modeling reveals threshold mechanism in CD95-induced apoptosis. *J Cell Biol*, 166(6):839–851, 2004.

W. J. Blake, M. KAErn, C. R. Cantor, and J. J. Collins. Noise in eukaryotic gene expression. *Nature*, 422(6932):633–7, 2003.

T. V. Bliss and G. L. Collingridge. A synaptic model of memory: long-term potentiation in the hippocampus. *Nature*, 361(6407):31–9, 1993.

M. T. Borisuk and J. J. Tyson. Bifurcation analysis of a model of mitotic control in frog eggs. *J Theor Biol*, 195(1):69 – 85, 1998.

A. Borst and F. E. Theunissen. Information theory and neural coding. *Nat Neurosci*, 2(11):947–57, 1999.

P. Boxler. A stochastic version of center manifold theory. *Probab. Theory Related Fields*, 83(4):509–545, 1989.

F. J. Bruggeman and H. V. Westerhoff. The nature of systems biology. *Trends Microbiol*, 15(1):45–50, 2007.

E. Bullinger. System analysis of a programmed cell death model. In *44th IEEE Conference on Decision and Control and the European Control Conference*, volume 8, pages 7994–7999, Seville, Spain, Dec 2005. IEEE.

W. B. Cannon. *The wisdom of the body*. W.W. Norton & Company, inc, New York, 1932.

J.-P. Changeux and S. J. Edelstein. Allosteric mechanisms of signal transduction. *Science*, 308(5727):1424–8, 2005.

S. M. Chase and E. D. Young. First-spike latency information in single neurons increases when referenced to population onset. *Proc Natl Acad Sci USA*, 104 (12):5175–80, 2007.

C. Chen, J. Cui, H. Lu, R. Wang, S. Zhang, and P. Shen. Modeling of the role of a Bax-activation switch in the mitochondrial apoptosis decision. *Biophys J*, 92(12):4304–15, 2007.

W. W. Chen, B. Schoeberl, P. J. Jasper, M. Niepel, U. B. Nielsen, D. A. Lauffenburger, and P. K. Sorger. Input-output behavior of ErbB signaling pathways as revealed by a mass action model trained against dynamic data. *Mol Syst Biol*, 5:239, 2009.

H.-Y. Chuang, M. Hofree, and T. Ideker. A decade of systems biology. *Annu Rev Cell Dev Biol*, 26:721–44, 2010.

O. Cinquin and J. Demongeot. Positive and negative feedback: striking a balance between necessary antagonists. *J Theor Biol*, 216(2):229–41, 2002.

J. A. Connor and C. F. Stevens. Prediction of repetitive firing behaviour from voltage clamp data on an isolated neurone soma. *J Physiol*, 213(1):31–53, 1971.

S. Cory and J. M. Adams. The Bcl2 family: regulators of the cellular life-or-death switch. *Nat Rev Cancer*, 2(9):647–56, 2002.

J. Cui, C. Chen, H. Lu, T. Sun, and P. Shen. Two Independent positive feedbacks and bistability in the Bcl-2 apoptotic switch. *PLoS ONE*, 3(1): e1469, 2008.

J. De Caluwé and G. Dupont. The progression towards Alzheimer's disease described as a bistable switch arising from the positive loop between amyloids and Ca(2+). *J Theor Biol*, 331:12–8, 2013.

M. Dixon and E. C. Webb. *Enzymes*. Academic Press, New York, NY, 1979.

G. Drion, A. Franci, V. Seutin, and R. Sepulchre. A novel phase portrait for neuronal excitability. *PLoS ONE*, 7(8):e41806, 2012.

T. Eissing, F. Allgöwer, and E. Bullinger. Robustness properties of apoptosis models with respect to parameter variations and intrinsic noise. *Syst Biol (Stevenage)*, 152(4):221–8, 2005.

T. Eissing, H. Conzelmann, E. D. Gilles, F. Allgöwer, E. Bullinger, and P. Scheurich. Bistability analyses of a caspase activation model for receptor-induced apoptosis. *J Biol Chem*, 279(35):36892–7, 2004.

T. Eissing, S. Waldherr, F. Allgöwer, P. Scheurich, and E. Bullinger. Response to bistability in apoptosis: roles of bax, bcl-2, and mitochondrial permeability transition pores. *Biophys J*, 92(9):3332–4, 2007.

S. Elmore. Apoptosis: a review of programmed cell death. *Toxicol Pathol*, 35 (4):495–516, 2007.

B. Ermentrout. *Simulating, Analyzing, and Animating Dynamical Systems: A Guide to XPPAUT for Researchers and Students*, volume 14. SIAM, Philadelphia, PA, 2002.

B. Ermentrout and D. H. Terman. *Mathematical foundations of neuroscience*, volume v. 35 of *Interdisciplinary applied mathematics*. Springer, New York, NY, 2010.

J. E. Ferrell, Jr. Tripping the switch fantastic: how a protein kinase cascade can convert graded inputs into switch-like outputs. *Trends Biochem Sci*, 21 (12):460–6, 1996.

J. E. Ferrell and E. M. Machleder. The biochemical basis of an all-or-none cell fate switch in Xenopus Oocytes. *Science*, 280(5365):895–898, 1998.

R. FitzHugh. Mathematical models of threshold phenomena in the nerve membrane. *Bull Math Biophys*, 17(4), 1955.

R. Fonseca, U. V. Nagerl, and T. Bonhoeffer. Neuronal activity determines the protein synthesis dependence of long-term potentiation. *Nat Neurosci*, 9(4): 478–80, 2006.

E. Forgoston and I. Schwartz. Escape rates in a stochastic environment with multiple scales. *SIAM J Appl Dyn Syst.*, 8(3):1190–217, 2009.

A. Franci, G. Drion, and R. Sepulchre. Modeling neuronal bursting: singularity theory meets neurophysiology. preprint, 2013a.

A. Franci, G. Drion, V. Seutin, and R. Sepulchre. A balance equation determines a switch in neuronal excitability. *PLoS Comput Biol*, 9(5):e1003040, 2013b.

U. Frey and R. G. Morris. Synaptic tagging and long-term potentiation. *Nature*, 385(6616):533–6, 1997.

U. Frey, M. Krug, K. G. Reymann, and H. Matthies. Anisomycin, an inhibitor of protein synthesis, blocks late phases of LTP phenomena in the hippocampal CA1 region in vitro. *Brain Res*, 452(1-2):57–65, Jun 1988.

D. Fricker and R. Miles. EPSP amplification and the precision of spike timing in hippocampal neurons. *Neuron*, 28(2):559–69, 2000.

S. Fulda and K.-M. Debatin. Extrinsic versus intrinsic apoptosis pathways in anticancer chemotherapy. *Oncogene*, 25(34):4798–811, 2006.

M. Fussenegger, J. E. Bailey, and J. Varner. A mathematical model of caspase function in apoptosis. *Nat Biotechnol*, 18(7):768–74, 2000.

T. S. Gardner, C. R. Cantor, and J. J. Collins. Construction of a genetic toggle switch in Escherichia coli. *Nature*, 403(6767):339–42, 2000.

W. Gerstner and W. M. Kistler. *Spiking Neuron Models: Single Neurons, Populations, Plasticity.* Cambridge University Press, 1 edition, 2002.

D. T. Gillespie. A general method for numerically simulating the stochastic time evolution of coupled chemical reactions. *J. Comput. Phys.*, 22(4):403 – 34, 1976.

D. T. Gillespie. Stochastic simulation of chemical kinetics. *Annu Rev Phys Chem*, 58(1):35–55, 2007.

A. Goldbeter and D. E. Koshland, Jr. Ultrasensitivity in biochemical systems controlled by covalent modification. Interplay between zero-order and multistep effects. *J Biol Chem*, 259(23):14441–7, 1984.

T. Gollisch and M. Meister. Rapid neural coding in the retina with relative spike latencies. *Science*, 319(5866):1108–11, 2008.

M. Golubitsky and D. G. Schaeffer. *Singularities and Groups in Bifurcation Theory*, volume 51 of *Applied mathematical sciences.* Springer-Verlag, New York, NY, 1985.

D. R. Green and G. I. Evan. A matter of life and death. *Cancer Cell*, 1(1): 19–30, 2002.

J. S. Griffith. Mathematics of cellular control processes II. Positive feedback to one gene. *J Theor Biol*, 20(2):209–16, 1968.

A. J. Gruber, S. A. Solla, and J. C. Houk. Dopamine induced bistability enhances signal processing in spiny neurons. In *Advances in Neural Information Processing Systems 15*, pages 165–72. MIT Press, 2002.

J. Guckenheimer and P. Holmes. *Nonlinear Oscillations, Dynamical Systems, and Bifurcations of Vector Fields*, volume 42 of *Applied mathematical sciences.* Springer-Verlag, New York, NY, 1983.

M. Hafner, P. Sacré, L. Symul, R. Sepulchre, and H. Koeppl. Multiple feedback loops in circadian cycles: robustness and entrainment as selection criteria. In *Seventh International Workshop on Computational Systems Biology*, pages 43–46, Luxembourg, Luxembourg, Jun 2010.

M. Hafner, H. Koeppl, M. Hasler, and A. Wagner. 'Glocal' robustness analysis and model discrimination for circadian oscillators. *PLoS Comput Biol*, 5(10): e1000534, 2009.

P. J. Hahn and D. M. Durand. Bistability dynamics in simulations of neural activity in high-extracellular-potassium conditions. *J Comput Neurosci*, 11 (1):5–18, 2001.

M. A. Henson. Dynamic modeling of microbial cell populations. *Curr Opin Biotechnol*, 14(5):460–7, 2003.

H. Hentze, I. Schmitz, M. Latta, A. Krueger, P. H. Krammer, and A. Wendel. Glutathione dependence of caspase-8 activation at the death-inducing signaling complex. *J Biol Chem*, 277(7):5588–95, 2002.

P. Heyward, M. Ennis, A. Keller, and M. T. Shipley. Membrane bistability in olfactory bulb mitral cells. *J Neurosci*, 21(14):5311–20, 2001.

D. J. Higham. An algorithmic introduction to numerical simulation of stochastic differential equations. *SIAM Review*, 43(3):525–46, 2001.

A. Hilfinger and J. Paulsson. Separating intrinsic from extrinsic fluctuations in dynamic biological systems. *Proc Natl Acad Sci USA*, 108(29):12167–72, 2011.

A. Hill. The possible effects of the aggregation of the molecules of haemoglobin on its dissociation curves. *J Physiol*, 40(Suppl):iv–vii, 1910.

M. M. Hill, C. Adrain, P. J. Duriez, E. M. Creagh, and S. J. Martin. Analysis of the composition, assembly kinetics and activity of native Apaf-1 apoptosomes. *EMBO J*, 23(10):2134–45, 2004.

B. Hille. *Ionic Channels of Excitable Membranes*. Sinauer Associates, Sunderland, MA, 1984.

A. L. Hodgkin, A L and A. F. Huxley. A quantitative description of membrane current and its application to conduction and excitation in nerve. *J Physiol*, 117(4):500–44, 1952.

D. A. Hoffman, J. C. Magee, C. M. Colbert, and D. Johnston. K+ channel regulation of signal propagation in dendrites of hippocampal pyramidal neurons. *Nature*, 387(6636):869–75, 1997.

J. J. Hopfield. Neural networks and physical systems with emergent collective computational abilities. *Proc Natl Acad Sci USA*, 79(8):2554–8, 1982.

C. C. Hsia. Respiratory function of hemoglobin. *N Engl J Med*, 338(4):239–47, 1998.

H. Huber, E. Bullinger, and M. Rehm. Systems biology approaches to the study of apoptosis. *Essentials of Apoptosis*, pages 283–97, 2009.

B. Ingalls. Sensitivity analysis: from model parameters to system behaviour. *Essays Biochem*, 45:177–93, 2008.

E. M. Izhikevich. *Dynamical Systems in Neuroscience: the Geometry of Excitability and Bursting.* MIT Press, Cambridge, MA, 2007.

F. Jacob and J. Monod. Genetic regulatory mechanisms in the synthesis of proteins. *J Mol Biol*, 3:318–56, 1961.

M. D. Jacobson, M. Weil, and M. C. Raff. Programmed cell death in animal development. *Cell*, 88(3):347–54, 1997.

R. S. Johansson and I. Birznieks. First spikes in ensembles of human tactile afferents code complex spatial fingertip events. *Nat Neurosci*, 7(2):170–7, 2004.

J. P. Keener and J. Sneyd. *Mathematical Physiology*, volume 8 of *Interdisciplinary applied mathematics.* Springer, New York, NY, 2nd edition, 2009.

N. Kellershohn and M. Laurent. Prion diseases: dynamics of the infection and properties of the bistable transition. *Biophys J*, 81(5):2517–2529, 2001.

Y. Kifer. The exit problem for small random perturbations of dynamical systems with a hyperbolic fixed point. *Israel Journal of Mathematics*, 40(1): 74–96, 1981.

S. Kikuchi, K. Fujimoto, N. Kitagawa, T. Fuchikawa, M. Abe, K. Oka, K. Takei, and M. Tomita. Kinetic simulation of signal transduction system in hippocampal long-term potentiation with dynamic modeling of protein phosphatase 2A. *Neural Netw*, 16(9):1389–98, 2003.

F. C. Kischkel, S. Hellbardt, I. Behrmann, M. Germer, M. Pawlita, P. H. Krammer, and M. E. Peter. Cytotoxicity-dependent APO-1 (Fas/CD95)-associated proteins form a death-inducing signaling complex (DISC) with the receptor. *EMBO J*, 14(22):5579–88, 1995.

H. Kitano. Systems biology: a brief overview. *Science*, 295(5560):1662–4, 2002.

H. Kitano. Biological robustness. *Nat Rev Genet*, 5(11):826–37, 2004.

H. Kitano. Towards a theory of biological robustness. *Mol Syst Biol*, 3:137, 2007.

H. Kitano. Violations of robustness trade-offs. *Mol Syst Biol*, 6(384), 2010.

H. Kobayashi, M. Kaern, M. Araki, K. Chung, T. S. Gardner, C. R. Cantor, and J. J. Collins. Programmable cells: interfacing natural and engineered gene networks. *Proc Natl Acad Sci USA*, 101(22):8414–9, 2004.

C. Koch. *Biophysics of Computation: Information Processing in Single Neurons.* Oxford University Press, New York, NY, 1999.

J. H. Kotaleski and K. T. Blackwell. Modelling the molecular mechanisms of synaptic plasticity using systems biology approaches. *Nat Rev Neurosci*, 11 (4):239–51, 2010.

B. P. Kramer, A. U. Viretta, M. Daoud-El-Baba, D. Aubel, W. Weber, and M. Fussenegger. An engineered epigenetic transgene switch in mammalian cells. *Nat Biotechnol*, 22(7):867–70, 2004.

H. Kramers. Brownian motion in a field of force and the diffusion model of chemical reactions. *Physica*, 7(4):284 – 304, 1940.

Y. A. Kuznestov. *Elements of Applied Bifurcation Theory*, volume 112 of *Applied mathematical sciences.* Springer, New York, NY, 3rd edition, 2004.

M. Laurent and N. Kellershohn. Multistability: a major means of differentiation and evolution in biological systems. *Trends Biochem Sci*, 24(11):418–22, 1999.

H. A. Lechner, D. A. Baxter, J. W. Clark, and J. H. Byrne. Bistability and its regulation by serotonin in the endogenously bursting neuron R15 in Aplysia. *J Neurophysiol*, 75(2):957–62, 1996.

R. H. Lee and C. J. Heckman. Bistability in spinal motoneurons in vivo: systematic variations in rhythmic firing patterns. *J Neurophysiol*, 80(2): 572–82, 1998.

S. Legewie, N. Blüthgen, and H. Herzel. Mathematical modeling identifies inhibitors of apoptosis as mediators of positive feedback and bistability. *PLoS Comput Biol*, 2(9), 2006.

B. Lindner, A. Longtin, and A. Bulsara. Analytic expressions for rate and CV of a type I neuron driven by white gaussian noise. *Neural Comput*, 15(8): 1760–87, 2003.

J. E. Lisman and A. M. Zhabotinsky. A model of synaptic memory: a CaMKII/PP1 switch that potentiates transmission by organizing an AMPA receptor anchoring assembly. *Neuron*, 31(2):191–201, 2001.

R. M. Locksley, N. Killeen, and M. J. Lenardo. The TNF and TNF receptor superfamilies: integrating mammalian biology. *Cell*, 104(4):487–501, 2001.

A. J. Lotka. *Elements of Physical Biology*. Williams and Wilkins Company, Baltimore, MD, 1925.

S. W. Lowe and A. W. Lin. Apoptosis in cancer. *Carcinogenesis*, 21(3):485–95, 2000.

L. Ma and P. Iglesias. Quantifying robustness of biochemical network models. *BMC Bioinformatics*, 3(1):38, 2002.

W. Maass and C. M. Bishop. *Pulsed Neural Networks*. MIT Press, Cambridge, MA, 1999.

R. Malinow, H. Schulman, and R. Tsien. Inhibition of postsynaptic PKC or CaMKII blocks induction but not expression of LTP. *Science*, 245(4920): 862–6, 1989.

M. Martina, J. H. Schultz, H. Ehmke, H. Monyer, and P. Jonas. Functional and molecular differences between voltage-gated K+ channels of fast-spiking interneurons and pyramidal neurons of rat hippocampus. *J Neurosci*, 18(20): 8111–25, 1998.

A. Mauroy, I. Mezic, and J. Moehlis. Isostables, isochrons, and Koopman spectrum for the action-angle representation of stable fixed point dynamics. *Phys. D*, page in press, 2013.

M. Miller, M. Hafner, E. Sontag, N. Davidsohn, S. Subramanian, P. E. M. Purnick, D. Lauffenburger, and R. Weiss. Modular design of artificial tissue homeostasis: robust control through synthetic cellular heterogeneity. *PLoS Comput Biol*, 8(7):e1002579, 2012.

P. Miller, A. M. Zhabotinsky, J. E. Lisman, and X.-J. Wang. The stability of a stochastic CaMKII switch: dependence on the number of enzyme molecules and protein turnover. *PLoS Biol*, 3(4):e107, 2005.

M. L. Molineux, F. R. Fernandez, W. H. Mehaffey, and R. W. Turner. A-Type and T-Type currents interact to produce a novel spike latency-voltage relationship in cerebellar stellate cells. *J Neurosci*, 25(47):10863–73, 2005.

J. Monod. From enzymatic adaptation to allosteric transitions. *Science*, 154 (3748):475–83, 1966.

J. Monod, J. P. Changeux, and F. Jacob. Allosteric proteins and cellular control systems. *J Mol Biol*, 6:306–29, 1963.

J. Monod, J. Wyman, and J. P. Changeux. On the nature of allosteric transitions: a plausible model. *J Mol Biol*, 12:88–118, 1965.

B. Müller-Hill. *The Lac Operon: a Short History of a Genetic Paradigm*. Walter de Gruyter, Berlin, DE, 1996.

D. Nijhawan, N. Honarpour, and X. Wang. Apoptosis in neural development and disease. *Annu Rev Neurosci*, 23:73–87, 2000.

A. Novick and M. Weiner. Enzyme induction is an all-or-none phenomenon. *Proc Natl Acad Sci USA*, 43(7):553–66, 1957.

J. T. Opferman and S. J. Korsmeyer. Apoptosis in the development and maintenance of the immune system. *Nat Immunol*, 4(5):410–5, 2003.

N. Otmakhov, J.-H. Tao-Cheng, S. Carpenter, B. Asrican, A. Dosemeci, T. S. Reese, and J. Lisman. Persistent accumulation of calcium/calmodulin-dependent protein kinase II in dendritic spines after induction of NMDA receptor-dependent chemical long-term potentiation. *J Neurosci*, 24(42): 9324–31, 2004.

E. M. Ozbudak, M. Thattai, I. Kurtser, A. D. Grossman, and A. van Oudenaarden. Regulation of noise in the expression of a single gene. *Nat Genet*, 31(1):69–73, 2002.

E. M. Ozbudak, M. Thattai, H. N. Lim, B. I. Shraiman, and A. Van Oudenaarden. Multistability in the lactose utilization network of *Escherichia coli*. *Nature*, 427(6976):737–40, 2004.

S. Palani and C. A. Sarkar. Synthetic conversion of a graded receptor signal into a tunable, reversible switch. *Mol Syst Biol*, 7:480, 2011.

L. Pauling. The oxygen equilibrium of hemoglobin and its structural interpretation. *Proc Natl Acad Sci USA*, 21(4):186–91, 1935.

J. R. Pomerening, E. D. Sontag, and J. E. Ferrell. Building a cell cycle oscillator: hysteresis and bistability in the activation of Cdc2. *Nat Cell Biol*, 5(4):346–51, 2003.

P. E. M. Purnick and R. Weiss. The second wave of synthetic biology: from modules to systems. *Nat Rev Mol Cell Biol*, 10(6):410–22, 2009.

A. Raj and A. van Oudenaarden. Nature, nurture, or chance: stochastic gene expression and its consequences. *Cell*, 135(2):216–26, 2008.

M. Rehm, H. Düßmann, R. U. Jänicke, J. M. Tavaré, D. Kögel, and J. H. M. Prehn. Single-cell fluorescence resonance energy transfer analysis demonstrates that caspase activation during apoptosis is a rapid process. *J Biol Chem*, 277(27):24506–14, 2002.

M. Rehm, H. J. Huber, H. Dussmann, and J. H. M. Prehn. Systems analysis of effector caspase activation and its control by X-linked inhibitor of apoptosis protein. *EMBO J*, 25(18):4338–49, 2006.

F. Rieke. *Spikes: Exploring the Neural Code.* MIT Press, Cambridge, MA, 1997.

C. P. Robert and G. Casella. *Monte Carlo Statistical Methods.* Springer, New York, NY, 1999.

L. Robert, G. Paul, Y. Chen, F. Taddei, D. Baigl, and A. B. Lindner. Predispositions and epigenetic inheritance in the Escherichia coli lactose operon bistable switch. *Mol Syst Biol*, 6:357, 2010.

A. Roberts. Normal form transforms separate slow and fast modes in stochastic dynamical systems. *Phys. A*, 387(1):12 – 38, 2008.

X. Saelens, N. Festjens, L. Vande Walle, M. van Gurp, G. van Loo, and P. Vandenabeele. Toxic proteins released from mitochondria in cell death. *Oncogene*, 23(16):2861–74, 2004.

A. Sanchez, S. Choubey, and J. Kondev. Regulation of noise in gene expression. *Annu Rev Biophys*, 42:469–91, 2013.

C. Scaffidi, S. Fulda, A. Srinivasan, C. Friesen, F. Li, K. J. Tomaselli, K. M. Debatin, P. H. Krammer, and M. E. Peter. Two CD95 (APO-1/Fas) signaling pathways. *EMBO J*, 17(6):1675–87, 1998.

C. Scaffidi, I. Schmitz, P. H. Krammer, and M. E. Peter. The role of c-FLIP in modulation of CD95-induced apoptosis. *J Biol Chem*, 274(3):1541–8, 1999.

M. Schliemann, T. Eißing, P. Scheurich, and E. Bullinger. Mathematical modelling of TNF-α induced anti-apoptotic signalling pathways in mammalian cells based on dynamic and quantitative experiments. In *Proceedings of the 2nd Foundations of Systems Biology in Engineering FOSBE*, pages pp. 545–552, Stuttgart, Germany, Sep 2007.

M. Schliemann, E. Bullinger, S. Borchers, F. Allgöwer, R. Findeisen, and P. Scheurich. Heterogeneity reduces sensitivity of cell death for TNF-stimuli. *BMC Syst Biol*, 5:204, 2011.

T. D. Seeley, P. K. Visscher, T. Schlegel, P. M. Hogan, N. R. Franks, and J. A. R. Marshall. Stop signals provide cross inhibition in collective decision-making by honeybee swarms. *Science*, 335(6064):108–11, 2012.

L. Serrano. Synthetic biology: promises and challenges. *Mol Syst Biol*, 3:158, 2007.

W. Sha, J. Moore, K. Chen, A. D. Lassaletta, C.-S. Yi, J. J. Tyson, and J. C. Sible. Hysteresis drives cell-cycle transitions in Xenopus laevis egg extracts. *Proc Natl Acad Sci USA*, 100(3):975–80, 2003.

J. E. Shoemaker and F. J. Doyle, 3rd. Identifying fragilities in biochemical networks: robust performance analysis of Fas signaling-induced apoptosis. *Biophys J*, 95(6):2610–23, 2008.

M. J. Solomon, M. Glotzer, T. H. Lee, M. Philippe, and M. W. Kirschner. Cyclin activation of p34cdc2. *Cell*, 63(5):1013–24, 1990.

S. L. Spencer and P. K. Sorger. Measuring and modeling apoptosis in single cells. *Cell*, 144(6):926–39, 2011.

S. L. Spencer, S. Gaudet, J. G. Albeck, J. M. Burke, and P. K. Sorger. Non-genetic origins of cell-to-cell variability in TRAIL-induced apoptosis. *Nature*, 459(7245):428–32, 2009.

J. Stelling, E. D. Gilles, and F. J. Doyle, 3rd. Robustness properties of circadian clock architectures. *Proc Natl Acad Sci USA*, 101(36):13210–5, 2004a.

J. Stelling, U. Sauer, Z. Szallasi, F. J. Doyle, 3rd, and J. Doyle. Robustness of cellular functions. *Cell*, 118(6):675–85, 2004b.

E. Stone and P. Holmes. Random perturbations of heteroclinic attractors. *SIAM J Appl Math*, 50(3):726–43, 1990.

R. Storchi, M. R. Bale, G. E. M. Biella, and R. S. Petersen. Comparison of latency and rate coding for the direction of whisker deflection in the subcortical somatosensory pathway. *J Neurophysiol*, 108(7):1810–21, 2012.

S. H. Strogatz. *Nonlinear Dynamics and Chaos: with Applications to Physics, Biology, Chemistry, and Engineering*. Addison-Wesley Pub., Reading, MA, 1994.

P. S. Swain, M. B. Elowitz, and E. D. Siggia. Intrinsic and extrinsic contributions to stochasticity in gene expression. *Proc Natl Acad Sci USA*, 99(20): 12795–800, 2002.

R. Thomas. The role of feedback circuits: positive feedback circuits are a necessary condition for positive real eigenvalues of the Jacobian matrix. *Ber Bunsenges Phys Chem*, 98(9):1148–51, 1994.

C. B. Thompson. Apoptosis in the pathogenesis and treatment of disease. *Science*, 267(5203):1456–62, 1995.

S. Thorpe, A. Delorme, and R. Van Rullen. Spike-based strategies for rapid processing. *Neural Netw*, 14(6-7):715–25, 2001.

C. D. Thron. Bistable biochemical switching and the control of the events of the cell cycle. *Nonlinear Analysis*, 30(3):1825–34, 1997.

L. Trotta, R. Sepulchre, and E. Bullinger. Delayed decision-making in bistable models. In *Proceedings of the 49th IEEE conference on Decision and Control*, pages 816–821, Atlanta, GA, Dec 2010.

L. Trotta, E. Bullinger, and R. Sepulchre. Global analysis of dynamical decision-making models through local computation around the hidden saddle. *PLoS ONE*, 7(3):e33110, 2012.

R. W. Tsien. Calcium channels in excitable cell membranes. *Annu Rev Physiol*, 45:341–58, 1983.

T. Turányi. Sensitivity analysis of complex kinetic systems. Tools and applications. *J Math Chem*, 5(3):203–48, 1990.

L. Tyas, V. A. Brophy, A. Pope, A. J. Rivett, and J. M. Tavaré. Rapid caspase-3 activation during apoptosis revealed using fluorescence-resonance energy transfer. *EMBO Rep*, 1(3):266–70, 2000.

J. J. Tyson and B. Novak. Temporal organization of the cell cycle. *Curr Biol*, 18(17):R759–68, 2008.

J. J. Tyson and B. Novák. Functional motifs in biochemical reaction networks. *Annu Rev Phys Chem*, 61(1):219–40, 2010.

J. J. Tyson, K. C. Chen, and B. Novak. Sniffers, buzzers, toggles and blinkers: dynamics of regulatory and signaling pathways in the cell. *Curr Opin Cell Biol*, 15(2):221–31, 2003.

M. Ullah and O. Wolkenhauer. Stochastic approaches in systems biology. *Wiley Interdiscip Rev Syst Biol Med*, 2(4):385–97, 2010.

M. Usher and J. L. McClelland. The time course of perceptual choice: the leaky, competing accumulator model. *Psychol Rev*, 108(3):550–92, 2001.

V. Volterra and M. Brelot. *Leçons sur la Théorie Mathématique de la Lutte pour la Vie*. Gauthier-Villars et cie, Paris, FR, 1931.

S. R. Williams, S. R. Christensen, G. J. Stuart, and M. Häusser. Membrane potential bistability is controlled by the hyperpolarization-activated current I(H) in rat cerebellar Purkinje neurons in vitro. *J Physiol*, 539(Pt 2):469–83, 2002.

H. R. Wilson and J. D. Cowan. Excitatory and inhibitory interactions in localized populations of model neurons. *Biophys J*, 12(1):1–24, 1972.

B. B. Wolf and D. R. Green. Suicidal tendencies: apoptotic cell death by caspase family proteinases. *J Biol Chem*, 274(29):20049–52, 1999.

G. Yao, C. Tan, M. West, J. R. Nevins, and L. You. Origin of bistability underlying mammalian cell cycle entry. *Mol Syst Biol*, 7:485, 2011.

Z. Zi, Z. Feng, D. A. Chapnick, M. Dahl, D. Deng, E. Klipp, A. Moustakas, and X. Liu. Quantitative analysis of transient and sustained transforming growth factor β signaling dynamics. *Mol Syst Biol*, 7:492, 2011.

O. Zohar, T. M. Shackleton, I. Nelken, A. R. Palmer, and M. Shamir. First spike latency code for interaural phase difference discrimination in the guinea pig inferior colliculus. *J Neurosci*, 31(25):9192–204, 2011.